Coordination Strategies of Connected and Automated Vehicles near On-ramp Bottlenecks on Motorways

Chen, N.

Publication date
2021

Document Version
Final published version

Citation (APA)
Chen, N. (2021). *Coordination Strategies of Connected and Automated Vehicles near On-ramp Bottlenecks on Motorways*. [Dissertation (TU Delft), Delft University of Technology].

Coordination Strategies of Connected and Automated Vehicles near On-ramp Bottlenecks on Motorways

Na CHEN

Delft University of Technology, 2021

This thesis was funded by China scholarship council, Rijkswaterstaat of the Ministry of Infrastructure and Water Management in the Netherlands, and Delft University of Technology.
The Netherlands Research School for Transport, Infrastructure and Logistics TRAIL is greatly acknowledged.

Coordination Strategies of Connected and Automated Vehicles near On-ramp Bottlenecks on Motorways

Dissertation

for the purpose of obtaining the degree of doctor

at Delft University of Technology

by the authority of the Rector Magnificus, Prof.dr.ir. T.H.J.J. van der Hagen,

chair of the Board for Doctorates

to be defended publicly on

Wednesday 22 December 2021 at 10:00 o'clock

by

Na CHEN

Master of Engineering in Traffic and Transportation Planning and Management,

Beijing Jiaotong University, China

born in Suzhou, China

This dissertation has been approved by the
promotor: Prof. dr. ir. B. van Arem
Copromotor: Dr. ir. M. Wang

Composition of the doctoral committee:

Rector Magnificus	Chairman
Prof. dr. ir. B. van Arem	Delft University of Technology, promotor
Dr. ir. M. Wang	Delft University of Technology, copromotor

Independent members:

Dr. S. Siri	University of Genova
Prof. dr. H. Nijmeijer	Eindhoven University of Technology
Prof. dr. ir. S.P. Hoogendoorn	Delft University of Technology
Dr. ir. H. Farah	Delft University of Technology
Prof. dr. R.M.P. Goverde	Delft University of Technology, reserve member

Other member:

Mr. T. Alkim	European Commission

TRAIL Thesis Series no. T2021/29, the Netherlands TRAIL Research School

TRAIL
P.O. Box 5017
2600 GA Delft
The Netherlands
E-mail: info@rsTRAIL.nl

ISBN: 978-90-5584-304-6

Printed in the Netherlands

Dedicated to my supervisors, family, and country

"Knowledge is power."

Francis Bacon

Preface

I acknowledge the generous financial support from China scholarship council, Rijkswaterstaat of the Ministry of Infrastructure and Water Management in the Netherlands, and Delft University of Technology.

I would like to express my deepest appreciation to my promotor and copromotor, Prof. dr. Bart van Arem and Dr. Meng Wang. Their guidance, suggestions, critical comments, and feedback have helped me in conducting research, publishing papers, and accomplishing my thesis. Besides, their experience and advice have helped me stay positive, strong, and healthy. I hope I can return the favor sometime in the future.

I am deeply indebted to Dr. Silvia Siri, Prof. dr. Henk Nijmeijer, Prof. dr. ir. Serge Hoogendoorn, Dr. ir. Haneen Farah, Prof. dr. Rob Goverde, and Mr. Tom Alkim for being members of my doctoral committee. Their feedback helped me improve the quality of my thesis.

I am extremely grateful to the Editors and reviewers of my papers for their constructive and encouraging feedback. I am greatly indebted to Mr. Tom Alkim, Mr. Marco Schreuder, and Mr. Remco Reints for the insightful discussions in my progress meetings.

I would also like to extend my deepest gratitude to my GO/NO GO committee members: Dr. ir. Haneen Farah, Dr. Javier Alonso Mora, Mr. Tom Alkim, and Dr. Meng Wang. Their GO decisions enabled me to continue my project. On the other hand, they gave me valuable advice.

The completion of my dissertation would not have been possible without the support of Dr. ir. Pengling Wang, Dr. Anqi Fu, Dr. ir. Freddy Antony Mullakkal-Babu, and Ms. Conchita van der Stelt. Dr. ir. Pengling Wang helped me check my codes for Chapter 2 and lent me a useful book related to control. Dr. Anqi Fu discussed with me about control methods for Chapter 2. Dr. ir. Freddy Antony Mullakkal-Babu discussed with me the approaches to control lateral motions of automated vehicles for Chapter 3. Ms. Conchita van der Stelt helped me check and print my thesis.

I cannot begin to express my thanks to my Mentor, Dr. Hemmo Abels. His patience, kindness, and ongoing encouragement were helpful to me.

I would like to extend my sincere thanks to Dr. ir. Xiao Liang and Dr. ir. Qu Hu for their kindness, time, and support during my pregnancy and after my delivery.

I very much appreciate my current and former colleagues from the department of Transport and Planning at Delft University of Technology. I would like to thank my officemates: Dr. ir. Lin Xiao, Dr. ir Paul van Gent, Dr. Hamid Saeedi, Dr. Silvia Varotto, Dr. Hari Nagalur Subraveti, Mr. Raeed Mohammed, Dr. Fanchao Liao, and Mr. Qinglin Li. They helped me drink plenty of water by frequently asking "coffee and tea." Discussions with them resolved my several confusions. I also wish to thank Dr. Victor Knoop, Dr. Juan Pablo N., Dr. Marie-Jette Wierbos, Dr. Maria J. Alonso Gonzalez, and Mr. Tín Nguyen for their kindness and knowledge. Special thanks to Dr. Yusen Chen, Prof. Jing Zhao, Dr. Vincent Gong, Dr. Yongqiu Zhu, Dr. Yihong Wang, Dr. Yufei Yuan, Dr. Kai Yuan, Ms. Zhuo Zhang, Ms. Yingqun Zhang, Dr. Yu Zhang, Ms. Xiaochen Ma, Dr. Mo Zhang, Dr. Yaqing Shu, Ms. Fei Yan, Ms. Wenjing Wang, Dr. Ding Luo, Ms. Rongqin Lu, Mr. Shi Sun, Dr. Bobing Wang, Mr. Zirui Li, Ms. Yuxia Yuan, Dr. Xinwei Wang, Dr. Xiaoxia Xiong, Ms. Haizi Wu, Mr. Ximing Chang, and Dr. Yan Feng, for all the chats, dinners, barbeques, and trips. Many thanks to the secretariat, particularly Ms. Dehlaila Da Costa Ricardo, for practical help and support. Many thanks to Mr. Edwin Scharp for handling the IT-related issues.

I am also grateful to all my teachers for their knowledge and guidance. I must also thank my colleagues from Service Desk, the Graduate School, and Human Resources for practical help and support. Particularly helpful to me was Dr. Wenhua Qu who gave me useful suggestions before I came to Delft. I gratefully acknowledge Nanhu Laboratory for providing working conditions.

Thanks should also go to all my friends, particularly Ms. Yanjiao Liang, Ms. Chunge Kou, Dr. Xiao Li, Dr. Dadi Zhang, Dr. Yunlong Guo, Ms. Lingjun Meng, Mr. Senlei Wang, Mr. Yuxin Liu, Dr. Haopeng Wang, Dr. Xiuxiu Zhan, Dr. Shi Xu, Dr. Jin Chang, Dr. Xiaoya Ma, Dr. Li Wang, Dr. Zhenwu Wang, Dr. Rui Li, Dr. Cong Xiao, Dr. Tiantian Du, Dr. Jian Fang, Dr. Xiang Fu, Ms. Zhaokun Guo, Dr. Baozhou Zhu, and Dr. He Wang, for celebrations, dinners, tours, helping me out, and inspiring me to do everything in an excellent way.

I deeply thank my parents for their love, attention, trust, and encouragement. I wish to thank my uncle, Dr. Shuming Yuan, my aunt, Ms. Hongling Ma, and my sister, Ms. Xi Chen, for their love and support. Thanks also to my aunt, Ms. Meiying Dou, for her attention and encouragement. I thank all my relatives for their attention and help. I also thank my parent-in-law, Ms. Jiaoe Hu, for loving and looking after Ruicheng.

Finally, I thank with love to my husband and son, Dr. Yande Jiang and Ruicheng Jiang. Yande helped me format my thesis and took care of Ruicheng when I was busy. In addition, Yande has consistently accompanied, helped, supported, and encouraged me. Ruicheng has brought love, joy, and happiness into my life. Their accompany and love have given me power.

Na Chen

Delft, November 2021

Contents

List of Figures

List of Tables

Chapter 1

Introduction

This chapter presents the research scope and highlights the main contributions of the thesis. The background of the thesis is first introduced. Then, the existing coordination strategies are briefly presented with a concise literature review and the idea of using model predictive control for trajectory control is described. The research needs, objectives, and contributions are discussed thereafter. Finally, we present the outline of the thesis.

1.1 Background

Highway traffic congestion is a societal problem faced by many countries (van den Broek et al., 2011; Milanés et al., 2011; Xie et al., 2017). It results in excessive travel delays, energy consumption, and carbon dioxide (CO_2) emissions (Skabardonis et al., 2003; Wen et al., 2020; Barth and Boriboonsomsin, 2009). On-ramps on highways are site-specific bottlenecks where mainline and on-ramp vehicles have to interact due to the mandatory lane-changing or merging demand of on-ramp vehicles. The "merging" demand from on-ramp vehicles can cause perturbations to the highway mainline traffic. The perturbations may bring mobility or efficiency loss (e.g. traffic congestion or breakdown) and safety problem (e.g. rear-end, side-swipe, and merge-related collisions) (Hirunyanitiwattana and Mattingly, 2006; McCartt et al., 2004; Jacobson et al., 2006). Improving merging efficiency and safety is vital to improve traffic operations near on-ramps. Traditional traffic management measures for on-ramp control include ramp metering and variable speed limit control (Arnold et al., 1998; Lin et al., 2004). The ramp metering uses traffic lights to regulate the entering of on-ramp vehicles into the merging area. Variable speed limit control regulates mainline traffic speeds to resolve stop-and-go waves. The two measures are extensively studied in the literature to reduce queue, collisions, travel time and delay, and emission and fuel consumption (Lin et al., 2004; Jacobson et al., 2006).

With the emergence of intelligent vehicles, new control approaches can be explored to improve traffic operations near on-ramps. Sensing and communication technologies can enhance intelligent vehicles' situation awareness and enable cooperative control (Wang et al., 2014b). Driving automation systems can fulfill lateral and longitudinal vehicle motion control actions (SAE International, 2021). They are designed to relieve the drivers from the driving tasks and bring ride comfort (Van Arem et al., 2006). With enhanced situation awareness, automated vehicles have the potential to keep smaller inter-vehicle distances, thus potentially improving roadway capacity (Xiao et al., 2018). Thus, they attract the attention of the public, researchers, and traffic operators.

To facilitate the research and implementation of automation in vehicles, SAE international provides a taxonomy for six levels of driving automation: level 0 (no driving automation), level 1 (driver assistance), level 2 (partial driving automation), level 3 (conditional driving automation), level 4 (high driving automation), and level 5 (full driving automation), based on the functionality of the driving automation system feature (SAE International, 2021). For automated vehicles with levels 3 to 5 driving automation, they are expected to accomplish all dynamic driving tasks automatically. Depending on the usage of communication technology to collect ambient traffic information, automated vehicles can be classified into autonomous automated vehicles (AAVs) and connected automated vehicles (CAVs). AAVs,e.g. vehicles equipped with adaptive cruise control in the market (Knoop et al., 2019), solely rely on their onboard sensors to collect surrounding vehicular states and make decisions for themselves without cooperation. Besides using on-board sensors, CAVs, e.g. vehicles equipped with cooperative

adaptive cruise control in the market (Wang et al., 2014b), further improve their situation awareness by exchanging vehicular state and control information with each other via vehicle-to-vehicle (V2V) communication and/or with infrastructure via vehicle-to-infrastructure (V2I) or vehicle-to-everything (V2X) communication. Communication among automated vehicles can maintain smaller inter-vehicle distance without sacrificing traffic stability when lane changing process exists (Van Arem et al., 2006; Ma et al., 2020). Traffic is stable if small changes in the speed of the leading vehicle are attenuated by following vehicles. To this end, CAVs have more potential to improve merging efficiency.

CAVs' impact on traffic operations depends on CAVs' acceptance by drivers and controllers' performance. Figure 1.1 shows the vehicle control structure and the interface between it and the infrastructure control structure. It is constructed by referring to an automated highway system (AHS) control structure (Hedrick et al., 1994; Raza and Ioannou, 1996). The infrastructure control is made up of a network and a link layer. The network layer issues routing instructions and traffic synchronization commands, and provides desired density distributions to the link layer. Based on the received desired density from the network layer and traffic flow measurements from the section, the link layer issues speed and headway commands to vehicles in its section, 1 or 2 kilometers stretch of highway.

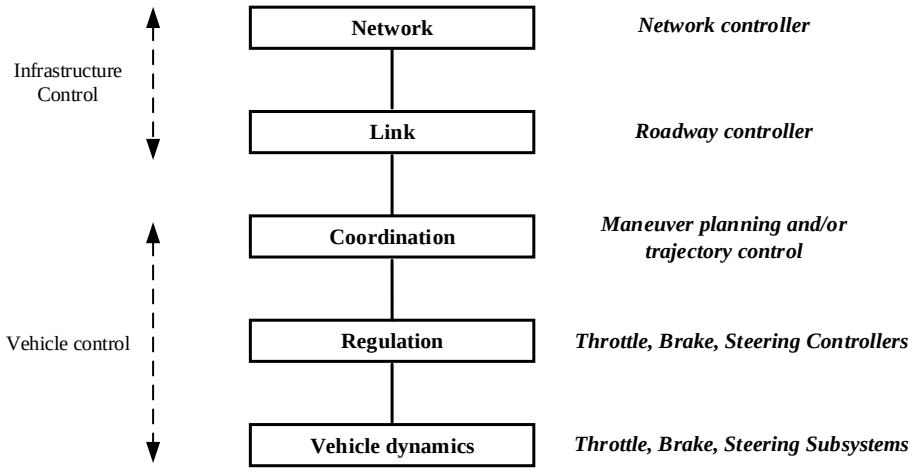

Figure 1.1: Vehicle control structure (Hedrick et al., 1994; Raza and Ioannou, 1996)

The vehicle control consists of three layers: coordination, regulation, and vehicle dynamics layers. The coordination layer communicates with the link layer, other CAVs, and drivers, schedules the desired maneuver of operation, and gives desired acceleration trajectories to the regulation layer. The regulation layer generates appropriate commands to vehicular actuators to follow the planned trajectories with throttle, brake, and steering controllers.

This thesis mainly concentrates on the coordination layer and considers interfaces between the coordination layer and the link and regulation layers. The maneuvers for CAVs include cruising, platooning, cooperative car-following, and lane changing.

1.2 Development of coordination strategies

Figure 1.2 shows a typical on-ramp merging scenario in mixed traffic. On-ramp vehicles travelling in lane 1 need to merge into mainline traffic. Coordination strategies make mainline CAVs facilitate the merging of on-ramp vehicles by generating desired gaps or/and speeds. Which mainline CAV in lane 2 creates a gap for which on-ramp CAV to merge into is represented by a merging sequence. The merging sequence is the specific sequence of vehicles from mainline and on-ramp traffic when passing through the merging area (Ntousakis et al., 2016). Existing coordination strategies for CAVs near on-ramps can be categorized into four groups based on main research focuses and assumptions. The four groups are described in the following subsections.

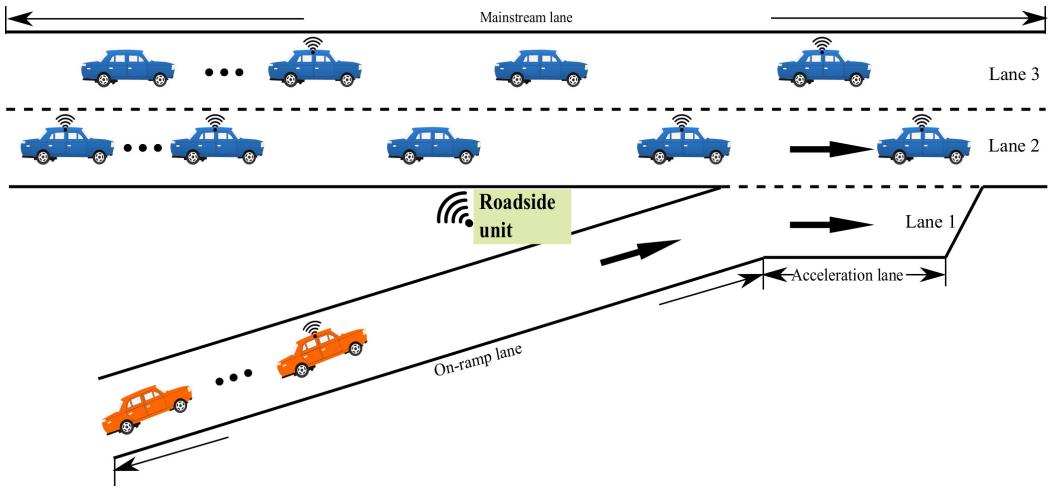

Figure 1.2: Schematic illustration of a typical on-ramp merging scenario in mixed traffic

1.2.1 Coordination strategies to achieve predefined final merging conditions at a fixed merging point

To have safe and efficient merging maneuvers, the design objectives of some coordination strategies are to make both mainline and on-ramp CAVs reach their desired inter-vehicle distances and merging speeds at a fixed merging point, where lateral maneuver is executed to accomplish merging process. The desired inter-vehicle distances can be based on a constant time gap or constant spacing (Xiao et al., 2018). In Wang et al. (2013), a virtual platoon forms by mapping the on-ramp CAV onto the main lane. Accordingly, mainline and on-ramp CAVs regulate their speed trajectories to have a

constant spacing at a fixed merging point, respectively. In Ntousakis et al. (2016), a merging sequence is assumed to be given. Each CAV regulates a longitudinal acceleration trajectory by minimizing the acceleration and its first and second derivatives during the on-ramp merging maneuver, subject to constraints on final vehicle speed and headway at a fixed merging point. Desired inter-vehicle distances are large and safe enough for merging. Noticeably, if the length of the on-ramp lane is short, an on-ramp CAV may not reach its desired inter-vehicle distance with its future preceding vehicle at a predefined merging point.

1.2.2 Coordination strategies to improve traffic operations

Improving traffic operations near on-ramps with CAVs is the control goal of many coordination strategies. They are applied to mainline CAVs or both mainline and on-ramp CAVs by mainly focusing on acceleration regulation. In Zhou et al. (2017), two cooperative rules are proposed for mainline CAVs to react to surrounding vehicles in advance. Mainline CAVs prepare large gaps to facilitate merging of detected on-ramp vehicles in advance, thus reducing travel time. In Scarinci et al. (2015), mainline CAVs act as leaders of different platoons. They are controlled to reduce speeds to create gaps for on-ramp vehicles to merge into, thus reducing the number of late-merging vehicles. In Xie et al. (2017), mainline and on-ramp CAVs are controlled together by a centralized cooperative merging strategy. Acceleration trajectories are regulated by minimizing a weighted sum of minus speeds and standard deviation of accelerations. In Rios-Torres and Malikopoulos (2017a), mainline and on-ramp CAVs are coordinated for a common goal. The goal is to minimize a weighted sum of accelerations and time intervals to enter into a merging zone. Only one CAV is allowed to enter in the merging zone each time to avoid lateral conflicts. In Letter and Elefteriadou (2017), with an assigned vehicle order, each CAV maximizes its average speed. Safe time gaps with the conflict trajectory are kept. Besides, vehicles are not allowed to exceed a predefined merging speed.

In Xie et al. (2017); Rios-Torres and Malikopoulos (2017a); Letter and Elefteriadou (2017), controllers are designed based on model predictive control (MPC) and the generated acceleration trajectories of CAVs lead to small values of the constructed control objectives, respectively. The performance of the MPC controllers is tested by assuming the prediction model used in the controller is the same as the actual vehicle dynamics model of the vehicle system. However, model mismatches may exist between the two models. Model mismatches may deteriorate the performance of the MPC controllers and even lead to string instability (Wang et al., 2016b). A platoon has string instability if the disruption of system states increase over the vehicle number in the platoon (Feng et al., 2019). Attenuating the detrimental influence of the model mismatches on the performance of the MPC controllers is important for practical usages.

1.2.3 Coordination strategies considering merging sequence with a single main lane

Merging sequences matter in improving traffic operations. Merging two conflicting streams of traffic into one is extensively researched, whereas merging sequences have been sparsely addressed (Wang et al., 2013; Ntousakis et al., 2016; Rios-Torres and Malikopoulos, 2017a; Xie et al., 2017; Letter and Elefteriadou, 2017). In Wang et al. (2013), a virtual vehicle is introduced by mapping an on-ramp CAV onto the main lane to form a merging sequence. A given merging sequence is assumed in Ntousakis et al. (2016). A first-in-first-out rule based on locations is used to establish merging sequence in Rios-Torres and Malikopoulos (2017a). In Xie et al. (2017), ramp vehicles are projected onto the main lane using a predefined fixed merging point as the reference. In Letter and Elefteriadou (2017), a merging sequence is scheduled by using vehicles' potential arrival times to a predefined fixed merging point. The aforementioned approaches may not establish optimal merging sequences.

One straightforward way to establish an optimal merging sequence is to evaluate all possible merging sequences with a certain performance indicator. In Athans (1969), given a merging sequence, the acceleration trajectories of vehicles are generated based on optimal control which minimizes CAVs' deviations to their desired states, including relative speed to the future directly preceding vehicle, acceleration, and gap error. The gap error is the difference between the actual gap and the desired gap. All merging sequences are then evaluated to choose the optimal one that brings the minimal value of the control objective. In Awal et al. (2013), feasible and prospective merging sequences are chosen by using estimated times of CAVs to reach a fixed merging point at a decision-making point. With a given merging sequence, CAVs utilize a traffic model which considers several vehicles ahead to generate speed. The chosen merging sequences are then evaluated to find the optimal one that brings minimal merging delay. Another way is to choose sub-optimal merging sequences by considering final desired or assumed vehicular states at a merging point. In Zhao et al. (2018), CAVs' minimum arrival times at an intersection are calculated by assuming that they accelerate to their maximum speed and keep the maximum speed to pass through the intersection, respectively. A CAV's maximum arrival times are calculated based on whether it can stop at the stop line with its maximum deceleration. If it cannot stop, its maximum arrival time is calculated based on its initial speed, distance to the stop line, and the maximum deceleration; otherwise, it is given the minimal arrival time plus a maximum delay. An upper-level optimization dynamically establishes merging sequences by minimizing the total travel time, subject to the minimal and maximum arrival times of CAVs, and safe entering and exiting time headway between consecutive vehicles. A lower-level optimization follows the decisions of the upper-level optimization and maximizes total vehicular speeds to generate acceleration trajectories for CAVs. In Duret et al. (2019), CAVs are assumed to maintain their free-flow speed between their initial positions and a merging position; and the final formed platoon settles down to equilibrium at the merging position. Thus the natural ordered sequence is achieved

by projecting vehicles' initial positions with the maximum speed along a shock wave starting from the merging point. An operational layer controller is designed based on MPC. It regulates acceleration trajectories of CAVs by minimizing a weighted sum of predicted headway errors, relative speeds to the directly preceding vehicles, and accelerations. A headway error is the deviation between the actual headway and the desired headway.

In summary, in Athans (1969) and Awal et al. (2013), future detailed trajectory planning approaches are utilized in seeking optimal merging sequences. In Zhao et al. (2018) and Awal et al. (2013), two-layer hierarchical control approaches are adopted. Higher layers establish merging sequences by making vehicles pass through conflict areas as quickly as possible; and lower layers regulate acceleration trajectories to reach maximum speeds or desired states. The merging sequences are established considering initial and vehicular states and cooperative merging processes start immediately. On-ramp CAVs are not given chances to travel to their desired speeds for certain time periods to create large inter-vehicle distances or small speed deviations for merging preparation.

1.2.4 Coordination strategies considering merging sequence with multiple main lanes

When CAVs drive in multiple main lanes near on-ramp merging areas, the majority of cooperative merging strategies prohibit mainline CAVs to change lane. Only few studies allow mainline CAVs to change lane to facilitate on-ramp merging. In Hu and Sun (2019), an on-ramp merging area with two main lanes is divided into a cooperative lane changing region and a cooperative merging region. In the cooperative lane changing region, a rule-based lane changing decision is applied to adjust upstream lane flow distribution so that downstream vehicle volume for the two main lanes after merging is balanced. The decision gives lane changing proportion of CAVs in the outer main lane. The mainline CAVs in the outer main lane are then randomly selected to change lane based on the proportion and all CAVs' acceleration trajectories are generated by maximizing the total speeds inside the lane changing region. In the cooperative merging region, each vehicle is controlled to maximize its speed, subject to safe inter-vehicle distance with the conflict trajectory and speed, acceleration, and jerk constraint. In Ding et al. (2021), an on-ramp merging area with two main lanes is divided into an induction zone and a merging zone. In the induction zone, the lane changing decisions for mainline CAVs in the outer main lane are given by maximizing the deviation between the saved time of on-ramp CAVs and the total delay caused by lane changing of mainline CAVs. In the merging zone, on-ramp CAVs use the first-in-first-out principle to merge into the mainline traffic. The upper and lower bound of an on-ramp CAV's time window for merging are roughly estimated based on its initial speed, position, and the predefined merging speed, and a set maximum waiting time. All on-ramp CAVs' arrival times are scheduled together by minimizing the total delay

caused to the mainline CAVs in the outer main lane. In Hang et al. (2021), a game theoretical approach is utilized to generate each vehicle's longitudinal acceleration. It minimizes a cost function which is constructed based on predicted vehicular states. During on-ramp merging, an on-ramp vehicle, its following vehicle in the adjacent lane, and the following vehicle's follower in another main lane play a coalitional game to check whether their overall cost can be reduced without sacrificing each vehicle's benefit.

The approaches in Hu and Sun (2019) and Ding et al. (2021) separate lane changing of mainline CAVs from merging of on-ramp CAVs into two regions. The lane changing behaviors of mainline CAVs are restricted in upstream predefined areas. In Hang et al. (2021), at most 3 vehicles are considered and their relative positions are restricted. The possibility for mainline CAVs to facilitate on-ramp merging by changing lane is restricted.

1.3 Research needs

The thesis is motivated by the following research needs:

N1 ***Robustness with respect to the mismatch between vehicle dynamics and coordination strategies models:*** A large model mismatch between vehicle dynamics and prediction models may deteriorate the performance of MPC controllers. Ensuring controllers' robustness is important and is a valuable research direction. A robust controller can maintain stability and an acceptable performance level in the presence of bounded modelling errors. However, the robustness of MPC coordination methods is rarely checked or researched.

N2 ***Safe lane changing condition not based on final desired inter-vehicle distances and speeds:*** Reaching desired inter-vehicle distances and zero relative speeds with preceding vehicles can ensure safe merging. In crowded traffic or with a short on-ramp lane, an on-ramp CAV may not reach its desired inter-vehicle distances with its future preceding and following vehicles when it arrives at a predefined merging point. In this case, how can the on-ramp CAV still join the mainline traffic safely? What are the safe inter-vehicle distances for the on-ramp CAV to change lane? These two questions need to be answered to check whether safe lane changing conditions can be relaxed without adhering to the desired inter-vehicle distances. Besides, after safe merging conditions are met, a driver is expected to take over and accomplish the lane changing maneuver in the literature. It is necessary to propose advanced cooperative merging strategies which allow on-ramp CAVs to accomplish merging automatically without the intervention of drivers.

N3 ***Optimal merging sequence planning:*** Merging sequence of two conflicting streams of traffic matter in improving merging efficiency. The optimal merging sequence is the best merging sequence based on a certain performance indicator. Whereas, how to

select the optimal merging sequence regarding traffic operations is rarely answered. Besides, some on-ramp CAVs may enter into the on-ramp lane or a control zone with low speeds when they are assigned merging sequences, respectively. Is it beneficial to make them accelerate to increase their speeds first before guiding them to their target slots?

N4 ***Cooperative merging control approach allowing mainline CAVs to change lane:*** Allowing mainline CAVs to change lane to facilitate on-ramp merging improves merging efficiency. Nevertheless, for on-ramp merging sections with multiple mainstream lanes, the majority of the existing cooperative merging strategies prohibit mainline vehicles to change lane. The state-of-the-art merging strategies that allow mainline CAVs to change lane constrain their lateral maneuver in a divided zone or allow at maximum two mainline CAVs to have this choice. It is valuable but challenging to systematically explore how a mainline CAV change lane helps to improve traffic operations.

1.4 Research objectives

The objective of this thesis is ***to design coordination strategies for CAVs near on-ramps considering controller performance, safe lane changing, maneuver planning, and trajectory control***. The main objective is broken into four sub-objectives which address the four research needs, respectively.

The first sub-objective is to develop a robust platooning control method. It mainly focuses on longitudinal coordination of CAVs.

The second objective is to develop a cooperative merging strategy which allows on-ramp CAVs to merge before they reach their desired inter-vehicle distances to preceding vehicles and their desired speeds, and assists CAVs to accomplish merging automatically. A merging sequence is assumed to be given.

The third objective is to develop a cooperative merging strategy which uses a new approach to seek the optimal merging sequence and regulates CAVs' lateral and longitudinal trajectories to accomplish merging. On-ramp CAVs are given chances to adjust their positions or speeds before being coordinated with mainline CAVs to prepare for merging.

The final one is to develop a cooperative merging strategy which allows mainline CAVs to change lane to facilitate the merging process of on-ramp CAVs. It establishes the dynamic optimal vehicle sequences in each lane and control acceleration trajectories for CAVs.

1.5 Research approach

Our designs are based on some assumptions and considerations. Firstly, we assume a small but representative on-ramp network (See Figure 1.2) on motorways throughout the thesis. Secondly, CAVs are assumed to be with level 4 driving automation. Finally, we are not studying the acceptance and comfort of CAVs, although smoothness of acceleration and comfort are taken into account in our proposed strategies.

Two types of traffic environment are considered by this thesis: a 100% CAV environment and mixed traffic. The 100% CAV environment merely has CAVs. For mixed traffic, CAVs coexist with human-driven vehicles.

Our four sub-objectives are consecutively addressed (See Figure 1.3) by designing four different coordination strategies for CAVs. Those four merging strategies mainly focus on different aspects, which are shown above and below the corresponding squares in Figure 1.3, and build on each other as illustrated by arrows.

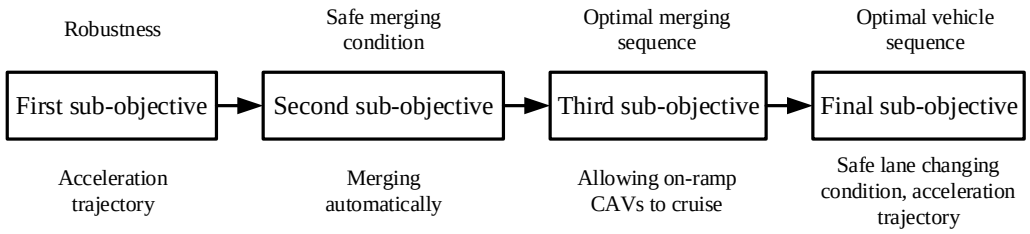

Figure 1.3: Research steps for the thesis

The first sub-objective is addressed in Chapter 2. A robust MPC approach is presented to coordinate acceleration trajectories of CAVs in homogeneous and heterogeneous platoons. In a homogeneous platoon, all vehicles are CAVs. A heterogeneous platoon comprises CAVs and human-driven vehicles. For a human-driven vehicle in a platoon, it can not be controlled but can be affected by surrounding CAVs' movement. Its behavior is roughly predicted with a car following model, intelligent driver model plus (IDM+). The vehicle dynamics model is assumed to have parametric uncertainties. As a result, it can be different from the nominal prediction model, which does not consider uncertainty, of nominal MPC. The robust MPC approach regulates acceleration trajectories of CAVs by minimizing the maximum value of a cost function brought by model uncertainties. The cost function is a weighted sum of predicted deviation from desired gap, deviation from directly predecessor's speed or desired speed, and accelerations of each vehicle in the controlled platoon in a future horizon. The optimal acceleration trajectories are computed in a receding horizon way based on the updated vehicular states. String stability is selected as a performance indicator. A fixed feedback delay is considered in simulation experiments.

A human-like coordination strategy is developed in Chapter 3 to address the second sub-objective. It is designed based on MPC. A merging sequence is assumed to be

given. Longitudinal accelerations of CAVs are generated by minimizing the same cost function as that in Chapter 2. A prediction-based safe lane changing condition is given. An on-ramp CAV turns left to the mainline traffic if it is in the acceleration lane and its time gaps with surrounding vehicles are larger than an accepted time gap for merging in a future horizon. Like human drivers, the accepted time gap for merging decreases as the on-ramp CAV approaches the end of the acceleration lane. Besides, it follows a human-like trajectory equation to accomplish lateral maneuver automatically. No collision is selected as a performance indicator.

A hierarchical control approach is proposed in Chapter 4 to address the third sub-objective. A tactical layer controller schedules optimal merging sequences for two conflicting traffic streams by solving a model-based optimization problem in a long future horizon. The same cost function as that in Chapter 2 is minimized. Future vehicles' behavior during merging is estimated by using surrogate linear models of real vehicle trajectories regulated by an operational layer controller. During the process, on-ramp vehicles are allowed to cruise for several seconds. The operational layer controller is designed based on MPC. It regulates acceleration trajectories by minimizing the same cost function as that in Chapter 2. The prediction-based merging condition and accepted time gaps for merging in Chapter 3 are used to determine lane change initiation times for on-ramp CAVs. The first-in-first-out merging rule is chosen in comparison with the tactical layer controller in scheduling merging sequences.

To address the final sub-objective, we extend the hierarchical control approach in Chapter 4 to allow mainline CAVs to change lane in Chapter 5. A uniform surrogate of real vehicle trajectories regulated by an operational controller is constructed to predict future cruising, car-following, and cooperative lane changing maneuvers of vehicles in the merging process. A planner Dynamic schedules vehicle sequence in each lane by minimizing predicted disturbances reflected by negative acceleration to upstream traffic in a long horizon. The operational controller is designed based on MPC. It regulates longitudinal trajectories for CAVs in each lane by minimizing the same cost function as that in Chapter 2. A mainline lane changer changes lane when its current and predicted time gaps with surrounding vehicles are larger than a predefined value. The safe merging condition in Chapter 3 is used for on-ramp CAVs. Besides, the operational controller gives the lane change initiation time instants for lane changers based on the current and predicted vehicular states. The first-in-first-out merging rule is chosen in comparison with the planner controller in scheduling vehicle sequences.

In chapter 5, we choose to use the first-in-first-out merging rule to establish merging sequences for comparison instead of the approach used in Chapter 4 because of two reasons. One is that the first-in-first-out merging rule is widely used. The other is that the tactical layer controller in Chapter 4 chooses a different objective function from the planner in Chapter 5. By using the same comparison method, we can check whether optimizing different objective functions lead to different optimal merging sequences or vehicle sequences.

1.6 Contributions

This thesis makes contributions to guarantee controller performance, safe merging conditions, as well as the longitudinal and lateral maneuver control of CAVs near on-ramps. The scientific and practical contributions of the thesis are highlighted below.

1.6.1 Scientific contributions

We present *a robust platooning control approach* (Chapter 2). A robust Min-Max MPC controller is proposed. The controller ensures the robustness of string stability and performance against parametric uncertainties of vehicle dynamics model and feedback delay. It can be used for platooning control in both the 100% CAV environment and mixed traffic.

A prediction-based safe lane changing condition is designed (Chapter 3). A CAV is allowed to accept smaller time gaps than its desired value for merging while it is approaching the end of the acceleration lane. It changes lane on the acceleration lane when its predicted time gaps are all larger than the accepted value in a control time horizon. The designed lane changing condition does not sacrifice traffic efficiency for safety.

A new approach to generate optimal merging sequence for two conflicting streams of traffic is proposed (Chapter 4). Instead of repeating future detailed merging process exhaustively, two surrogate linear models of real vehicle trajectories regulated by an operational layer controller are utilized to represent interactions among CAVs during merging. The optimal merging sequence is established by minimizing a constructed control objective based on the predicted vehicular states in a long time horizon. During the process, an on-ramp CAV is allowed to travel with its desired speed for a short time period before preparing itself to move to the target slot.

A hierarchical cooperative merging control approach allowing mainline CAVs to change lane for facilitating on-ramp merging is proposed (Chapter 5). Mainline CAVs can change lane at any location. All CAVs' maneuvers are planned together to improve traffic operations. Besides, acceleration trajectories are controlled in a centralized way. No transition is needed between lane changing and merging facilitating process. We discuss under which conditions mainline CAVs may be instructed to change lane and analyze the correlation between lane changers' lane change time instants.

1.6.2 Practical contributions

Our proposed robust control approach can support CAV developers to develop robust controllers and road operators and public authorities to assess under which conditions the developed CAVs can be admitted.

Our designed prediction-based lane changing condition serves as a basis to develop lane changing strategies that do not sacrifice traffic efficiency for safety and safe lane changing conditions in mixed traffic.

Our proposed approaches to generate optimal merging or vehicle sequences can be used by researchers when they mainly focus on longitudinal acceleration regulation for CAVs. Besides, they are supported to design new cooperative merging strategies. Traffic operators are given recommendations on using the first-in-first-out merging rule to have optimal or sub-optimal merging sequences. Those recommendations are based on the decisions of our proposed new approach to generating optimal merging sequences for two streams of traffic.

1.7 Outline of the dissertation

Figure 1.4 illustrates the outline of the thesis. It consists of 6 chapters. The lines with arrows depict the relationship between the chapters. Chapter 1 introduce the research objectives and highlights the main contributions. The following four chapters address sub-objectives proposed in Section 1.4, respectively.

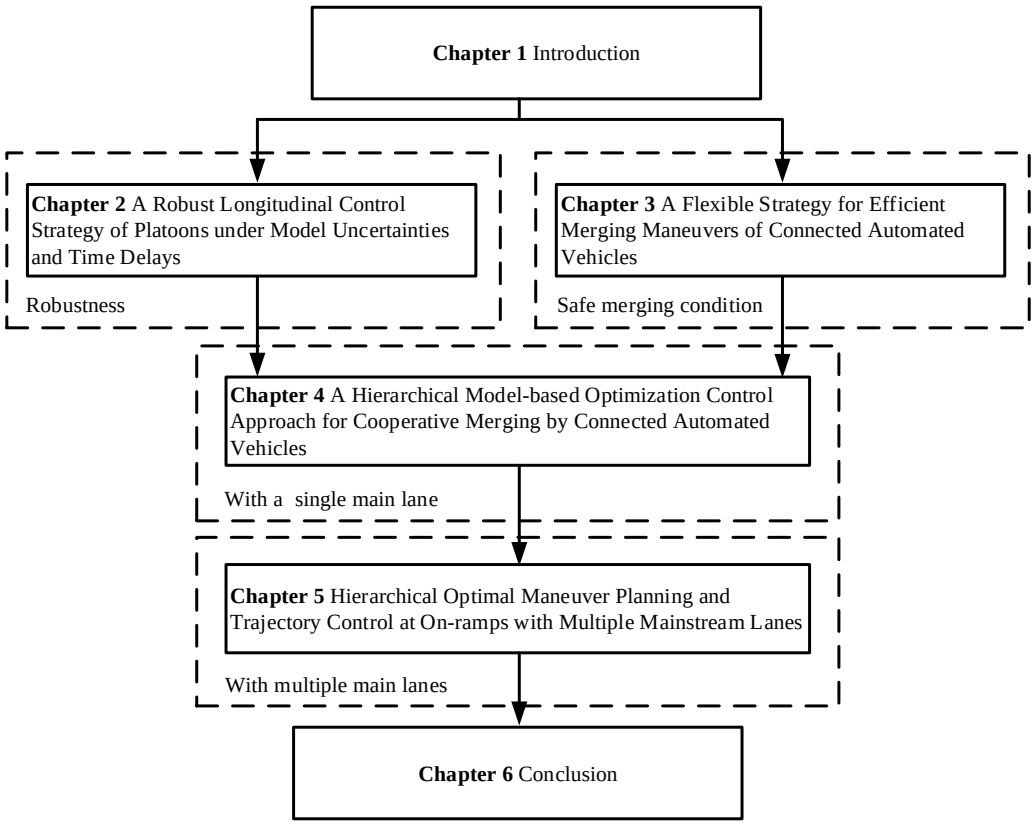

Figure 1.4: The outline of the thesis

Chapter 2 deals with a robust platooning control approach. A robust Min-Max MPC controller is developed. It is robust to keep string stability.

In chapter 3, we present a prediction-based merging condition. It supports on-ramp CAVs to change lane safely before it reaches its desired inter-vehicle distance to its future directly preceding vehicle and speed. Besides, it is controlled to accomplish on-ramp merging automatically without the intervention of drivers.

Chapter 4 designs a hierarchical control approach for the cooperative merging of CAVs. An upper-level controller schedules an optimal merging sequence for two conflicting streams of traffic and time instants for on-ramp CAVs to be coordinated together with mainline CAVs for merging. A lower-level controller regulates longitudinal acceleration trajectories and time instants for on-ramp CAVs to change lane.

Chapter 5 proposes a hierarchical cooperative merging control approach to allow mainline CAVs to change lane to facilitate on-ramp merging. An upper-level controller plans dynamic optimal vehicle sequences in each lane in a long time horizon. A lower-level controller generates longitudinal acceleration trajectories and time instants for lane changers to change lane.

Chapter 6 summarizes the main findings and gives future research directions.

Chapter 2

A robust longitudinal control strategy of platoons under model uncertainties and time delays

This chapter addresses the first sub-objective. We design a robust and flexible platooning control strategy for CAVs. Ignoring time delays and model uncertainties may render the performance of cooperative driving systems unsatisfactory or even unstable. We present a centralized control method, where the leader of a CAV platoon collects information from followers, computes the desired accelerations of all controlled vehicles, and broadcasts the desired accelerations to followers. The robust platooning is formulated as a Min-Max Model Predictive Control problem, where optimal accelerations are generated to minimize the cost function under the *worst case*, where the worst case is taken over the possible models. The proposed method can be applied to both homogeneous platoon and heterogeneous platoon with mixed human-driven and automated controlled vehicles. A third-order linear vehicle model with fixed feedback delay and stochastic actuator lag is used to predict the platoon behavior. Actuator lag is assumed to vary randomly with unknown distributions but a known upper bound. The designed strategy is tested by simulating homogeneous and heterogeneous platoons in a number of typical and extreme scenarios to assess the system stability and performance. The test results demonstrate that the designed control strategy for CAV can ensure stability and the robustness of performance against model uncertainties and feedback delay and outperforms the deterministic MPC based platooning control.

This chapter is an edited version of the article:

Chen, N., Wang, M., Alkim, T., and Van Arem, B., "A robust longitudinal control strategy of platoons under model uncertainties and time delays", *Journal of Advanced Transportation*, vol. 2018, Article ID 9852721, 13 pages, 2018. https://doi.org/10.1155/2018/9852721

2.1 Introduction

Today's traffic systems are facing serious congestion (Ghasemi et al., 2015). Automated vehicles using advanced sensing, communication and control technologies have the potential to increase road capacity and improve traffic operations (Van Arem et al., 2006; Dey et al., 2016; Wang et al., 2016a). Adaptive cruise control (ACC) systems has already entered the market (VanderWerf et al., 2001; Xu and Sengupta, 2003; Naus et al., 2010). An automated vehicle equipped with ACC uses its on-board sensors to detect the ambient environment and regulates its speeds to increase ride comfort. Vehicle-to-vehicle and vehicle-to-infrastructure communications extend the visibility of automated vehicles and enable the so-called connected automated vehicles (Rios-Torres and Malikopoulos, 2017b). When a group of CAVs travel with short inter-vehicle headways or gaps, a platoon is formed (Li et al., 2016). CAVs have more potential to improve traffic performance compared to individual automation, since they can share information and coordinate their behavior to ensure shorter inter-vehicle distances safely as demonstrated by field tests (Van Arem et al., 2006; Tak et al., 2016; Wang et al., 2014a; Michaud et al., 2006; Milanés et al., 2014). With V2I communication between a road side device and electric vehicles, the traffic stability can be improved with CAVs (Li et al., 2018).

The successful implementation of platooning entails to address some challenges, including feedback delay, actuator lag, measurement inaccuracy and heterogeneity in traffic (Naus et al., 2010; Jin and Orosz, 2014; Wang et al., 2016b; Xiao and Gao, 2010). Feedback delay and actuator lag are known to have detrimental effects on string stability (Xiao and Gao, 2010; Wang et al., 2016b). Control approaches using platoon leader or predecessor acceleration as feedforward term can compensate delay (Öncü et al., 2014; Jin and Orosz, 2014; Ghasemi et al., 2015). Another delay compensation strategy is based on a predictive control approach (Wang et al., 2016b). Measurement noise can be handled by using filtering and data fusion techniques (Ryu and Gerdes, 2004). The heterogeneity of traffic can be considered by using cooperative control strategies where a joint objective is optimized within the platoon (Wang et al., 2014b).

Although different methods have been proposed to address the aforementioned challenges, most of them are based on deterministic modeling of vehicle system dynamics and have not been tested systematically against uncertainties. There is no guarantee that existing platooning control systems generate satisfactory performance with model uncertainties. An adaptive fuzzy sliding mode control approach is proposed to deal with the model uncertainties, and functional approximation technique is employed to replace the unknown vehicle functions (Guo et al., 2017). However, the reliability of using functional approximation technique is not clear. Besides, vehicle speeds can be adjusted through electronic throttle (ET) control. With V2V communication, the opening angle of the ET of the preceding vehicle is available. The following vehicle then adjusts adaptively its ET to avoid collision and follow the speed of the preceding

vehicle. Using extended state observer to estimate the change of throttle opening angel and total disturbance, a double-loop integral sliding-mode controller for electronic throttle is designed (Li et al., 2015). This controller has robustness to parametric uncertainties of the ET model. An H-infinity control method for a CAV platoon is proposed considering the uncertain vehicle dynamics (Gao et al., 2016). The robust control is designed considering the differences among dynamics for CAVs in the platoon. The feasibility of this control method to a heterogeneous platoon comprised of CAVs and human-driven vehicle is not given. The robust control for the CAV platooning control has not fully explored.

The objective of this chapter is to design a robust controller considering the model uncertainties involved in the longitudinal vehicle dynamics. The robust control is designed by considering the parametric uncertainties in the dynamics model of platoons expressed by a third-order linear vehicle model. The robust platooning is then formulated as a Min-Max Model Predictive Control (MM-MPC) problem, where optimal desired accelerations are generated to minimize the cost function under the *worst case*. The controller regulates platoon desired accelerations over a time horizon to minimize the cost function representing driving safety, efficiency and ride comfort, subject to speed limits, plausible desired acceleration range and minimal net spacing. The designed control strategy is flexible in such a way that it can be applied to the homogeneous platooning control where all the vehicles in the controlled platoon are CAVs and the heterogeneous platooning control where CAVs and human-driven vehicles are mixed.

The remaining of the chapter is organized as follows. We will first introduce longitudinal dynamics models for a CAV, homogeneous and heterogeneous platoons with CAVs. The proposed robust MM-MPC controllers for a single homogeneous and heterogeneous CAV platoon are presented separately. After that, the simulation experiments are designed to verify the performance of the controllers followed by the discussion of the simulation results of the CAV platoons under different control strategies. Finally we conclude the findings and present future research directions.

2.2 Dynamics models

This section presents a longitudinal vehicle dynamics model for state prediction for a single CAV and CAV platoon dynamics model considering actuator lag.

2.2.1 Single vehicle dynamics model

We introduce a longitudinal dynamics model for a single vehicle n, following an exogenous head vehicle, with x_n, v_n, a_n and l_n denoting the location, speed, actual acceleration and vehicle length of the subject vehicle n. For a single CAV n, the system

state $\mathbf{Z}$ is described by the gap error Δs, relative speed Δv_n to the preceding vehicle $n-1$, and a_n, i.e. $\mathbf{Z} = (\Delta s_n, \Delta v_n, a_n)^T$, and the control variable is defined as $\mathbf{U} = u_n$, where u_n is the desired acceleration given to vehicle n. Δs_n is the deviation between the real gap/net spacing $s_n = x_{n-1} - x_n - l_n$ and the desired gap s_n^d to vehicle $n-1$, i.e. $\Delta s = s_n - s_n^d$. We employ the Constant Time Gap (CTG) policy that is the frequently used by researchers and largely used in the commercial ACC systems to determine the desired gap (Wang et al., 2014a), i.e. $s_n^d = v_n \cdot t^d + s_0$, where t^d is the desired time gap and s_0 is the minimum gap at stand still. For simplicity, the time argument is dropped.

A third-order model (Equation (2.1)) is used to express the longitudinal dynamics model for vehicle n (Wang et al., 2016b; Liang and Peng, 1999). The system dynamics is then described by Equation (2.2).

$$\dot{x}_n = v_n; \quad \ddot{x}_n = a_n; \quad \dddot{x}_n = \frac{1}{\tau_n^A} \cdot (u_n - \ddot{x}_n) \tag{2.1}$$

where, τ_n^A denotes the engine time lag for the nth vehicle.

$$\frac{d}{dt}\mathbf{Z} = \frac{d}{dt}\begin{pmatrix} x_{n-1} - x_n - l_n - s_n^d \\ v_{n-1} - v_n \\ a_n \end{pmatrix} = \begin{pmatrix} v_{n-1} - v_n - a_n \cdot t^d \\ a_{n-1} - a_n \\ \frac{u_n - a_n}{\tau_n^A} \end{pmatrix} = \mathbf{f}(\mathbf{Z}, \mathbf{U}, \mathbf{d}) \tag{2.2}$$

where,

$$A = \begin{bmatrix} 0 & 1 & -t^d \\ 0 & 0 & -1 \\ 0 & 0 & -\frac{1}{\tau_n^A} \end{bmatrix}; B = \begin{bmatrix} 0 \\ 0 \\ \frac{1}{\tau_n^A} \end{bmatrix}; C = \begin{bmatrix} 0 \\ 1 \\ 0 \end{bmatrix}; \mathbf{d} = a_{n-1}$$

$\mathbf{d}$ denotes the exogenous disturbance to the vehicle system, which is the actual acceleration of the preceding vehicle $n-1$. If the preceding vehicle is a CAV, the subject vehicle will receive a_{n-1} via V2V communication. When using the V2V communication to obtain the value of $\mathbf{d}$ is not feasible, the disturbance can be modeled using $a_{n-1} = 0$, i.e. the vehicle $n-1$ is assumed to travel at the same detected speed in the prediction horizon (Wang et al., 2016b).

2.2.2 Homogeneous platoon dynamics model

For a homogeneous CAV platoon (e.g. Figure 2.1(a)) with $N \geq 2$ vehicles, the system state variable is defined as $\mathbf{Z}^P = (\Delta s_1, \Delta v_1, a_1, \Delta s_2, \Delta v_2, a_2, \cdots, \Delta s_N, \Delta v_N, a_N)^T$, the command variable is defined as $\mathbf{U}^P = (u_1, u_2, \cdots, u_N)^T$, and the disturbance is defined as $\mathbf{d}^P = \mathbf{a_p}$, where $\mathbf{a_p}$ is the exogenous head vehicle of the platoon. For each of the vehicle in the homogeneous CAV platoon, the single CAV dynamics model can be applied. Thus the matrix-form system dynamics model for a CAV platoon with N vehicles can be expressed with:

$$\frac{d}{dt}\mathbf{Z}^P = \frac{d}{dt}(\Delta s_1, \Delta v_1, a_1, \Delta s_2, \Delta v_2, a_2, \cdots, \Delta s_N, \Delta v_N, a_N)^T = \mathbf{g}(\mathbf{Z}^P, \mathbf{U}^P, \mathbf{d}^P) \tag{2.3}$$

$$\mathbf{g}(\mathbf{Z}^P, \mathbf{U}^P, \mathbf{d}^P) = A^P \cdot \mathbf{Z}^P + B^P \cdot \mathbf{U}^P + C^P \cdot \mathbf{d}^P \tag{2.4}$$

where,

$$A^P = \begin{bmatrix} A_1^{3\times3} & 0^{3\times3} & \cdots & 0^{3\times3} \\ 0^{3\times2} & A_2^{3\times4} & \cdots & 0^{3\times3} \\ \vdots & \vdots & \ddots & \vdots \\ 0^{3\times2} & 0^{3\times3} & \cdots & A_N^{3\times4} \end{bmatrix}; B^P = \begin{bmatrix} B_1 & & \mathbf{0} \\ & \ddots & \\ \mathbf{0} & & B_N \end{bmatrix}; C^P = \begin{bmatrix} C & \mathbf{0} \\ \mathbf{0} & \mathbf{0} \end{bmatrix};$$

$$A_1^{3\times3} = \begin{bmatrix} 0 & 1 & -t^d \\ 0 & 0 & -1 \\ 0 & 0 & -\frac{1}{\tau_1^A} \end{bmatrix}; A_i^{3\times4} = \begin{bmatrix} 0 & 0 & 1 & -t^d \\ 1 & 0 & 0 & -1 \\ 0 & 0 & 0 & -\frac{1}{\tau_i^A} \end{bmatrix}, i = 2,3,\cdots,N;$$

$$B_k = \begin{bmatrix} 0 \\ 0 \\ \frac{1}{\tau_n^A} \end{bmatrix}, k = 1,2,\cdots,N.$$

2.2.3 Heterogeneous platoon dynamics model

When a platoon is comprised of a CAV(s) and a human-driven vehicle(s), a heterogeneous platoon is formed. A heterogeneous CAV platoon is given as shown in Figure 2.1(b). For this platoon, the state and control variables can be defined as $\mathbf{Z}^{HP} = (\Delta s_1, \Delta v_1, a_1, \Delta s_2, \Delta v_2, \Delta s_3, \Delta v_3, a_3, \Delta s_4, \Delta v_4)^T$ and $\mathbf{U}^{HP} = (u_1, u_3)^T$, and the exogenous disturbance is $\mathbf{d}^{PH} = (a_p, a_2, a_4)^T$. For the human-driven vehicles, the actual accelerations cannot be controlled directly but can be calculated using a car-following model. We use IDM+ to model the collision-free car-following behavior as expressed with Equation (2.5) and Equation (2.6), where α is the maximum acceleration, b is the desired deceleration, and s^* is the dynamic desired headway (Schakel et al., 2012; Treiber et al., 2000). To this end, the dynamics model of the heterogeneous platoon is as shown in Equation (2.7) and Equation (2.8).

$$\frac{dx}{dt} = v, \frac{dv}{dt} = a \tag{2.5}$$

$$\frac{dv}{dt} = \alpha \cdot \min[1 - (\frac{\mathrm{v}}{\mathrm{v}_0})^4, 1 - (\frac{\mathrm{s}^*(\mathrm{v}, \Delta\mathrm{v})}{\mathrm{s}})^2] \tag{2.6}$$

where,

$$s^*(v, \Delta v) = \frac{s_0 + v \cdot T - v \cdot \Delta v}{2 \cdot \sqrt{\alpha \cdot b}}$$

$$\frac{d}{dt}\mathbf{Z}^{HP} = \frac{d}{dt}(\Delta s_1, \Delta v_1, a_1, \Delta s_2, \Delta v_2, \Delta s_3, \Delta v_3, a_3, \Delta s_4, \Delta v_4)^T = \mathbf{h}(\mathbf{Z}^{HP}, \mathbf{U}^{HP}, \mathbf{d}^{HP}) \tag{2.7}$$

$$\mathbf{h}(\mathbf{Z}^{HP},\mathbf{U}^{HP},\mathbf{d}^{HP}) = A^{HP}\cdot\mathbf{Z}^{HP} + B^{HP}\cdot\mathbf{U}^{HP} + C^{HP}\cdot\mathbf{d}^{HP} \tag{2.8}$$

where,

$$A^{HP} = \begin{bmatrix} A_{n=1} & 0^{3\times2} & 0^{3\times3} & 0^{3\times2} \\ 0^{2\times2} & D^{2\times3} & 0^{2\times3} & 0^{2\times2} \\ 0^{3\times2} & 0^{3\times3} & A_{n=3} & 0^{3\times2} \\ 0^{2\times2} & 0^{2\times3} & 0^{2\times2} & D^{2\times3} \end{bmatrix}; B^{HP} = \begin{bmatrix} 0^{2\times1} & 0^{2\times1} \\ \frac{1}{\tau_1^A} & 0 \\ 0^{4\times1} & 0^{4\times1} \\ 0 & \frac{1}{\tau_3^A} \\ 0^{2\times1} & 0^{2\times1} \end{bmatrix};$$

$$C^{HP} = \begin{bmatrix} C & 0^{3\times1} & 0^{3\times1} \\ 0^{2\times1} & E & 0^{2\times1} \\ 0^{3\times1} & C & 0^{3\times1} \\ 0^{2\times1} & 0^{2\times1} & E \end{bmatrix}; D = \begin{bmatrix} 0 & 0 & 1 \\ 1 & 0 & 0 \end{bmatrix}; E = \begin{bmatrix} -T \\ -1 \end{bmatrix}$$

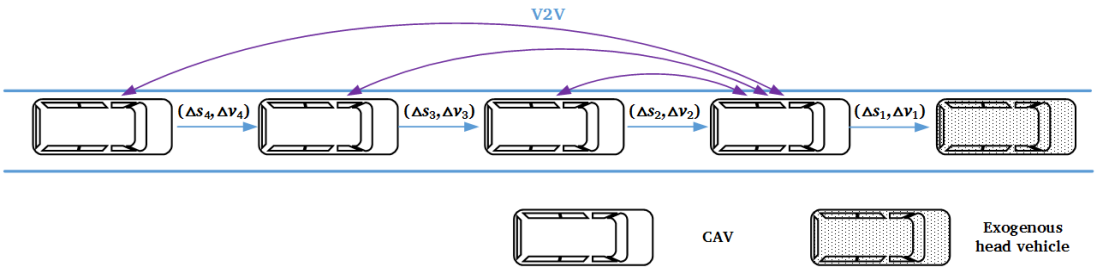

(a) A homogeneous platoon

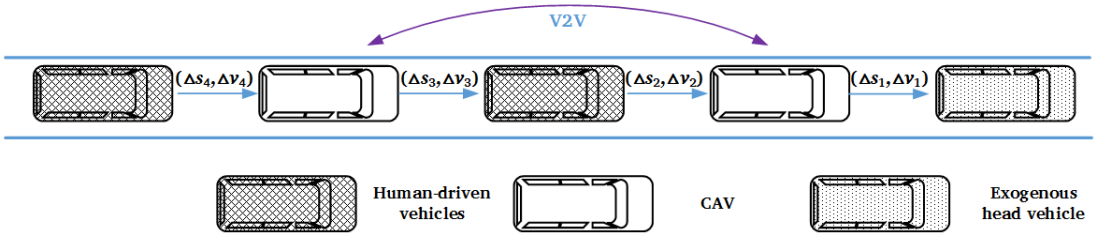

(b) A heterogeneous platoon

Figure 2.1: The platooning formations

2.3 Design of robust controller for platoon operation

In this section we develop a robust controller to determine the control command by minimizing a running cost function.

2.3.1 Design assumptions

The homogeneous platooning controller is designed based on the following assumptions:

- The CAVs are homogeneous. They have the same vehicle length, desired acceleration boundary, speed limits and variable actuator lag.
- The accurate feedback information on positions, speeds and actual accelerations of controlled vehicles can be obtained via on-board sensors and V2V communication, but are subject to a fixed feedback delay τ^S. The received state at time t is actually measured at time $t-\tau^S$ (Wang et al., 2016b). As a result of the feedback delay, the initial condition of the system state is not accurate.
- The controller updates the control command at regular time intervals.
- The CAVs are subjected to the stochastic actuator lag $\tau^A(t)$, with $\tau^A(t) \in [\alpha, \beta]$, $(0 < \alpha < \beta)$ (Jia and Ngoduy, 2016; Rajamani and Shladover, 2001).

2.3.2 Platooning control formulation

Min-Max model predictive control problem

There are several paradigms for robust control of linear systems: H_2, H_∞, "multi-model" paradigm and "linear system with a feedback uncertainty" paradigm (Kothare et al., 1996; Duan et al., 2006). For linear systems as in Equation (2.4), the "multi-model" paradigm works by discovering different linearly independent combination of $[A^P\ B^P]$. The "linear system with a feedback uncertainty" paradigm can be converted into the form of "multi-model" essentially (Kothare et al., 1996).

The stochastic actuator lag τ^A can result in different dynamics models. Thus "multi-model" paradigm is chosen. The robust platooning controller is designed by combining MPC method and the robust control (Wang et al., 2014a). We formulate the platooning control problem as a MM-MPC problem (Kothare et al., 1996). To achieve a system-optimal performance, we use a centralized control method. The leader of a CAV platoon collects information from followers, computes the desired accelerations of itself and all followers, and broadcasts the desired accelerations to followers. The designed controller regulates platoon desired accelerations over a time horizon $[t_0, t_0+T_p]$ to minimize a cost function J representing driving safety, efficiency and ride comfort. It is formulated as Equation (2.9):

$$\min_{\mathbf{U}^p[t_0,t_0+T_p]} \max_{[A^PB^P]\in S^P} J(\mathbf{Z}^P, \mathbf{U}^P) = \min_{\mathbf{U}^p[t_0,t_0+T_p]} \max_{[A^PB^P]} \left(\int_{t_0}^{t_0+T_p} L(\mathbf{Z}^P(t), \mathbf{U}^P(t))dt\right) \quad (2.9)$$

subject to:

- the system dynamics model of Equation (2.3).
- the initial condition: $\widetilde{\mathbf{Z}}^P_{t_0} = \mathbf{Z}^P(t_0-\tau^S)$
- the constraints on state $\mathbf{Z}^P(t)$ and $\mathbf{U}^P(t)$

where L denotes the running cost. $\widetilde{\mathbf{Z}}_{t_0}^P$ represents the initial state for the controlled vehicle system at t_0.

Cost specification for controller

The cost function L is defined as Equation (2.10), where three different cost terms representing safety, efficiency and control are included.

$$L = \underbrace{c_1 \cdot \sum_{i=1}^{N} (\Delta s_i)^2}_{\text{safety}} + \underbrace{c_2 \cdot \sum_{i=1}^{N} (\Delta v_i^2)}_{\text{disruption}} + \underbrace{c_3 \cdot \sum_{i=1}^{N} (u_i)^2}_{\text{control}} \tag{2.10}$$

where, c_1, c_2, and c_3 are weight parameters.

The safety cost term implies that the vehicles tend to reach the desired gap. The disruption cost works by making the following vehicles in the platoon to follow the speeds of their preceding vehicles. The control cost penalizes large values of desired acceleration.

Constraints specification

The constraints on state and control variables are specified as constraints on speeds, gaps and desired accelerations:

- Speed constraint: $v_i \in [0, v_{max}]$.
- Gap constraint: $x_p - x_1 - l_1 \geq s_0$; $x_i - x_{i+1} - l_i \geq s_0$.
- Acceleration constraint: $u_i \in [a_{min}, a_{max}]$.

2.3.3 Solution approach

A nominal MPC does not consider uncertainties. It uses a fixed $[A^P\ B^P]$ as the dynamics model to design the controller. We use Sequential Quadratic Programming (SQP) algorithm to generate the optimal control trajectory (Boggs and Tolle, 1995). When the model uncertainties are considered, we have to solve a MM-MPC problem. The concept of minimizing the *worst case* is applied to solve the MM-MPC problem, i.e. minimizing the largest cost or *worst case* value of J when a deterministic τ^A is used in the dynamics model to predict the future states of the vehicle systems (Liang and Peng, 1999). To have the largest cost, each possible value of τ^A should be involved. With infinite possibilities of τ^A, the computation is theoretically infinite by utilizing brute-force search. For simplicity, we discretize the continuous range of the values of τ^A into M intervals of equal size and only consider the M+1 endpoints' values. The solution

method of the the 'min-max' problem is formulated as an algorithm as shown in Algorithm 1. The M+1 values correspond to M+1 different models. When one model is utilized for prediction, a nominal-MPC formulation forms. Algorithm 1 solves M+1 nominal-MPC formulations and selects the solution to the one having the maximum cost.

Data: Sensor delay τ^S, the boundary of actuator lag $\tau^A \in [\alpha, \beta]$, (delayed) system state $\mathbf{Z}^P(t_0 - \tau^S)$, M intervals
Result: Optimal control input u^* in the horizon $[t_0, t_0 + T_p)$
initialization;
for $i \leftarrow$ 1:M+1
$\tau_i^A \leftarrow \alpha$+($i$-1) $\cdot \frac{\beta-\alpha}{M}$; $u_i \leftarrow$ the solution of optimal control problem of Equation (2.9) with $\tau^A \leftarrow \tau_i^A$; $J_i \leftarrow$ the total cost with $u_i[t_0, t_0 + T_p]$ using Equation (2.9)
end
for $i \leftarrow$ 2:M+1
if $J_1 < J_i$
$J_1 \leftarrow J_i$; $u_1[t_0, t_0 + T_p] \leftarrow u_i[t_0, t_0 + T_p]$
end
end
$u^*[t_0, t_0 + T_p] = u_1[t_0, t_0 + T_p]$

Algorithm 1: The solution for the 'min-max' problem

2.4 Design of robust controller for heterogeneous platoon operation

In this subsection, we first illustrate how to propose a formulation for heterogeneous platooning control like homogeneous platooning control, and then give the detailed design description.

For a platoon of heterogeneous followers like Figure 2.1(b), the CAVs can predict the human-driven vehicles' behaviors by using IDM+ (Wang et al., 2014b). Robust heterogeneous platooning control can then be achieved by optimizing a joint cost function same as Equation (2.9 and Equation (2.10 for the whole platoon.

2.4.1 Design assumptions

The robust heterogeneous platooning controller is designed under the following additional assumptions compared to homogeneous controller design:

- The locations and speeds of the human-driven vehicles can be detected by the on-board sensors equipped on the CAVs.

- The controller has imperfect knowledge of the car-following behavior. This imperfection is represented by uncertainties in the parameters of IDM+.

2.4.2 Platooning control formulation and solution

The heterogeneous platooning controller is also formulated as a Min-Max model predictive control problem as shown in Equation (2.11), where the superscript H is used to represent the notations for heterogeneous platooning control. It uses the same format of cost function as the homogeneous platooning controller except that the control cost of the human driven vehicles is represented by the actual accelerations. The variations of τ^A and the uncertainties in α and b of IDM+ are considered.

$$\min_{\mathbf{U}^H[t_0,t_0+T_p]} \max_{[A^H B^H]} J(\mathbf{Z}^H, \mathbf{U}^H) = \min_{\mathbf{U}^H[t_0,t_0+T_p]} \max_{[A^H B^H]} \left(\int_{t_0}^{t_0+T_p} \iota(\mathbf{Z}^H(t), \mathbf{U}^H(t)) dt \right) \tag{2.11}$$

$$\iota = \underbrace{c_1 \cdot \sum_{i=1}^{4} (\Delta s_i)^2}_{\text{safety}} + \underbrace{c_2 \cdot \sum_{i=1}^{4} (\Delta v_i^2)}_{\text{disruption}} + \underbrace{c_3 \cdot ((u_1)^2 + (u_3)^2 + (a_2)^2 + (a_4)^2)}_{\text{control}} \tag{2.12}$$

subject to:

- the system dynamics model of Equation (2.7) and the dynamics model of human-driven vehicles of Equation (2.5).
- the initial condition and the constraints: they are the same as that described in the homogeneous platooning controller design.

The Min-Max model predictive control problem for the heterogeneous includes the variation of τ^A and the uncertainties in α and b of IDM+. The solution for this problem is essentially the same as that used in the homogeneous platooning controller design. We discretize the continuous range of the values of τ^A with the same method as that used in the homogeneous platooning controller design. After that, the problem is solved as for the homogeneous platooning controller design.

2.5 Simulation experimental design

This section presents the experimental design to assess the performance of the designed platooning controllers, including selected simulation scenarios, controller parameter settings, and the performance indicators.

2.5.1 Simulation scenarios

To test the robustness of the robust MM-MPC controller for a homogeneous CAV platoon and the flexibility of the controller to a heterogeneous platoon control, different simulation scenarios are used. Generally τ^S is between 0.1-0.3 s (Wang et al., 2016b). We choose $\tau^S = 0.2$ s. $\tau^A(t) \in [0.2, 0.8]$ s is chosen as designed bound of τ^A. We compare the designed robust controller with a deterministic nominal MPC controller using a fixed $\tau^A = 0.2$ s. The two controllers are compared under the designed scenario with $\tau^A(t) \in [0.2, 0.8]$ s, and unplanned scenario with $\tau^A(t) \in [0.8, 0.9]$ s, i.e. the actuator lag of vehicle systems are outside the assumed bounds (Kothare et al., 1996). The selected simulation scenarios are as shown in Table 2.1. The heterogeneous platooning controller are tested with imperfect knowledge of the car-following behavior of human-driven vehicles by using different parameters of IDM+ used by human-driven vehicles in the platoon. The selected scenarios are as shown in Table 2.2.

Table 2.1: Simulation scenarios for a homogeneous platooning control test

τ^A (s)	Control strategy
[0.2,0.8]	Nominal MPC ($\tau^A = 0.2$)
[0.2,0.8]	Robust MM-MPC ($\tau^A(t) \in [0.2, 0.8]$
[0.8,0.9]	Nominal MPC ($\tau^A = 0.2$)
[0.8,0.9]	Robust MM-MPC ($\tau^A(t) \in [0.2, 0.8]$

Table 2.2: Simulation scenarios for a heterogeneous platooning control test

τ^A (s)	α (m/s^2)	b (m/s^2)	Control strategy
[0.2,0.8]	1.1	2	Nominal MPC ($\tau^A = 0.2$, α= 1.25, b=2.09)
[0.2,0.8]	1.1	2	Robust MM-MPC ($\tau^A(t) \in [0.2, 0.8]$, $\alpha = 1.25$, $b = 2.09$)
[0.8,0.9]	1.1	2	Nominal MPC ($\tau^A = 0.2$, α= 1.25, b=2.09)
[0.8,0.9]	1.1	2	Robust MM-MPC ($\tau^A(t) \in [0.2, 0.8]$, $\alpha = 1.25$, $b = 2.09$)

2.5.2 Parameter settings

We choose $N = 4$ to demonstrate platoon control, since it can sufficiently show the performances of the controlled platoon as shown in Figure 2.1(a) and Figure 2.1(b) (Milanés et al., 2014). The parameter setting for CAVs in the homogeneous and heterogeneous platooning controllers is the same. The platoons follow an exogenous head vehicle that has a designated speed profile. The total simulation time is 50 seconds (s). To clearly show the performances of the controllers, we use a step function of acceleration for the exogenous head vehicle. It starts with an initial speed of 25 m/s and decelerates with -4 m/s^2 from 3 to 5 s and then accelerates with 1 m/s^2 from 27 s to 35 s. For other time slots, its acceleration is 0 m/s^2. For the controllers, the parameters are set as: $t^d = 1$ s (Xiao and Gao, 2011), $s_0 = 2$ m, $T_p = 5$ s, $c_1 = 0.6$, $c_2 = 0.5$, $c_3 =$

0.6, a_{max} =1.5 m/s^2, $a_{\min}$ = -8 m/s^2, l_i = 4 m (i = 1,2,3,4), M = 19 and $v_{\max}$ = 120/3.6 m/s.

The controller parameters have been manually tuned. The controller tracks the exogenous head vehicle responsively and results in small overshoots and no oscillations in the case where sensor delay τ^S is 0.2 s and no actuator lag exists. In the same case, the time horizon T_p is chosen by preliminary simulations. The total running cost barely changes with higher values of T_p. Systematic tuning methods of MPC can be found in (Garriga and Soroush, 2010).

For the heterogeneous platooning control, we assume the controller has imperfect knowledge of the human-driven vehicles. The controller assumes that the parameters of the IDM+ are α = 1.25 m/s^2, b = 2.09 m/s^2, and T = 1.2 s, while actually the parameters of the IDM+ are α = 1.1 m/s^2, b = 2 m/s^2, and T = 1.2 s. Both simulation time step and controller sampling step are 0.2 s. The simulation starts with equilibrium conditions for each CAV and human-driven vehicle.

2.5.3 Performance assessment indicators

Several indicators are selected to assess the performance of the CAV platoon under different control strategies : (1) total running cost of all controlled vehicles in simulation; (2) total running costs of the first controlled vehicle (1st vehicle) and the last one (4th vehicle); (3) maximum absolute actual acceleration, relative speed and gap error for the first and last controlled vehicle; (4) string stability. A platoon has string stability if the disruption of system states reduce over the vehicle number in the platoon (Feng et al., 2019).

2.6 Simulation results and discussion

In this section, the simulation results are shown and analyzed and the discussion is presented thereafter.

2.6.1 Homogeneous platooning control performance

The simulations are performed separately with the nominal MPC controller (deterministic controller with actuator lag τ^A = 0.2 s) and the robust MM-MPC controller. The performances are shown with figures of the variation of actual acceleration, relative speed, and gap error as shown in Figure 2.2 and of assessment indicators are shown in second and third columns in Table 2.3. As depicted in Figure 2.2, the nominal MPC and the designed robust MM-MPC controller generate reasonable behavior when $\tau^A(t) \in [0.2, 0.8]$ s. When the exogenous head vehicle decelerates, the relative

speed and gap error of the first vehicle become negative while other vehicles are still in the equilibrium states, and the cost of the controller starts to increase. Both controllers work by reducing the costs and give control commands to reduce the relative speeds and gap errors caused by the deceleration of the exogenous head vehicle. The first vehicle then starts to decelerate. After that the second vehicle's relative speed and gap error become negative as well and costs are generated, and the controller has to reduce the costs caused by the relative speeds and gap errors of the first and second vehicles while considering the control costs. It can easily be observed in Figure 2.2 that the changes of actual accelerations start from the first vehicle to the last vehicle sequentially.

The behavior of the first vehicle is more sensitive to the behavior of the the exogenous head vehicle, and this can be reflected in Figure 2.2 and values of costs in Table 2.3. Both controllers can settle to new equilibrium where the cost is zero after certain time, and the maximum of absolute actual acceleration, relative speed and gap error of the 4th vehicle is smaller than these of the first vehicle. To this end, they can ensure string stability.

Table 2.3: Performance results: homogeneous platooning controllers

Indicators	Nominal MPC	MM-MPC	Nominal MPC	MM-MPC
	$\tau^S = 0.2$ s, $\tau^A(t) \in [0.2, 0.8]$s		$\tau^S = 0.2$ s, $\tau^A(t) \in [0.8, 0.9]$s	
$\sum_{i=1}^{4} J_i$	617,57	615,19	936,75	689,59
J_1	248,43	248,65	352,58	308,49
J_4	99,99	99,01	187,37	98,39
$\max \lvert\Delta v_1^+\rvert$ (m/s)	1,13	1,16	1,24	1,16
$\max \lvert\Delta v_4^+\rvert$ (m/s)	0,96	0,97	1,30	0,93
$\max \lvert a_1^+\rvert$ (m/s^2)	1,19	1,25	1,30	1,30
$\max \lvert a_4^+\rvert$ (m/s^2)	0,97	0,97	1,23	1,03
$\max \lvert\Delta s_1^+\rvert$ (m)	0,66	0,74	2,05	0,93
$\max \lvert\Delta s_4^+\rvert$ (m)	0,41	0,40	0,89	0,41
$\max \lvert\Delta v_1^-\rvert$ (m/s)	4,13	4,17	4,24	4,15
$\max \lvert\Delta v_4^-\rvert$ (m/s)	1,92	1,90	2,14	1,84
$\max \lvert a_1^-\rvert$ (m/s^2)	4,34	4,35	4,49	4,15
$\max \lvert a_4^-\rvert$ (m/s^2)	2,20	2,17	2,38	1,95
$\max \lvert\Delta s_1^-\rvert$ (m)	2,11	2,09	3,17	3,12
$\max \lvert\Delta s_4^-\rvert$ (m)	0,20	0,19	0,68	0,25

2.6.2 Robustness of MM-MPC controller

When it comes to the scenario with $\tau^A(t) \in [0.8, 0.9]$ s, the performances of the nominal MPC controller (deterministic controller with actuator lag $\tau^A = 0.2$ s) and the designed robust MM-MPC controller differs as shown in Figure 2.3 and the assessment indicators are shown in fourth and fifth columns in Table 2.3. The nominal MPC controller

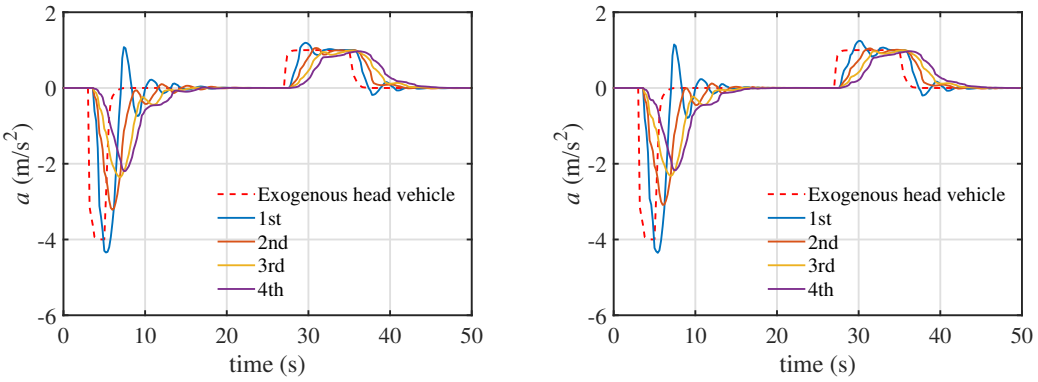

(a) Nominal MPC actual acceleration

(b) MM-MPC actual acceleration

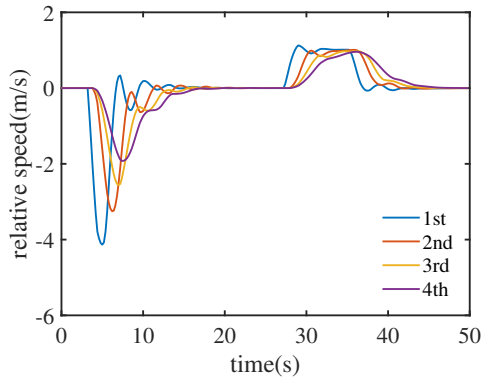

(c) Nominal MPC relative speed

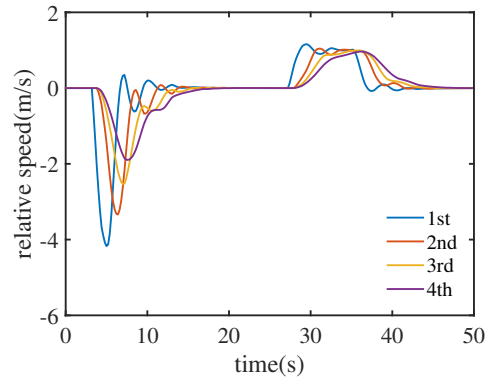

(d) MM-MPC relative speed

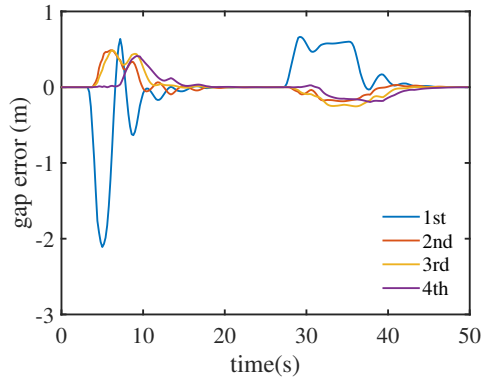

(e) Nominal MPC gap error

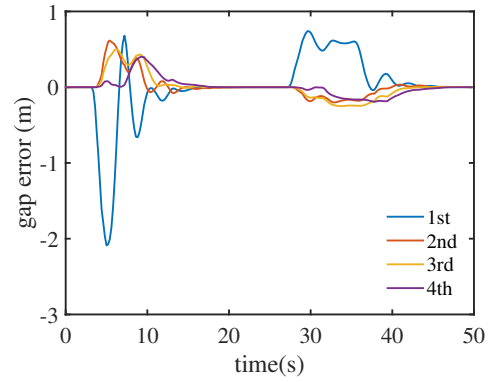

(f) MM-MPC gap error

Figure 2.2: Comparison of nominal MPC ($\tau^A = 0.2$ s) and MM-MPC (designed with $\tau^A(t) \in [0.2, 0.8]$ s) for homogeneous platooning control while actual $\tau^A(t) \in [0.2, 0.8]$ s

can plausibly reach a new equilibrium state; however, that cannot be achieved within the simulation time as shown in Figure 2.3(a), 2.3(c) and 2.3(e). There exists many oscillations but it may ensure string stability since the maximum of absolute actual acceleration, relative speed and gap error of the 4th vehicle is smaller than these of the first vehicle as shown in Table 2.3. By comparison, the robust MM-MPC controller can still settle to new equilibrium, and thus can ensure local and string stability. Besides, the total cost of the platoon using MM-MPC controller is 26.38% lower than that using the nominal MPC controller. This illustrates that the MM-MPC controller is quite robust against large model uncertainties. As opposed to the robust MM-MPC controller, the nominal MPC controller cannot handle large model uncertainties.

2.6.3 Heterogeneous platooning control performance

The nominal MPC controller and the designed robust MM-MPC controller for the heterogeneous platoon is tested with imperfect knowledge of the car-following model IDM+. The simulations are conducted with different parameter settings of the IDM+ used in the controllers and the human-driven vehicles. The performances of the nominal MPC controller (deterministic controller with actuator lag $\tau^A = 0.2$ s) and the designed robust MM-MPC controller are shown in Figure 2.4 and Figure 2.5, and Table 2.4.

Table 2.4: Performance results: heterogeneous platooning controllers

Indicators	Nominal MPC	MM-MPC	Nominal MPC	MM-MPC
	$\tau^S = 0.2$ s, $\tau^A(t) \in [0.2, 0.8]$s		$\tau^S = 0.2$ s, $\tau^A(t) \in [0.8, 0.9]$s	
$\sum_{i=1}^{4} J_i$	938,74	933,82	1120,52	988,19
J_1	249,38	250,08	348,66	301,35
J_4	212,97	211,75	229,23	209,92
$\max \lvert\Delta v_1^+\rvert$ (m/s)	1,12	1,11	1,23	1,21
$\max \lvert\Delta v_4^+\rvert$ (m/s)	1,55	1,55	1,59	1,58
$\max \lvert a_1^+\rvert$ (m/s^2)	1,22	1,15	1,26	1,25
$\max \lvert a_4^+\rvert$ (m/s^2)	0,80	0,80	0,81	0,81
$\max \lvert\Delta s_1^+\rvert$ (m)	1,02	1,03	1,71	1,07
$\max \lvert\Delta s_4^+\rvert$ (m)	14,59	14,65	14,41	14,59
$\max \lvert\Delta v_1^-\rvert$ (m/s)	4,11	4,15	4,17	4,08
$\max \lvert\Delta v_4^-\rvert$ (m/s)	2,14	2,14	2,46	2,19
$\max \lvert a_1^-\rvert$ (m/s^2)	4,41	4,41	4,47	4,19
$\max \lvert a_4^-\rvert$ (m/s^2)	2,04	2,01	2,46	2,09
$\max \lvert\Delta s_1^-\rvert$ (m)	2,14	2,14	2,99	2,96
$\max \lvert\Delta s_4^-\rvert$ (m)	16,28	16,55	17,97	16,31

When $\tau^A(t) \in [0.2, 0.8]$ s, the performances of nominal MPC controller and the designed robust MM-MPC controller are similar. They both generate reasonable behavior as analyzed in homogeneous platooning control performance and settle to the

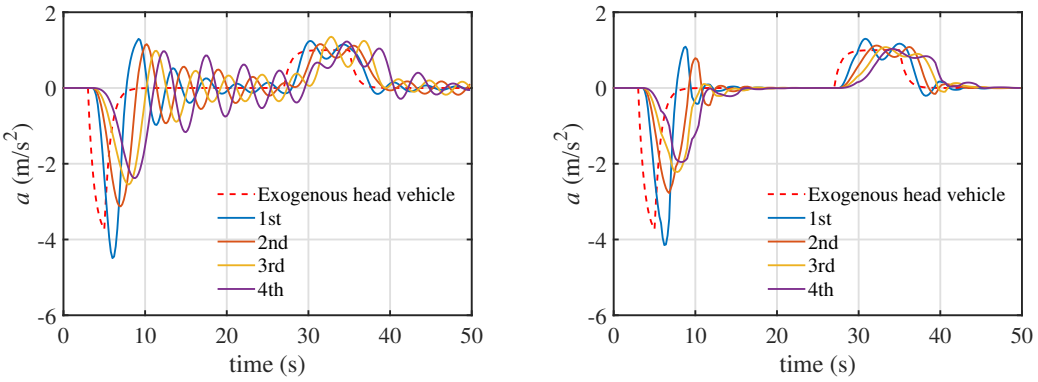

(a) Nominal MPC actual acceleration

(b) MM-MPC actual acceleration

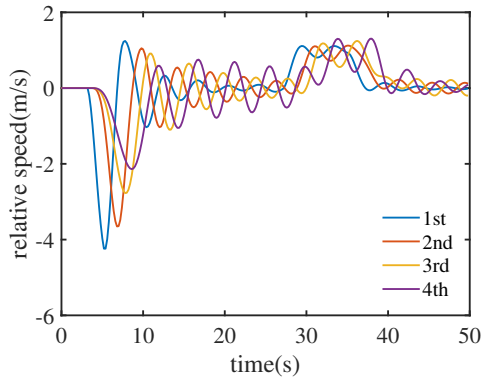

(c) Nominal MPC relative speed

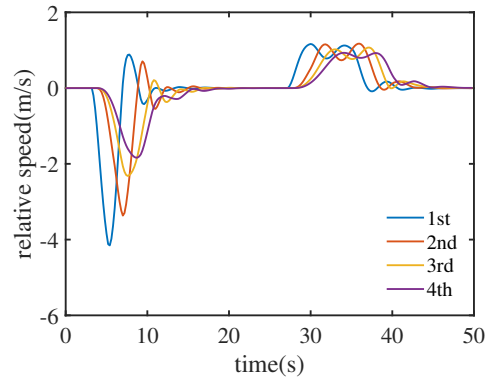

(d) MM-MPC relative speed

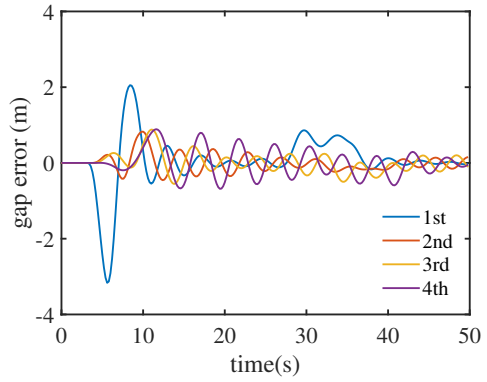

(e) Nominal MPC gap error

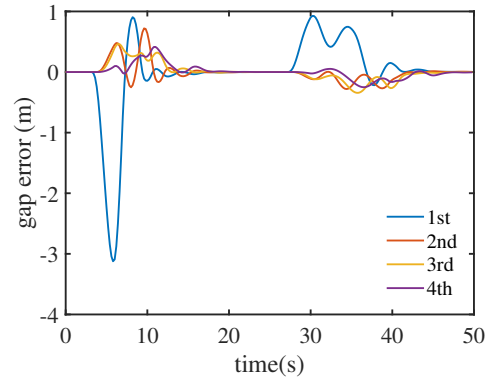

(f) MM-MPC gap error

Figure 2.3: Comparison of nominal MPC ($\tau^A = 0.2$ s) and MM-MPC (designed with $\tau^A(t) \in [0.2, 0.8]$ s) for homogeneous platooning control while actual $\tau^A(t) \in [0.8, 0.9]$ s

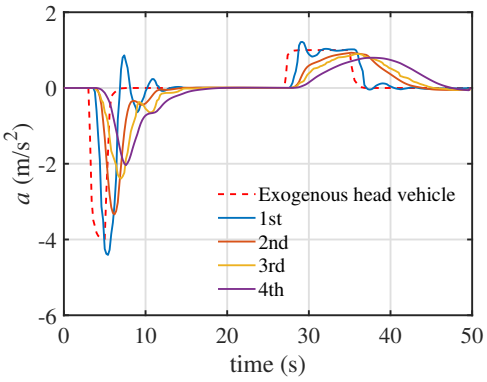

(a) Nominal MPC actual acceleration

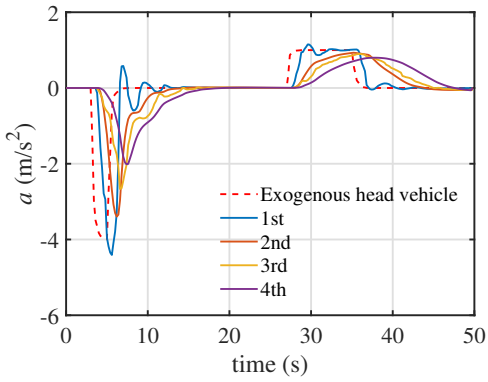

(b) MM-MPC actual acceleration

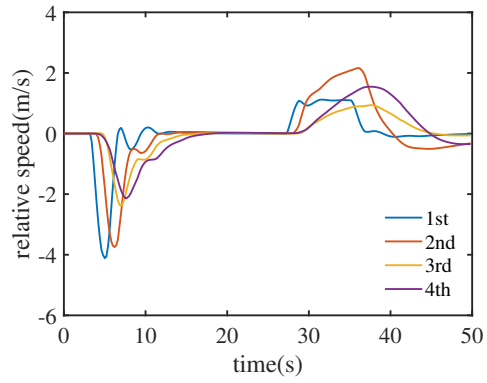

(c) Nominal MPC relative speed

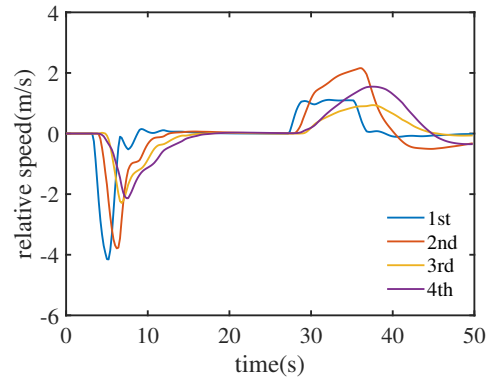

(d) MM-MPC relative speed

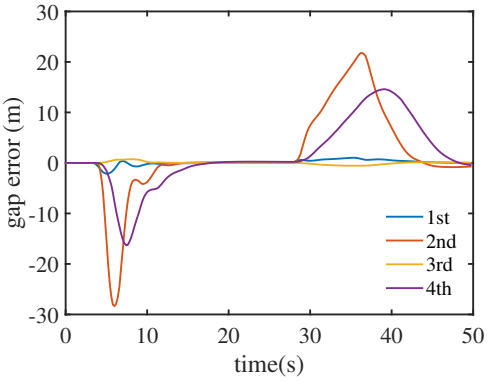

(e) Nominal MPC gap error

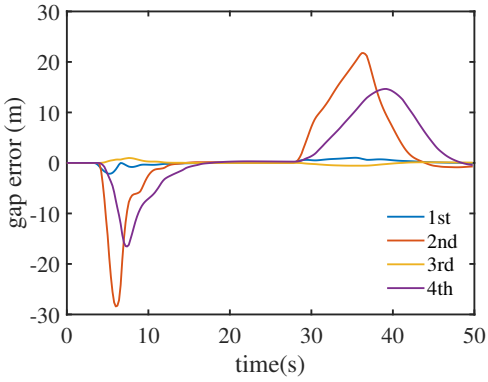

(f) MM-MPC gap error

Figure 2.4: Comparision of nominal MPC ($\tau^A = 0.2$ s) and MM-MPC (designed with $\tau^A(t) \in [0.2, 0.8]$ s) for heterogeneous platooning control while actual $\tau^A(t) \in [0.2, 0.8]$ s

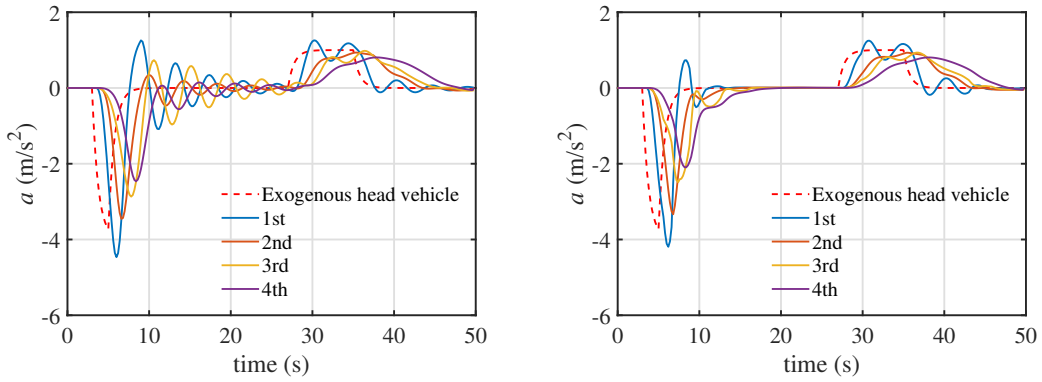

(a) Nominal MPC actual acceleration

(b) MM-MPC actual acceleration

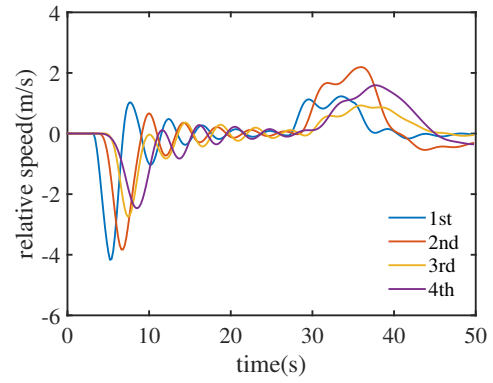

(c) Nominal MPC relative speed

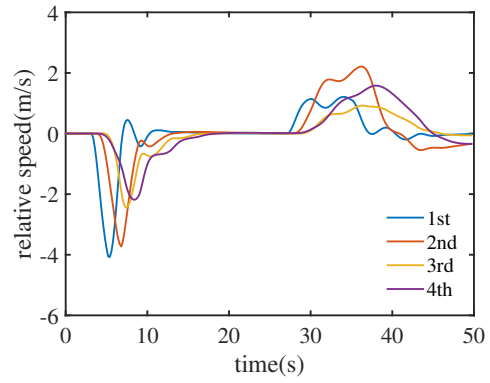

(d) MM-MPC relative speed

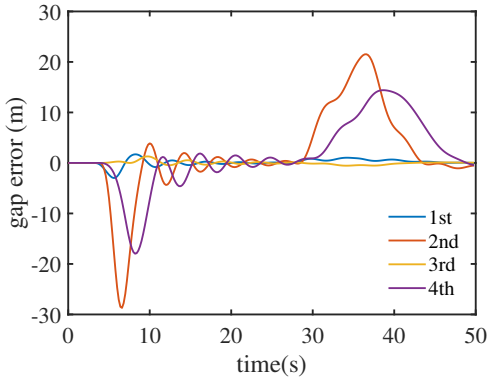

(e) Nominal MPC gap error

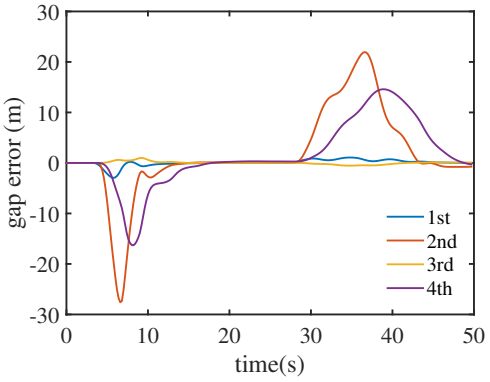

(f) MM-MPC gap error

Figure 2.5: Comparision of nominal MPC ($\tau^A = 0.2$ s) and MM-MPC (designed with $\tau^A(t) \in [0.2, 0.8]$ s) for heterogeneous platooning control while actual $\tau^A(t) \in [0.8, 0.9]$ s

new equilibrium state within the simulation time. However, when it comes to $\tau^A(t) \in [0.8, 0.9]$ s, the nominal MPC controller has more oscillations before reaching the new equilibrium state. The ability to reach a new equilibrium state and keep string stability is plausible for the nominal MPC controller while obvious for the MM-MPC controller. Besides, MM-MPC controller brings 12.55% total platoon cost reduction compared with the nominal MPC controller.

The simulation results confirm the feasibility and robustness of the MM-MPC controller to homogeneous platooning control and flexibility to heterogeneous platooning control.

2.6.4 Discussion

The nominal MPC controller chooses $\tau^A = 0.2$ s. This choice is based on preliminary simulations. $\tau^A = 0.5$ s is not chosen because utilizing 0.5 s results in more oscillations and brings higher total cost where the actual actuator lag is 0.2 s.

The solution method for MM-MPC is clear and obvious enough; however, the relation of M and the length of the bound of $\tau^A(t)$ is not deeply explored. It is noticeable that the larger M is, the longer the computation time will be. There is a tradeoff between the computation time and the performance when choosing the value of M. The solution method can be replaced by using linear matrix inequalities (Kothare et al., 1996).

Even through the controllers have imperfect knowledge of the car-following model, the good performance of the controller can be kept. This implies the controllers are not sensitive to the parameters of the car-following model, and the controllers for homogeneous platooning control may be converted for heterogeneous platooning control easily. It is noticeable, the positive benefits of using MM-MPC controller are larger with homogeneous platooning than with the heterogeneous platooning. This may be explained by the fact that the controller cannot give command to the human-driven vehicle directly. The simulation results show the feasibility and robustness of the MM-MPC controller to homogeneous platooning control and flexibility to heterogeneous platooning control.

The simulation results indicate that with model uncertainties, the robust control is needed for guaranteeing the benefits of the designed controller. This chapter focuses on using the parameter uncertainties to represent the model uncertainties. However, we have not explored other methods of representing model uncertainties. Developed CAVs are suggested to be tested under different scenarios before being brought into the market.

2.7 Conclusion

This chapter proposed a robust MM-MPC controller for vehicle homogeneous and heterogeneous platooning control, taking into account the feedback delay and model parametric uncertainties. Unlike the deterministic MPC, the robust MM-MPC controller is formulated as a 'min-max' problem and generates the desired acceleration by selecting the solution of the *worst case*. Simulation results suggest the robustness and flexibility of the proposed MM-MPC controller with reference to the nominal deterministic MPC controller within and outside of the specified parameter range, respectively. In all situations, the robust MM-MPC controller outperforms the nominal MPC controller and the benefits of the robust MM-MPC is much more pronounced where the uncertainties are outside specified parameter range. However, the computation time of the robust MM-MPC is larger than the nominal MPC. In the solution algorithm to robust MM-MPC, several nominal MPC formulations are solved.

Application of the MM-MPC controller in heterogeneous platoon control seems to validate the flexibility of the proposed control approach and further indicate the robustness of the controller against uncertainties in mixed traffic. The proposed controller has the potential to improve traffic operations due to its robust performance against uncertainties and system delays. The flexibility to mixed traffic shows that MM-MPC controller may be applied to different platooning formations with more CAVs or human-driven vehicles. Nevertheless, it should be tested under these platooning formations to validate this potential.

This research will be extended to robust control design under stochastic feedback delay and input uncertainties in addition to model parametric uncertainties. Future research is also directed to the analytic approach using Lyapunov theory to guarantee string stability of vehicle platoons and robust lane change control in mixed traffic to improve traffic operations. In the next chapter, a human-like cooperative merging strategy is developed. CAVs on mainline and on-ramp lanes are coordinated together to accomplish on-ramp merging. A safe prediction-based lane-changing condition is given.

Chapter 3

A human-like flexible strategy for efficient merging maneuvers of connected automated vehicles

---

Chapter 1 presents a robust platooning control approach. This chapter focuses on coordination of CAVs in two adjacent lanes. The second sub-objective is addressed. We propose a strategy for CAVs to guide on-ramp vehicles to mainline traffic efficiently while ensuring safe interactions with the mainline vehicles. Point-mass kinematic models are used to describe 2-D vehicle motion and receding horizon control is used to generate optimal trajectories of interacting vehicles. The strategy determines the optimal merging time instant for merging vehicles and accelerations of all involving vehicles to minimize the deviation from the preceding vehicles' speed, deviation from preferred inter-vehicle gaps, accelerations, and the merging time instant. The strategy builds on a pre-determined order of vehicles passing the conflict zone but is not restricted to fixed merging points as many methods assumed in the literature. It resembles human-like behavior in the sense that on-ramp CAVs accept smaller time gaps for merging when approaching the end of the acceleration lane. The on-ramp CAVs are controlled longitudinally and laterally to finish the merging process automatically. The feasibility and performance of the proposed strategy are demonstrated through numerical simulations.

This chapter is an edited version of the article:

Chen, N., Wang, M., Alkim, T., and Van Arem, B., "A flexible strategy for efficient merging maneuvers of connected automated vehicles". *18th COTA International Conference of Transportation Professionals*, 2018, pp. 46 –55.

3.1 Introduction

Connected Automated Vehicles, enabled by V2V or V2I communications, have the potential to bring driving comfort and increase traffic performance (Van Arem et al., 2006). The performance of automated vehicles depends on the design of their decision-making systems. For automated vehicles to fully replace human drivers, their controllers should handle different foreseen scenarios in real traffic. On-ramp merging is a common but challenging task for drivers. Inappropriate merging maneuvers can lead to traffic perturbation and even crashes. When on-ramps are activated, considerable vehicle hours are lost. With the possibility of cooperation among CAVs and coordination between CAVs and infrastructure, the merging process can be improved, thus leading to safer and more efficient traffic.

Different cooperative merging strategies have been designed. Wang et al. (2013) proposes to convert merging into a virtual platooning control problem. The conversion is based on mapping an on-ramp vehicle or platoon onto the mainstream lane to form a virtual platoon. The motions of all vehicles in the virtual platoon are controlled by using a geometric method which makes inter-vehicle distances reach a constant value at a fixed merging point. (Milanés et al., 2011) also uses a geometric method to plan desired inter-vehicle distances laterally and longitudinally. Formulating merging as a constrained nonlinear optimization problem or a MPC formulation is another stream of approach. Based on MPC, a cooperative path generation method is designed to regulate the acceleration trajectories of one on-ramp and one mainstream vehicle together (Cao et al., 2015). A longitudinal trajectory planning methodology to facilitate the merging process works by minimizing the engine effort and passenger discomfort (Ntousakis et al., 2016). The control target is, at a fixed merging point, the speed of the controlled vehicle equals to its putative leader and the controlled vehicle reaches its desired time-headway. The objectives of minimizing the engine effort and passenger discomfort are reached by minimizing the acceleration and its first and second derivatives of the controlled vehicle. Using Hamiltonian analysis, an analytical optimal solution format is available offline. In Rios-Torres and Malikopoulos (2017a), acceleration trajectories are generated to reduce fuel consumption. The controller minimizes the square of accelerations. An analytical solution is achieved. To avoid collision, the potential collision zone comprised of the acceleration lane and the mainstream lane is treated as a merging zone. Only one vehicle is allowed to enter into before its driver takes over and completes the final lane changing maneuver (Rios-Torres and Malikopoulos, 2017a). This concept of using a merging zone to avoid conflicts is also used in Xie et al. (2017). The designed merging strategy reduces travel time and increases average speed by minimizing the standard deviation of accelerations and the opposite values of vehicles' speeds (Xie et al., 2017). A longitudinal and lateral control strategy is proposed by evaluating discrete lane change decisions and continuous accelerations jointly based on receding horizon control and dynamic game theory (Wang et al., 2015). The discrete lane change time instants and directions are given in the prediction horizon according to the predicted desired lane sequence.

The role of infrastructure is considered by some merging strategies. A slot-based method is proposed in Marinescu et al. (2012). CAVs travel within virtual slots generated by traffic management system (Marinescu et al., 2012). For on-ramps with ramp metering, CAVs in the mainstream lane collect gaps based on the fundamental diagram theory, and then the ramp metering regulates on-ramp vehicles to use the collected gaps for merging (Scarinci et al., 2015). In Jin et al. (2017), the infrastructure sends signals to the upstream CAVs to make gaps for the upcoming merging vehicles.

The majority of existing methods ignore the lateral motion of merging CAVs and only longitudinal motion is controlled. The merging starts when the longitudinal inter-vehicle gaps for merging vehicles reach a constant spacing or a constant time gap at a fixed merging point. The lateral motion is then completed by drivers or controlled using a simple geometric method. The merging condition is rigid and has no flexible acceptable gaps depending on the urgency of the merge; and the merging can thus fail in dense traffic without sufficiently large gaps. However, human drivers behave differently. When reaching closer to the terminal of the acceleration lane, drivers accept smaller gaps (Daamen et al., 2010). This increases the traffic efficiency to a certain degree. Therefore, it is better for on-ramp CAVs to have human-like behavior to increase the feasibility of finding an acceptable gap for merging.

This chapter proposes a strategy for CAVs to optimally guide the on-ramp vehicles to the mainline traffic efficiently while ensuring safe interactions with the mainline vehicles. Point-mass kinematic models are used to describe 2-D vehicle motion and receding horizon control is used to generate optimal trajectories of interacting vehicles. The strategy determines optimal merging time for on-ramp vehicles and acceleration trajectories for all involving vehicles by minimizing the deviation from the directly preceding vehicles' speed, deviation from preferred inter-vehicle gaps, accelerations, and the time spent in the acceleration lane. The strategy builds on a pre-determined order of passing the conflict zone but is not restricted to fixed merging points. It resembles some human-like behavior in the sense that on-ramp vehicles accept smaller time gaps for merging when approaching the end of the acceleration lane. The performance of the strategy is demonstrated through numerical simulations.

The remaining of the chapter is organized as follows. Firstly, cooperative merging concepts and operational preliminaries are stated. After that, vehicle dynamics models are presented. The formulation of the cooperative merging strategy is given. Finally, the design of simulations and experimental results are illustrated.

3.2 Cooperative merging concepts and operational preliminaries

We consider a typical merging scenario with one mainstream lane and an on-ramp lane connected with an acceleration lane (see Figure 3.1). We postulate a future passing

order of the vehicles at the conflict zone (Ntousakis et al., 2016). For on-ramp vehicle 2 in Figure 3.1, its putative leader and putative follower in the target lane are numbered as vehicle 1 and 3, respectively.

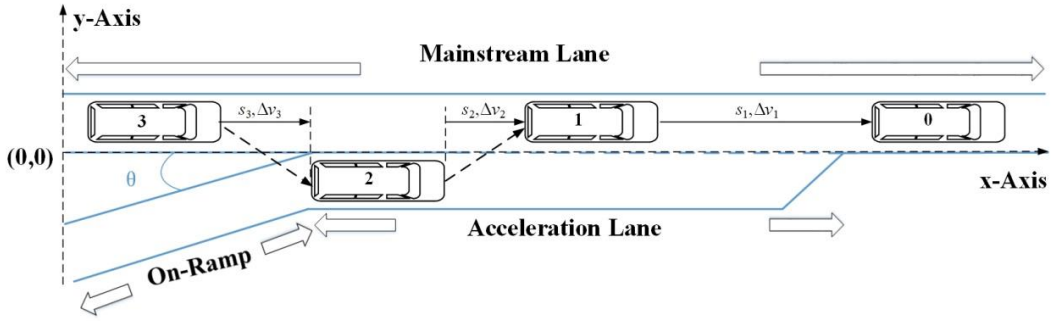

Figure 3.1: A typical merging scenario with one mainstream lane and an on-ramp connected with an acceleration lane

The three vehicles are CAVs whose longitudinal and lateral accelerations are controlled. We do not consider communication imperfection, nor any measurement noise in this chapter. A receding horizon control method is used to design the merging strategy. At the current time instant, the interacting vehicles communicate their current states represented by the inter-vehicle gap and relative speeds. With the communicated information, the controller predicts the future motions of the three vehicles using vehicle dynamics models and decides the optimal acceleration trajectories of all three vehicles and the initiation time of lane change for vehicle 2 over a time horizon T^p. The decisions are generated to optimize a performance index or cost function of the whole CAV group, reflecting safety, efficiency, and control effort. The lane change of vehicle 2 can be triggered when the predicted time gaps to vehicle 1 and 3 are larger than a minimum time gap in the predicted future. Only the first sample of the acceleration trajectories is implemented. At the next time instant, the whole procedure is repeated with updated vehicular information.

3.2.1 Vehicle dynamics models

The system we considered consists of the three vehicles shown in Figure 3.1. The passing order of the three vehicles is as shown with two dotted arrow lines in Figure 3.1. x_i, y_i, v_{ix}, v_{iy}, a_{ix} and a_{iy} are denoted as the longitudinal location, lateral location, longitudinal speed, lateral speed, longitudinal acceleration, and lateral acceleration of vehicle i ($i = 1,2,3$). The merging process is that vehicle 2 moves laterally and longitudinally from the acceleration lane to the mainstream lane while vehicle 1 and 3 move longitudinally. For simplicity, the time argument is dropped where no misunderstanding exists.

The state variable and control variable are defined $X = (s_1, \Delta v_1, s_2, \Delta v_2, s_3, \Delta v_3, y_2)^T$ and $U = (a_{1x}, a_{2x}, a_{3x}, t_2^l)^T$ respectively, where $s_i = x_{i-1} - x_i - l_i$ and $\Delta v_i = v_{i-1} - v_i$

$(i = 1,2,3)$ denote gap (or net spacing) and relative speed of vehicle i with respect to vehicle $i-1$ respectively, t_2^l denotes the merging time instant for vehicle 2 and l_i denotes the length of vehicle i. y_2 is the lateral position of vehicle 2. It is a continuous function of t_2^l as shown in Equation 3.1, where h denotes the lane width. Point mass models are chosen to describe the motion of a vehicle. A second order dynamics is used to represent both the longitudinal and lateral motion of vehicles, as shown in Equation 3.2 and Equation 3.3.

$$y_2 = \begin{cases} -h/2 & t \le t_2^l \\ f(t_2^l) & t_2^l < t < t_2^l + t_m \\ h/2 & t \ge t_2^l + t_m \end{cases} \tag{3.1}$$

$$\dot{x_i} = v_{ix}, \dot{v_{ix}} = a_{ix} \tag{3.2}$$

$$\dot{y_i} = v_{iy}, \dot{v_{iy}} = a_{iy} \tag{3.3}$$

The admissible values of lateral and longitudinal accelerations are subject to the physical characteristics of vehicles (Mehar et al., 2013). To this end, the system state dynamics is as shown in Equation 3.4.

$$\frac{d}{dt}X = (\Delta v_1, a_0 - a_1, \Delta v_2, a_1 - a_2, \Delta v_3, a_2 - a_3, \dot{y_2})^T \tag{3.4}$$

3.3 Cooperative merging strategy design

This section gives a detailed description of the formulation of the cooperative merging approach for CAVs.

3.3.1 Cooperative merging control formulation

The objectives of the cooperative merging controller are to efficiently and safely facilitate the on-ramp merging vehicle to merge into the mainstream traffic. MPC method is applied to design the controller. At each time instant t_0, the controller solves an optimal control problem as shown in Equation 3.5 and Equation 3.6.

$$\min_{U[t_0,t_0+T_p]} J(X,U) = \min_{U[t_0,t_0+T_p]} \int_{t_0}^{t_0+T_p} L(X,U)dt \tag{3.5}$$

$$L = \underbrace{c_1 \cdot \sum_{i=1}^{3} (\Delta s_i)^2}_{\text{safety}} + \underbrace{c_2 \cdot \sum_{i=1}^{3} (\Delta v_i)^2}_{\text{disruption}} + \underbrace{c_3 \cdot \sum_{i=1}^{3} (a_{ix})^2}_{\text{control}} + \underbrace{c_4 \cdot t_2^l}_{\text{lane switch}} \tag{3.6}$$

where c_1, c_2, and c_3 are weight parameters. $\Delta s_i = s_i - s_i^d$ denotes the gap error, i.e. the deviation of the real gap to the desired gap. The desired gap s_i^d is determined by using a constant time gap, i.e. $s_i^d = v_i \cdot t_d + s_0$, where s_0 is the minimum gap at standstill. T_p is the prediction horizon.

The cost function is comprised of safety, disruption, control, and lane switch costs. With the safety cost, the CAVs have a tendency to reach the desired gap. The disruption cost implies that CAVs follow the speeds of their preceding CAVs according to the future passing order. The control cost penalizes large values of desired longitudinal accelerations. The lane switch cost represents the cost for late merging and thus the time spent in the acceleration lane is penalized. When an on-ramp vehicle have large enough inter-vehicle distances with its future preceding and following vehicles, it is instructed to change lane in the acceleration immediately to reduce the lane switch cost.

The optimal control problem is subject to the following constraints on state and control variables:

1) the system dynamics models represented by Equation 3.2 and Equation 3.3.

2) the initial condition: $X(t_0) = \tilde{X}(t_0)$, where $\tilde{X}(t_0)$ represents the initial state for the controller at t_0.

3) state constraints of speed bound: $v_i \in [0, v^{limit}]$, where v^{limit} represent the speed limits.

4) admissible acceleration bound: $a_{ix} \in [a^i_{min}, a^i_{max}]$, where $-a^i_{min}$ and a^i_{max} denote the largest deceleration and acceleration respectively.

Vehicle 2 starts to merge when its predicted time gap with vehicle 1 and vehicle 3 are lager than a threshold $t_g(x_2)$. $t_g(x_2)$ is dependent on vehicle 2's position in the acceleration lane. The chosen simple relationship between $t_g(x_2)$ and x_2 is linear as shown in Figure 3.2, where x_s and x_e denote the start and end locations of the acceleration lane respectively, and t_g^{max} and t_g^{min} denote the maximum and minimum time gap for the acceptance of the merging CAV and the putative follower during the merging process, respectively.

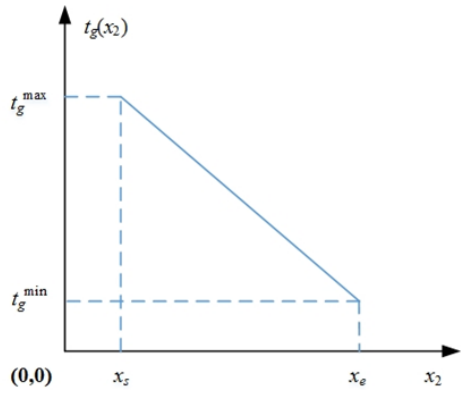

Figure 3.2: The linear relationship of desired net gap headway and the location of CAV 2 in the acceleration lane

The solution to the constrained optimization problem is based on the Pontryagin's Minimum Principle. The optimal longitudinal accelerations are first obtained, after that the controller compares the predicted gaps between vehicle 1 and 2 and between vehicle 2 and 3 with the acceptable gap to have the differences in the prediction horizon. When the on-ramp CAV is traveling in the acceleration lane, the first time instant that satisfies all the differences are non-negative is the optimal merging time instant.

To have the optimal longitudinal accelerations, we use $X_1 = (s_1, s_2, s_3)^T$, $X_2 = (\Delta v_1, \Delta v_2, \Delta v_3)^T$ and $S^d = (s_1^d, s_2^d, s_3^d)^T$ and construct its Hamiltonian function as shown in Equation 3.7 considering Equation 3.4 and Equation 3.6.

$$H = c_1 \cdot (X_1 - S^d) + c_2 \cdot X_2^2 + c_3 \cdot \sum_{i=1}^{3} (a_{ix})^2 + \lambda_1 \cdot X_2 + \lambda_2 \cdot \sum_{i=1}^{3} (a_{(i-1)x} - a_{ix}) \tag{3.7}$$

where λ_1 and λ_2 are co-state variables. The necessary conditions for optimality are as shown in Equation 3.8.

$$\dot{\lambda_1} = -\frac{\partial H}{\partial X_1}; \dot{\lambda_2} = -\frac{\partial H}{\partial X_2} \tag{3.8}$$

subject to initial state conditions and terminal conditions: $\lambda_1(t_0 + T_p) = 0$ and $\lambda_2(t_0 + T_p) = 0$. The process then turns to two-point boundary value problem. It is then solved with a gradient method (Wang et al., 2015).

3.3.2 Human-like lane change

The lateral motion of CAV 2 resembles a human-like behavior. When the lane changing maneuver starts, it follows an empirical human-like lane change path model shown in Equation 3.9, where t_m and h represent the lane change execution time and the lane

width respectively (Samiee et al., 2016). The positive value of h indicates lane change to the right side of the road.

$$f(t_2^l) = \left(\frac{-6h}{t_m^5}\right)(t-t_2^l)^5 + \left(\frac{15h}{t_m^4}\right)(t-t_2^l)^4 + \left(\frac{-10h}{t_m^3}\right)(t-t_2^l)^3 - h/2 \tag{3.9}$$

3.4 Simulations and results

This section designs two experiments to test the performance of the designed merging strategy to achieve cooperative on-ramp merging with short time gap acceptance characteristics.

3.4.1 Experiment Design

The merging controller parameters are set as follows: $c_4 = 0.5$, $T_p = 6$ s, $t_d = 1$ s, $v^{\text{limit}} = 30$ m/s, $a^i_{min} = -2$ m/s^2 $(i = 1,2,3)$, $a^i_{max} = 2$ m/s^2 $(i = 1,2,3)$, $t_m = 2$ s, $s_0 = 2$ m, $t_g^{min} = 0.25$ s (Daamen et al., 2010), and $t_g^{max} = 1$ s. The combinations of c_1, c_2, and c_3 are listed in Table 3.1. The simulation time step is 0.1 s. A feedback delay $\tau^s = 0.2$ s due to discrete sampling process is introduced in simulation, i.e. $X(t) = X(t-\tau^s)$. Thus the performance of the strategy is tested against model mismatch. The length of the acceleration lane is 300 m, setting $x_s = 0$ m and $x_e = 300$ m.

To prove the efficiency of the controller, the two experiments are designed. The settings are as shown in Table 3.2 and Table 3.3. In experiment 1, the initial inter-vehicle distances between CAV 2 and CAV 1 and between CAV 2 and CAV 3 are the same; while in experiment 2, the inter-vehicle distance of CAV 2 and CAV 3 is 0, and the merging situation is much more difficult than the first experiment. The speed of CAV 1 is set constant for the two experiments and the simulation time is 30 s.

Table 3.1: Combinations of c_1, c_2, and c_3

Number	c_1	c_2	c_3
1	0.1	0.5	0.5
2	0.2	0.5	0.5
3	0.1	0.6	0.5
4	0.1	0.5	0.6

3.4.2 Results and analysis

When c_1=0.1, c_2=0.5, and c_3=0.5, vehicle trajectories in experiment 1 are shown in Figure 3.3 and Figure 3.4. The merging strategy generates reasonable behaviors of

Table 3.2: Initial conditions for experiment 1

i	x_i (m)	y_i (m)	v_{ix} (m/s)	l_i (m)
1	18	3.5/2	30	4
2	0	-3.5/2	30	4
3	-18	3.5/2	30	4

Table 3.3: Initial conditions for experiment 2

i	x_i (m)	y_i (m)	v_{ix} (m/s)	l_i (m)
1	32	3.5/2	30	4
2	0	-3.5/2	30	4
3	-4	3.5/2	30	4

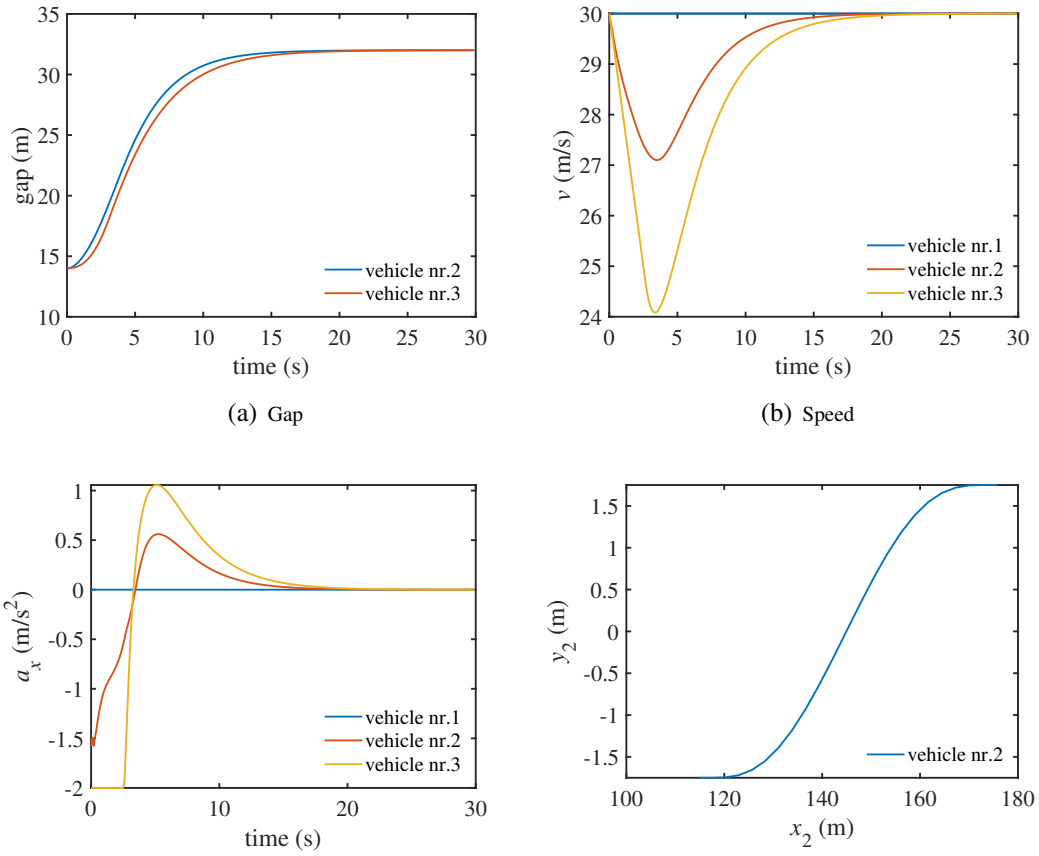

(a) Gap

(b) Speed

(c) Longitudinal acceleration

(d) Lateral motion trajectory

Figure 3.3: Simulation results of experiment 1

CAVs. Initially, the actual gaps of CAV 2 and 3 are smaller than their desired gaps, and the gap errors are negative. To reduce the gap errors, CAV 2 and 3 decelerate to reduce their speeds, and then their desired gaps decrease. However, after the deceleration of CAV 2 and 3, the relative speeds start to be positive and the values of the longitudinal accelerations are non-zero. And then there exists a trade-off for these cost terms. Finally, the following vehicles settle down to the equilibrium states where desired gaps are 32 m, speeds are 30 m/s, and longitudinal accelerations are zero. In the lateral dimension, according to differences of the predicted gaps of merging CAV 2 to CAV 1 and CAV 3 to the accepted gap as shown in Figure 3.4(b), the merging time instant is $t_2^l = 4.3$ s. The merging trajectory is as shown in Figure 3.3(d). Before merging, the predecessor of CAV 3 is CAV 1; however, after merging it turns to be CAV 2. Accordingly, the visual gap of CAV 3 to its preceding CAV in the mainstream lane reduces sharply and then gradually increases to reach the equilibrium state, as shown in Figure 3.4(a).

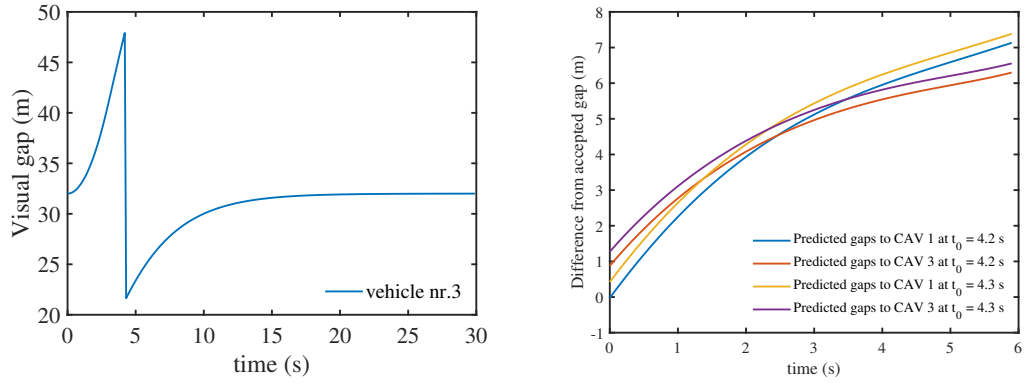

(a) Distance gaps of CAV 3

(b) Predicted gap differences

Figure 3.4: Experiment 1: (a) distance gap of CAV 3 to its preceding CAV in the mainstream; (b) the difference of the predicted gaps to the accepted gaps over the prediction horizon at several different simulation time

For different combinations of c_1, c_2, and c_3, the corresponding values of t_2^l are listed in Table 3.4. Table 3.4 shows that the second combination lead vehicle 2 to merge earlier. This may indicate that vehicle 2 can accomplish merging earlier if c_1 is given a larger value.

Table 3.4: The corresponding values of t_2^l for different combinations of weights in experiment 1

Number	c_1	c_2	c_3	t_2^l
1	0.1	0.5	0.5	4.3
2	0.2	0.5	0.5	4.1
3	0.1	0.6	0.5	4.3
4	0.1	0.5	0.6	4.3

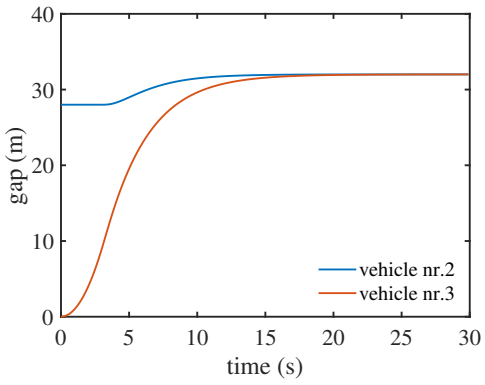

(a) Gap

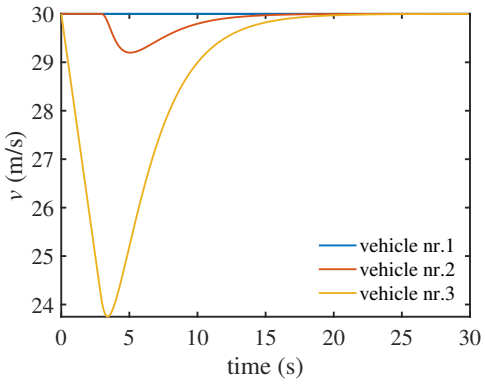

(b) Speed

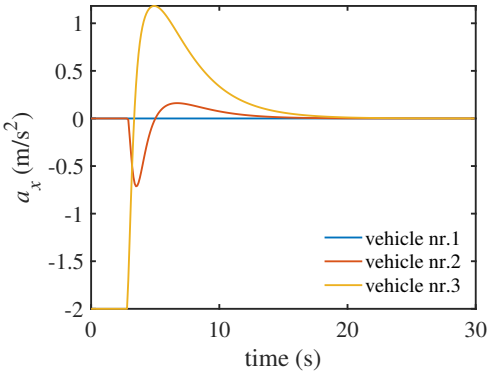

(c) Longitudinal acceleration

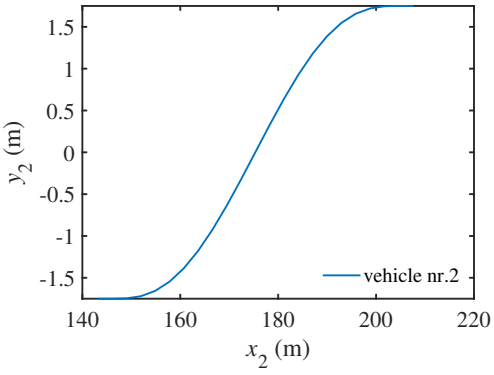

(d) Lateral motion trajectory

Figure 3.5: Simulation results of experiment 2

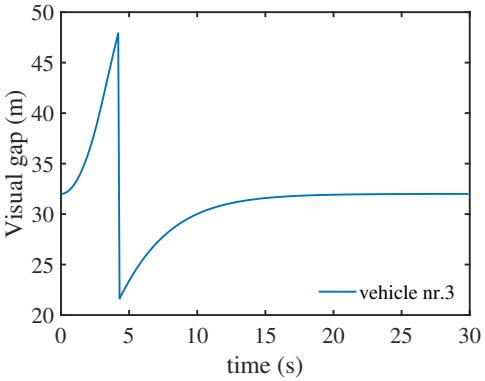

(a) Distance gaps of CAV 3

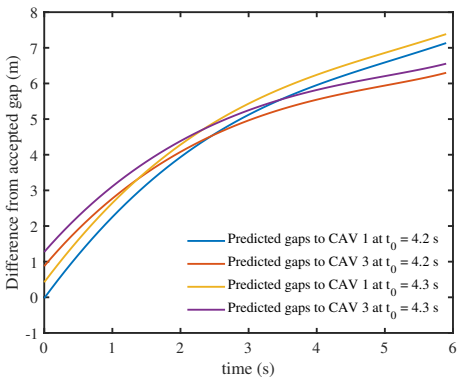

(b) Predicted gap differences

Figure 3.6: Experiment 2: (a) distance gap of CAV 3 to its preceding CAV in the mainstream; (b) the difference of the predicted gaps to the accepted gaps over the prediction horizon at several different simulation time

The simulation results of experiment 2 are shown in Figure 3.5 and Figure 3.6. The controller still generates reasonable behaviors for CAVs in this challenging scenario.

Longitudinally, the initial gap for CAV 3 is 0 and the gap error is large and negative. The controller gives commands for CAV 3 to decelerate. The behavior of CAV 2 is affected by the trade-off of different cost terms and it starts with constant speeds. With deceleration, the gap error of CAV 3 reduces; however, its relative speed becomes positive. By trading off different cost terms, CAV 2 and 3 finally reaches the equilibrium state as that in experiment 1. Laterally the merging time instant is $t_2^l = 5$ s as shown in Figure 3.6(b).

For different combinations of c_1, c_2, and c_3, the corresponding values of t_2^l are listed in Table 3.5. Like Table 3.5, Table 3.5 demonstrates that a larger c_1 brings a smaller value of t_2^l. Besides, Table 3.5 suggests that a larger c_2 may result in a larger value of t_2^l.

Table 3.5: The corresponding values of t_2^l for different combinations of weights in experiment 2

Number	c_1	c_2	c_3	t_2^l
1	0.1	0.5	0.5	5
2	0.2	0.5	0.5	4.7
3	0.1	0.6	0.5	5.1
4	0.1	0.5	0.6	5

The simulation results seem to indicate the feasibility of the designed controller to complete merging automatically and safely, and the capability of on-ramp CAVs to accept small gaps for merging. Even though only two settings of initial states of CAVs are given in this chapter, many other possible settings have been tested by us. By performing simulations with different weights, we find that a larger value for c_1 or a small value for c_2 may make the on-ramp CAV start to merge earlier.

3.5 Conclusion

This chapter proposes a cooperative merging control strategy for on-ramp CAVs to complete the merging task automatically and safely. The controller is designed based on model predictive control. It regulates the longitudinal motions of CAVs and gives the initiation times of lane change for merging vehicles. On-ramp CAVs are allowed to accept smaller time gaps for merging while approaching the end of the acceleration lane. When an on-ramp vehicle travels in the acceleration lane and its predicted inter-vehicle distances to its future preceding and following vehicles in the mainline lane are larger than the accepted values in the predicted time horizon, respectively, it turn left to join mainline the traffic. The lateral lane changing maneuver is automatically controlled to follow an empirically lateral acceleration trajectory without the intervention of a driver. The feasibility of the designed controller to complete merging automatically and safely and the capability to accept small gaps for merging may be demonstrated by numerical experiments. Besides, experimental results suggest the proposed

approach generates feasible and smooth trajectories at challenging initial conditions even when feedback delay is not considered by the controller.

The proposed cooperative merging control strategy uses a predefined merging sequence. A future research direction is to seek optimal merging sequence. Besides, future research will focus on ensuring safe and automatic merging maneuvers in mixed traffic. In the next chapter, we propose a hierarchical control approach. The optimal merging sequence for two conflicting streams of traffic is scheduled. Longitudinal acceleration trajectories for CAVs are regulated to achieve safe and efficient merging and time instants for on-ramp CAVs to change lane are given based on the safe merging condition presented in this chapter.

Chapter 4

A hierarchical model-based optimization control approach for cooperative merging by connected automated vehicles

---

Chapter 3 uses a predefined merging sequence. This chapter presents a new approach to determine the optimal merging sequence. It addresses the third sub-objective. We put forward a hierarchical control approach for CAVs to achieve efficient and safe merging operations. Gap selection and dynamic speed profiles of interacting vehicles at on-ramps affect the safety and efficiency of highway merging sections. A tactical layer controller employs a second-order car-following model with a cooperative merging mode to represent a cooperative merging process and generates an optimal dynamic vehicle merging sequence. An operational layer controller is designed based on model predictive control. It uses a third-order vehicle dynamics model and optimizes desired accelerations for CAVs and the time instants when the on-ramp CAVs initiate the lane-changing executions respectively. Both the tactical layer controller and operational layer controller derive their control commands by minimizing the same objective function for different time horizons. The performance of the proposed hierarchical control framework and a benchmark on-ramp merging method using a *first-in-first-out* rule to determine the merging sequence is demonstrated under 135 scenarios. The experimental results show the superiority of the hierarchical control approach.

This chapter is an edited version of the article:

Chen, N., Van Arem, B., Alkim, T., and Wang, M., "A hierarchical model-based optimization control approach for cooperative merging by connected automated vehicles", *IEEE Transactions on Intelligent Transportation Systems*, 2020, doi: 10.1109/TITS.2020.3007647.

4.1 Introduction

Highway traffic congestion and traffic incidents are societal problems, and they bring great economic loss to the public. On-ramps on highways are typical bottlenecks where improper on-ramp merging behavior brings loss to traffic efficiency and safety easily (Milanés et al., 2011). The loss to a great extent is caused by improper merging sequences and motions of involved vehicles during merging processes (Pueboobpaphan et al., 2010; Morales and Nijmeijer, 2016; Li et al., 2014; Feng et al., 2015; Chen and Englund, 2016; Yang et al., 2016).

With the development of control and telematic technologies, Connected Automated Vehicles potentially improve highway operations near on-ramps (Van Arem et al., 2006; Jin et al., 2018; Ntousakis et al., 2016; Rios-Torres and Malikopoulos, 2017a; Shladover et al., 2012; Rios-Torres and Malikopoulos, 2017b; Zhou et al., 2017). In high driving automation CAVs exchange their current and/or anticipated information with each other via Vehicle-to-Vehicle communication and/or with the road infrastructure via Vehicle-to-Infrastructure communication to enhance situation awareness and/or maneuver in a coordinated way (Van Arem et al., 2006; Wang et al., 2014b; Rios-Torres and Malikopoulos, 2017b; Chen et al., 2018c). CAVs have the potential to follow selected or established merging sequences, and to accomplish or to facilitate difficult merging tasks automatically by behaving cooperatively. Many trajectory-planning approaches exist. They mainly belong to (cooperative) adaptive cruise control, geometric methods, and optimal control. (Milanés et al., 2011; Rios-Torres and Malikopoulos, 2017b; Ntousakis et al., 2016).

By contrast, fewer methods are available to establish optimal merging sequences. To improve traffic efficiency, mainline vehicles are allowed to yield for merging of on-ramp vehicles (Wang et al., 2013; Rios-Torres and Malikopoulos, 2017a,0). The existing cooperative merging strategies generally utilize proactive merging sequences. The merging sequences are given before on-ramp vehicles reaching at merging points (Wang et al., 2013; Awal et al., 2013; Rios-Torres and Malikopoulos, 2017b).

This chapter aims to design a cooperative merging strategy for CAVs to achieve safe and efficient traffic under 100% CAV market penetration. The cooperative merging strategy is based on a hierarchical control approach, where a tactical controller and an operational layer controller work together to select gaps for the merging of on-ramp CAVs, to regulate CAVs' desired accelerations, and to determine time instants when the on-ramp CAVs initiate lane-changing executions respectively. The superiority of the proposed cooperative hierarchical control approach over a benchmark control approach, using a *first-in-first-out* method to determine merging sequences and the same operational layer controller to regulate vehicular motions, is verified numerically at a microscopic level under 135 scenarios with different initial conditions and desired time gap settings.

The remainder of the chapter is organized as follows. In Section 4.2 the relevant literature on establishing merging sequences is critically reviewed and summarized. The

following section presents the designed cooperative merging control architecture. Section 4.4 elaborates on the design of the tactical controller and operational layer controller. After that, we introduce simulation experiments design in Section 4.5, followed by an analysis and a discussion of simulation results in Section 4.6. Finally, Section 4.7 concludes the study.

4.2 Literature review on establishing merging sequences

Existing cooperative merging strategies have two types of means to establish merging sequences. One means is based on explicit rules. The methods belong to this means are thus called 'rule-based methods' for simplicity. Another means is based on the predicted values of a global or local performance indicator relating to traffic operations. Prediction-based approaches are called 'optimal methods' for simplicity.

The rule-based methods include *virtual mapping*, the *first-in-first-out* method, *heuristic* methods, and *others*. The *virtual mapping* method establishes merging sequences by comparing initial path lengths of vehicles to a fixed merging point (Milanés et al., 2011; Wang et al., 2013; Rios-Torres and Malikopoulos, 2017b). A vehicle closer to the merging point passes through it earlier. When a control zone is defined, *first-in-first-out* method establishes merging sequences by comparing the enter times of vehicles into the control zone (Rios-Torres and Malikopoulos, 2017a). A vehicle that enters into the control zone earlier leaves earlier. An upper layer controller of a two-layer local merging control method utilizes a *heuristic* method to establish merging sequences (Schmidt and Posch, 1983; Posch and Schmidt, 1984). The upper layer controller prescribes a constant merging velocity. It makes vehicles entering into the control zone adjust their speeds first to the merging velocity based on constant accelerations and then continue to move. Thus, the expected leaving times of vehicles can be calculated. A merging sequence is then established by sorting the expected leaving times of vehicles. *Others* includes all other methods using plausibly reasonable rules to establish merging sequences, such as selecting one mainline CAV to yield for the merging of an on-ramp vehicle or appointing virtual slots for CAVs (Pueboobpaphan et al., 2010; Scarinci et al., 2015; Marinescu et al., 2012). In Pueboobpaphan et al. (2010), the first downstream mainline CAV, which is estimated within a safety zone when an on-ramp human-driven vehicle arrives at a merging point, yields for merging of an on-ramp human-driven vehicle. Because human-driven vehicles' arriving times and speeds at the start of an acceleration lane are not perfectly predicted, sometimes mainline CAVs generate unnecessarily large gaps. Mainline CAVs can act as leaders to collect gaps for merging of on-ramp vehicles by using the fundamental diagram in traffic flow theory (Scarinci et al., 2015).

Optimal methods evaluate all or some selected merging sequences by using the predicted values of a performance indicator relating to traffic operations and establish the optimal one for merging of on-ramp vehicles. Athans (1969) uses optimal platooning

control to generate accelerations of vehicles and compares the values of an objective function during on-ramp merging process with different merging sequences. The merging sequence that corresponds to the minimal value of the objective function is optimal. However, the process to establish the optimal merging sequence may be time-consuming when many vehicles are involved. An optimal merging sequence can also be established during a merging process (Cao et al., 2014). Cao et al. (2014) utilizes a trajectory equation with uncertain parameters as potential merging paths of an on-ramp vehicle and designs on-ramp merging control based on MPC. Uncertain parameters in the potential merging paths and vehicles' longitudinal accelerations are generated by minimizing a weighted sum of several penalty functions. Awal et al. (2013) calculates a CAV's safe vehicular speed by considering several vehicles ahead of it within a specified distance. Where no merging exists, the nature arriving times of CAVs at a merging point can be estimated. Reasonable merging sequences are established by comparing these estimated arriving times. The predicted merging delays with these reasonable merging sequences are then compared to determine the optimal merging sequence. Zhao et al. (2018) proposes a bi-level programming model for autonomous intersection control. An upper-level controller estimates the earliest and latest arrival times of CAVs into an intersection and establishes an optimal passing sequence of vehicles by minimizing the sum of arriving times of CAVs in two different roads, subject to safe minimal time intervals. A lower-level controller optimizes every vehicle's trajectory to follow the allocated arrival time and maximizes the terminal speed. Xu et al. (2019) gives optimal merging sequences through a genetic approach. A car-following model is used to update vehicles' accelerations and vehicles' accelerations are assumed to be constant in divided time intervals. Duret et al. (2019) proposes a model-based bi-level control strategy for splitting a platoon of trucks near network merges. A supervisory tactical strategy uses a first-order Newell car-following model with bounded acceleration and deceleration to describe the follower-the-leader behavior of vehicles. A natural ordered sequence is given by projecting vehicles' position-time with the maximum flow speed along a shock wave on two lanes to a shock wave starting from a leader's position. The optimal ordering sequence is established to make the projections in a time-ordered set. The existing optimal methods tend to arrange passing times of vehicles over a merging point or repeat future detailed merging process exhaustively with different merging sequences to find an optimal one.

Both the rule-based methods and the optimal methods establish merging sequences by using numerical criteria. The numerical criteria employed by the rule-based methods are based on values related to vehicles' initial or estimated future positions and/or speeds. Merging sequences selected by utilizing the rule-based methods do not have obvious advantages over other possible merging sequences. The optimal methods repeat future detailed merging process exhaustively with different merging sequences to choose optimal ones. Compared with the rule-based methods, the optimal methods evaluate all or some merging sequences and adopt selected global or local performance indicators relating to traffic operations to establish optimal merging sequences. The optimal methods to a great extent ensure utilizing the established merging sequence

improves traffic operations. However, the existing optimal methods rely on accurate vehicle dynamics models and detailed trajectory planning process. These methods' flexibility is limited. They may not work properly to establish optimal merging sequences when mismatches exist. Besides, with the existing optimal methods, on-ramp CAVs start to adapt their speeds and positions to prepare merging into selected gaps respectively when they enter into on-ramp lanes. This neglects the possibilities of allowing on-ramp vehicles to drive with their desired speeds for certain time periods respectively to reduce their speed deviations to mainline vehicles' or adjust their positions to have large inter-vehicle distances. Chances to improve traffic operations may thus be ignored to some extent. This chapter proposes a novel hierarchical model-based optimization control approach to plan vehicular trajectories for CAVs. This approach can establish optimal merging sequences when mismatches exist and allow on-ramp vehicles to travel with their desired speeds for certain time periods respectively.

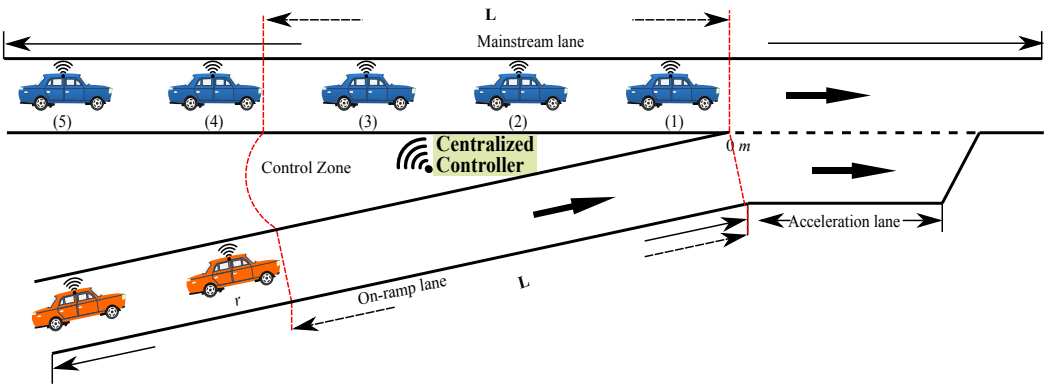

Figure 4.1: A typical on-ramp merging scenario

4.3 Cooperative merging control architecture

Figure 4.1 shows a typical on-ramp merging scenario considered in this chapter. All vehicles are CAVs with SAE Level 4 Automation, and they are assumed to be automatically controlled by the operational layer controller. On-ramp CAVs need to merge into mainstream traffic before reaching the end of an acceleration lane. Located near the start of the acceleration lane, a roadside centralized controller, which acts as the tactical layer controller, regularly collects vehicular information provided by in-vehicle estimators through V2I communication. The operational layer controller is located in CAVs, regulating CAVs' motions.

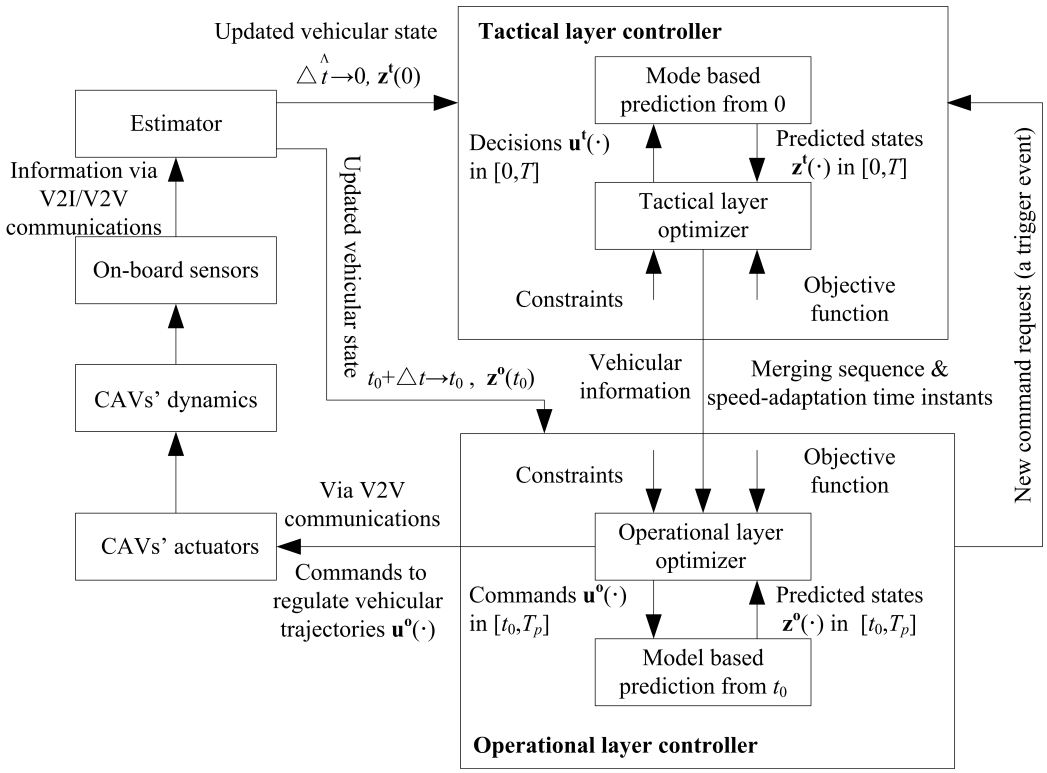

Figure 4.2: Hierarchical architecture of the merging control system

A hierarchical control architecture (See Figure 4.2) is designed to achieve safe and efficient merging of the on-ramp CAVs. It includes two controllers, CAVs' actuators, CAVs' dynamics, on-board sensors, and estimators. These components are connected by communications networks. CAV's actuators execute decision from the operational layer controller, thus changing CAVs' motion. The tactical layer controller and operational layer controller assume that the estimator equipped on each CAV gives accurate vehicular information detected by sensors, including position, speed, and actual acceleration of that CAV. With $\mathbf{Z^t}(0)$, the value of a state variable defined by the tactical layer controller at time 0 s, the tactical layer controller computes optimal future vehicle merging sequences (or equivalently selects gaps for the on-ramp CAVs to merge respectively) and speed-adaptation time instants for on-ramp vehicles to maximize efficiency and comfort while respecting safety and maneuver constraints in a time horizon T. A speed-adaptation time instant is the time instant when an on-ramp CAV starts to adapt its speed and position to prepare merging into the target gap. The maximal efficiency and comfort are to be achieved when the value of an objective function is minimal. The objective function is a weighted sum of deviations of inter-vehicle gaps to desired gaps, relative speeds to their direct predecessors, and actual accelerations of all the vehicles, subject to constraints on velocities, actual accelerations, and inter-vehicle gaps. To predict CAVs' future dynamics in the merging process, the tactical layer controller employs a second-order multi-regime model with a car-following mode and a cooperative merging mode. The transition of the two modes is separated by an on-ramp CAV's speed-adaptation time instant and a time instant when it accom-

plishes the lateral maneuver. The tactical layer controller transmits the optimal future vehicle merging sequence and speed-adaptation time instants to the operational layer controller as a command every $\Delta\hat{t}$, if the command is accepted by the operational layer controller. If the command is rejected and a request is made by the operational layer controller, a new command is to be established by the tactical layer controller before $\Delta\hat{t}$.

With the command received from the tactical layer controller and $\mathbf{Z^o}(t_0)$, the value of the state variable defined by the operational layer controller at the current time t_0, the operational layer controller rejects the command when no feasible solution is found for an on-ramp vehicle. If the on-ramp vehicle is far away from the end of the acceleration lane, the operational layer controller then requests a new command from the tactical layer controller. A request is a trigger event for the tactical layer controller to establish a new decision without waiting until $\Delta\hat{t}$. However, if the on-ramp vehicle is close to the end of the acceleration lane, the operational layer controller chooses the next slot after the established target slot directly for the on-ramp vehicle.

When the tactical command is accepted, the operational layer controller computes longitudinal desired acceleration trajectories for CAVs and lane-changing initiation time instants in a shorter time horizon $T_p < T$ by using MPC. A lane-changing initiation time instant is the time instant when a merging vehicle initiates the lane-changing execution. The operational layer controller utilizes a third-order longitudinal dynamics model as a state prediction model and minimizes the same specification of the objective function as the tactical layer controller. When an on-ramp vehicle has a sufficient gap, it steers towards the main lane and executes merging. The gap acceptance criterion for the on-ramp CAV is that its current and predicted inter-vehicle time gaps to its future direct predecessor and follower in the whole prediction horizon T_p are larger than a certain time gap, depending on the on-ramp vehicle's location on the acceleration lane. When the on-ramp CAV's lane-changing initiation time is given, its lateral motion is modeled with a lateral trajectory equation (Samiee et al., 2016), which is elaborated in Appendix 4.7. The operational layer controller updates its commands with a fixed frequency $1/\Delta t$.

4.4 Merging control formulation

This section elaborates on the design of the tactical layer controller and operational layer controller. For clarity, only one on-ramp vehicle r is considered to establish a merging sequence and its speed-adaptation time instant. The process applies to scenarios where multiple on-ramp vehicles exist as well.

4.4.1 Tactical layer controller establishing a merging sequence and speed-adaptation time instant

For the tactical layer controller, the state variable is defined as $\mathbf{Z^t} = (x_1, v_1, a_1, x_2, v_2, a_2, \cdots, a_N, x_r, v_r, a_r)^T$, where x_i, v_i, and a_i (i=1,2,...,N), x_r, v_r, and a_r denote mainline CAV i's location, speed, and actual acceleration, on-ramp CAV's location, speed, and actual acceleration respectively. For notation simplicity, the time argument is dropped when no ambiguity exists. The decision variable is defined as $\mathbf{U^t} = (\vec{f}_r, t^p)^T$, where $\vec{f}_r$ is a row vector denoting the merging sequence and t^p stands for the speed-adaptation time instant of the on-ramp CAV. When $t < t^p$, the size of $\vec{f}_r$ is N, and the value of $\vec{f}_r$ is (1,2,...,N). After t^p, the on-ramp vehicle starts to adapt its speed and position to prepare merging into the target gap and the size of $\vec{f}_r$ is increased to N+1, and the value of the vector is (1,2,...,k-1,r,k,...N), with $\vec{f}_r(k)$=r, $\vec{f}_r(k-1)$=$k-1$, and $\vec{f}_r(k+1)$=k. To this end, k is the on-ramp CAV's position in the mainline platoon after accomplishing merging.

Closed loop system dynamics model

A second-order model with a feedback law is used to express the longitudinal behavior of a CAV. The open-loop system dynamics for each vehicle are described in Equation (4.1). Because the second-order vehicle dynamics model is used, no extra time is needed to reach a new desired acceleration.

$$\dot{x}_i = v_i, \dot{v}_i = a_i, i = 1, 2, \cdots, N, r \tag{4.1}$$

Considering cases when there is a conflict between the merging vehicle and the mainline traffic during the on-ramp merging process, vehicles' motions are categorized into two modes: car-following and cooperative merging. The cooperative merging mode only applies to the on-ramp CAV and its potential direct follower from t^p to the first time instant when the on-ramp CAV is on the main lane.

The car-following operation is modeled by a Helly car-following model, as shown in Equation (4.2) (Brackstone and McDonald, 1999).

$$\begin{aligned} a^{cf}_{\vec{f}_r(i)}(t) \quad = \quad & D_1 \cdot \Delta v_{\vec{f}_r(i)}(t-\Delta\hat{t}) \\ & + D_2 \cdot (s_{\vec{f}_r(i)}(t-\Delta\hat{t}) - s^d_{\vec{f}_r(i)}(t-\Delta\hat{t})) \end{aligned} \tag{4.2}$$

where, D_1 and D_2 are parameters, $\Delta v_{\vec{f}_r(i)} = v_{\vec{f}_r(i-1)} - v_{\vec{f}_r(i)}$, $s_{\vec{f}_r(i)} = x_{\vec{f}_r(i-1)} - x_{\vec{f}_r(i)} - l_{veh}$, and $s^d_{\vec{f}_r(i)} = v_{\vec{f}_r(i)} \cdot t_d + s_0$ are CAV $\vec{f}_r(i)$'s relative speed, inter-vehicle gap and desired inter-vehicle gap to its (potential) direct predecessor. l_{veh}, t_d, and s_0 denote vehicle length, desired time gap and the minimum inter-vehicle gap at standstill respectively.

For the on-ramp vehicle, before t^p, it travels to reach its desired speed v^{limits} as shown in Equation (4.3), a special car-following mode. When multiple on-ramp vehicles exist, a following on-ramp vehicle uses the vehicular information of its direct preceding on-ramp vehicle in the car-following mode to generate its actual acceleration if its direct preceding vehicle is close to it.

$$a_r = D_3 \cdot (v^{\text{limits}} - v_r(t - \Delta\hat{t})) \tag{4.3}$$

The cooperative merging mode works by adjusting the inter-vehicle gaps between the on-ramp CAV (CAV $\vec{f}_r(k)$) and its potential direct follower (CAV $\vec{f}_r(k+1)$) and predecessor (CAV $\vec{f}_r(k-1)$) till these gaps are large enough for the on-ramp CAV to execute merging. During the adjustment, the on-ramp CAV and its potential follower accelerate or decelerate comfortably to create suitable inter-vehicle gaps. We utilize the same criterion of acceptable time gap for lane changing in our previous work (Chen et al., 2018a). For lane changing, the on-ramp vehicle tends to accept a smaller inter-vehicle time gap to its potential direct predecessor and follower when it is approaching the acceleration lane's end as shown in Equation (4.4) (Chen et al., 2018a), where x_s, x_e, and $t_g^{\min}$ denote the start and end longitudinal position of the acceleration lane, and the minimum acceptable time gap respectively.

$$t_g(t) = (x_{\vec{f}_r(k)(t)} - ac_s) \cdot (t_g^{\min} - t_d)/(ac_e - ac_s) + t_d \tag{4.4}$$

The cooperative merging operation is modeled by a piecewise function, as shown in Equation (4.5). To ensure comfort, when a vehicle is in the cooperative merging mode, its actual acceleration is bounded within [d_{com},a_{com}], standing for the acceptable range of acceleration during the cooperative merging process. If the vehicle accelerates, its acceleration is constrained to be less than a_{com}.If it decelerates, its its deceleration is constrained to be larger than d_{com}.

$$a_{\vec{f_r}(j)} = \begin{cases} \min(a_{com}, \min(a^{cf}_{\vec{f_r}(j)}, a_{\max})), & a^{cf}_{\vec{f_r}(j)} \geq 0, \\ \max(d_{com}, \max(a^{cf}_{\vec{f_r}(j)}, d_{\max})), & a^{cf}_{\vec{f_r}(j)} < 0, \end{cases} \tag{4.5}$$

where, the value of j is k or $k+1$. $a_{\max}$ and $d_{\max}$ denote maximum positive and minimum negative acceleration of vehicles respectively. $a_{\max}$ and $d_{\max}$ are assumed constant for all CAVs simply, but they can be different for different CAVs in the design.

Tactical decision problem formulation

To improve traffic efficiency and safety, the tactical layer controller aims to make the following vehicles to have the same speed as the first downstream vehicle, ensure inter-vehicle spacing $s_{\vec{f}_r(i)}$ to be as desired value $s^d_{\vec{f}_r(i)}$, and reduce the effort of changing

vehicular states which is reflected by actual accelerations. The formulation is as shown in Equation (4.6) and Equation (4.7). The time period T is long enough for the on-ramp vehicle to merge in the mainstream lane and relax to the equilibrium state.

$$\begin{aligned}\min_{\mathbf{U^t}} J(\mathbf{Z^t},\mathbf{U^t}) \quad = \quad & \min_{\mathbf{U^t}}\Big(\int_0^{0+T} \iota(\mathbf{Z^t},\mathbf{U^t})dt\Big) \\ & + c_4\cdot\Big(\sum_{2}^{N+1}(\Delta v_{\vec{f}_r(i)}(0+T))^2\Big) \\ & + c_5\cdot\Big(\sum_{2}^{N+1}(\Delta s_{\vec{f}_r(i)}(0+T))^2\Big)\end{aligned} \tag{4.6}$$

$$\iota = c_1\cdot\sum_i(\Delta s_{\vec{f}_r(i)})^2 + c_2\cdot\sum_i(\Delta v^2_{\vec{f}_r(i)}) + c_3\cdot\sum_i(a_{\vec{f}_r(i)})^2 \tag{4.7}$$

$$\Delta s_{\vec{f}_r(i)} = s_{\vec{f}_r(i)} - s^d_{\vec{f}_r(i)},\ i = 2,3,\cdots,M(t) \tag{4.8}$$

subject to:

- the system dynamics model shown in Equation (4.1), car-following mode shown in Equation (4.2) and Equation (4.3) and cooperative merging mode shown in Equation (4.5).
- the initial condition: $\mathbf{Z^t}(0)$=$\widetilde{\mathbf{Z}}^{\mathbf{t}}(0)$.
- speed constraints: $0 \le v_{\vec{f}_r(i)} \le v^{\text{limits}}$.
- gap constraints: $s_{\vec{f}_r(i)} \ge s_0$.
- acceleration constraints: $d_{\max} \le a_{\vec{f}_r(i)} \le a_{\max}$.

where, $\Delta s_{\vec{f}_r(i)}$ denotes vehicle $\vec{f}_r(i)$'s gap error, c_1, c_2, c_3, c_4, and c_5 are weight parameters, and $M(t)$ is the size of $\vec{f}_r(t)$. Before t^p, $M(t)$=N and the on-ramp CAV is not included. During $t < t^p$, the on-ramp CAV travels with its desired speeds, generating zero value of the objective function. While $t \ge t^p$, $M(t)$=N+1, including the on-ramp CAV at t^p. The on-ramp vehicle steers towards the main lane when its lane changing conditions are first met. The lane changing conditions are: 1) $d_{com} \le a^{cf}_{\vec{f}_r(k)}$, $a^{cf}_{\vec{f}_r(k+1)} \le a_{com}$, 2) on-ramp CAV $\vec{f}_r(k)$ is on the acceleration lane, and 3) on-ramp CAV $\vec{f}_r(k)$'s inter-vehicle time gaps to its potential direct predecessor and follower are larger than t_g, as shown in Equation (4.4). After a lane changing maneuver time t_m, the on-ramp CAV accomplishes on-ramp merging process and is on the main lane.

The tactical layer controller is formulated as a mixed-integer quadratic programming problem (See Equation (4.6)). The on-ramp CAV needs to change lane before reaching the end of the acceleration lane. Thus, t^p has an upper bound. Besides, we discretize the possible values of t^p to be multiples of the time step $\Delta\hat{t}$. As the choices of k and

t^p are finite, the problem can be solved iteratively by giving different values to k and t^p. The optimal $\mathbf{U^t}$ is then transmitted to the operational layer controller. To ensure safety, the tactical layer controller does not give the on-ramp CAV's lane-changing initiation time instant as a command, because the tactical controller and operational layer controller have mismatches regarding vehicle dynamics model and vehicular motions. According to current and predicted inter-vehicle time gaps, the operational layer controller then decides lane-changing initiation time based on a gap acceptance criterion (Chen et al., 2018a).

4.4.2 Operational layer controller regulating vehicular trajectory

Operational layer controller formulation

Receiving the optimal combination of the merging sequence $\vec{f}_r$ and t^p of the on-ramp vehicle, the operational layer controller regulates vehicles' longitudinal desired accelerations and determines the on-ramp CAV's lane-changing initiation time instant t^l to reach efficient and safe traffic performance. Before t^l is determined, the evaluation frequency of the desired accelerations and t^l by the operational layer controller is a fixed $1/\Delta t$. After the on-ramp vehicle starts to steer towards the main lane at t^l, t^l is not evaluated. The operational layer controller is designed based on MPC. With the vehicular information at time t_0, the operational layer controller generates the optimal longitudinal desired accelerations and determines t^l within future T_p time horizon, shorter than T.

For the operational layer controller, the state variable is defined as $\mathbf{Z^o}$=$(s_{\vec{f}_r(1)}, \Delta v_{\vec{f}_r(1)}, \Delta a_{\vec{f}_r(1)}, \cdots, \Delta a_{\vec{f}_r(M(t))}, y_r)^T$, where $\Delta a_{\vec{f}_r(i)}$=$a_{\vec{f}_r(i-1)}$ - $a_{\vec{f}_r(i)}$ is CAV $\vec{f}_r(i)$'s relative actual acceleration to its (future) direct predecessor. The control variable is defined as $\mathbf{U^o} = (u_{\vec{f}_r(1)}, \cdots, u_{\vec{f}_r(M(t))}, \xi_r, t^l)^T$, where $u_{\vec{f}_r(i)}$ is the desired acceleration of CAV $\vec{f}_r(i)$ and ξ_r is the lane-changing acceptability of the on-ramp vehicle $\vec{f}_r(k)$. When lane-changing conditions are not met, $\xi_r(t)$ equals to 0. When the on-ramp vehicle accepts the lane-changing conditions, $\xi_r(t)$ becomes 1, the on-ramp vehicle starts to steer towards the main lane, and the corresponding time instant is t^l. The longitudinal vehicle dynamics model used by the operational layer controller is expressed with a third-order model, as shown in Equation (4.9), Equation (4.10) and Equation (4.11) (Sheikholeslam and Desoer, 1993; Liang and Peng, 1999; Wang et al., 2016b). An actuator lag τ^A is the time duration needed for a vehicle $\vec{f}_r(i)$ to change its actual acceleration $a_{\vec{f}_r(i)}$ to its given desired acceleration $u_{\vec{f}_r(i)}$. τ^A of vehicles herein are assumed constant, but there is no restriction on their homogeneity in our design.

$$\dot{s}_{\vec{f}_r(i)} = \Delta v_{\vec{f}_r(i)}, i = 2, 3, \cdots, M(t) \tag{4.9}$$

$$\Delta \dot{v}_{\vec{f}_r(i)} = \Delta a_{\vec{f}_r(i)} \tag{4.10}$$

$$\Delta \dot{a}_{\vec{f}_r(i)} = \frac{u_{\vec{f}_r(i-1)} - u_{\vec{f}_r(i)} - \Delta a_{\vec{f}_r(i)}}{\tau^A} \tag{4.11}$$

When the on-ramp vehicle starts to change lane, i.e. $\xi_r(t) = 1$, its lateral path during the lane changing process is designed to follow a polynomial equation (Samiee et al., 2016), as shown in Equation (4.21) and Equation (4.22) in Appendix 4.7.

We use a MPC method to formulate the control problem of the operational layer controller (Wang et al., 2014b; Chen et al., 2018c), as shown in Equation (4.12). The objective function specification is as shown in Equation (4.13).

$$\begin{aligned} \min_{\mathbf{U^o}} \zeta(\mathbf{Z^o}, \mathbf{U^o}) \quad = \quad & \min_{\mathbf{U^o}} \Big(\int_{t_0}^{t_0+T_p} \psi(\mathbf{Z^o}, \mathbf{U^o}) dt \Big) \\ & + c_4 \cdot \sum_{2}^{M(t)} (\Delta v_{\vec{f}_r(i)}(t_0+T_p))^2 \\ & + c_5 \cdot \sum_{2}^{M(t)} (\Delta s_{\vec{f}_r(i)}(t_0+T_p))^2 \end{aligned} \tag{4.12}$$

$$\psi = \underbrace{c_1 \cdot \sum_i (\Delta s_i)^2}_{\text{safety}} + \underbrace{c_2 \cdot \sum_i (\Delta v_i^2)}_{\text{disruption}} + \underbrace{c_3 \cdot \sum_i (u_i)^2}_{\text{control}} \tag{4.13}$$

$$i = 2, 3, \cdots, M(t)$$

The operational layer controller has the same specification of an objective function as the tactical layer control. However, the operational layer controller generates the CAVs' desired accelerations by minimizing the objective function. Minimizing the first two items implies that vehicles tend to reach equilibrium states, where the inter-vehicle gaps are their desired values and relative speeds are zeros, safety being ensured and disruption attenuated. Penalizing large positive or small negative accelerations saves control effort. The lane-changing acceptability ξ_r is not controlled as the longitudinal accelerations, but it is affected by the predicted inter-vehicle gaps and speeds. For an open-loop control of the operational layer controller, the lane-changing acceptability ξ_r is determined by using Equation (4.14). When the on-ramp vehicle is on the acceleration lane and the inter-vehicle gaps between it, ordering k after merging, and its future direct predecessor and follower are larger enough within future time horizon T_p, it changes lane.

$$\begin{aligned} \xi_r \quad = \quad & \prod_{j=t_0}^{t_0+T_p} (s_{\vec{f}_r(k)}(j) - v_{\vec{f}_r(k)} \cdot t_g - s_0 \geq 0) \cdot \\ & (s_{\vec{f}_r(k+1)}(j) - v_{\vec{f}_r(k+1)} \cdot t_g - s_0 \geq 0) \end{aligned} \tag{4.14}$$

where, t_g is calculated by using the position of the on-ramp vehicle at t_0, $x_{\vec{f}_r(k)}(t_0)$, when the on-ramp vehicle is on the acceleration lane.

The control process is subject to below constraints:

- the system dynamics model shown in Equation (4.9), Equation (4.10) and Equation (4.11).
- an initial state: $\mathbf{Z^o}(t_0) = \widetilde{\mathbf{Z^o}}(t_0)$
- speed constraints: $0 \leq v_{\vec{f}_r(i)} \leq v^{\text{limits}}$.
- gap constraints: $s_{\vec{f}_r(i)} \geq s_0$.
- acceleration constraints: $d_{\max} \leq u_{\vec{f}_r(i)} \leq a_{\max}$.

Solution to the optimal control problem

The generation of optimal longitudinal desired accelerations for the formulated MPC problem is achieved by using Pontryagin's Minimum Principle (Wang et al., 2015; Duret et al., 2019).

$$X_1 = (s_{\vec{f}_r(1)}, \cdots, s_{\vec{f}_r(M(t))})^T \tag{4.15}$$

$$X_2 = (\Delta v_{\vec{f}_r(1)}, \cdots, \Delta v_{\vec{f}_r(M(t))})^T \tag{4.16}$$

$$X_3 = (\Delta a_{\vec{f}_r(1)}, \cdots, \Delta a_{\vec{f}_r(M(t))})^T \tag{4.17}$$

$$S^d = (s^d_{\vec{f}_r(1)}, \cdots, s^d_{\vec{f}_r(M(t))})^T \tag{4.18}$$

We define X_1, X_2, X_3, and S^d as shown in Equation (4.15)-(4.18) and create the corresponding Hamiltonian function of the optimization problem as shown in Equation (4.19). For the first mainline vehicle, its relative speeds, relative actual accelerations and gap errors are zeros, if it travels with a constant speed.

$$\begin{aligned} H \quad = \quad & c_1 \cdot (X_1 - S^d)^2 + c_2 \cdot X_2^2 + c_3 \cdot \sum_i u^2_{\vec{f}_r(i)} \\ & + \lambda_1 \cdot X_2 + \lambda_2 \cdot X_3 \\ & + \lambda_3 \cdot \sum_i \frac{u_{\vec{f}_r(i-1)} - u_{\vec{f}_r(i)}}{\tau^A} - \lambda_3 \cdot \frac{X_3}{\tau^A} \end{aligned} \tag{4.19}$$

$$\dot{\lambda}_1 = -\frac{\partial H}{\partial X_1}; \dot{\lambda}_2 = -\frac{\partial H}{\partial X_2}; \dot{\lambda}_3 = -\frac{\partial H}{\partial X_3} \tag{4.20}$$

where, λ_1, λ_2, and λ_3 are co-state variables of X_1, X_2, and X_3 respectively. To have the optimal longitudinal desired accelerations, Equation (4.9), Equation (4.10), Equation (4.11) and Equation (4.20) need to be solved. The terminal conditions for Equation (4.20) are $\lambda_1(t_0+T_p)=2\cdot c_5\cdot(X_1(t_0+T_p)-S^d(t_0+T_p))$, $\lambda_2(t_0+T_p)=2\cdot c_4\cdot(X_2(t_0+T_p))$, and $\lambda_3(t_0+T_p)=0$. We are faced with a two-point boundary-value problem which is solved by using an iterative algorithm used in (Wang et al., 2014a).

For the on-ramp CAV, before t^p, it runs with its desired speeds until reaching the speed limits. It utilizes Equation (4.12) to generate its desired acceleration by making $\Delta v_r = v^{\text{limits}} - v_r$ and $\Delta s_r = 0$. When multiple on-ramp vehicles exist, a following on-ramp vehicle utilizes its direct preceding vehicle's information to regulate its desired acceleration by Equation (4.12) and the generated value of the objective function is included in the tactical layer controller and the operational layer controller to calculate the total value of the objective function.

4.5 Simulation experiments design

In this section, we describe numerical experiment settings to test the designed hierarchical cooperative merging strategy and give its detailed parameter settings. Performance indicators used to show the traffic operations with the proposed strategy are given.

4.5.1 Simulation scenarios

To test the performance of the proposed hierarchical control approach, we design 135 scenarios with different initial conditions, desired time gap settings, and different numbers of on-ramp vehicles. The initial conditions include the on-ramp CAVs' initial speed and the initial relative position (RP) of the first on-ramp CAV to the space between mainline CAV 3 and 4. For simplicity, we use percentages to represent RPs. If the first on-ramp CAV simultaneously enters with the mainline CAV 3 and CAV 4, respectively, into the control zone, the RP is indicated by 0% and 100%, respectively. The control zone (See Figure 4.1) is used by a benchmark control method. The RPs are set to be 0%, 20%, 40%, 60% and 80%. The desired time gap t_d varies among 0.6 s, 0.8 s, and 1 s. The on-ramp CAVs' initial speed changes among 15 m/s, 20 m/s, and 25 m/s. The acceleration lane's longitudinal start point is 0 meter (m), and its endpoint is 300 m. The initial first on-ramp vehicle's rear position is -62 m.

There are five mainline CAVs, N=5. Their initial speeds are 25 m/s. Initially, for 90 scenarios, one on-ramp CAV exists. Mainline vehicles start in equilibrium states for 45 scenarios and in non-equilibrium states for the other 45 scenarios respectively. When vehicles start in non-equilibrium states, the inter-vehicle distance between initial vehicle 1 and 2 is 0.5 times of the desired inter-vehicle distance of the vehicle 2 and

other vehicles have desired inter-vehicle distances to their direct preceding vehicles respectively. Another 45 scenarios starting with two on-ramp CAVs are included as well. For these 45 scenarios, all vehicles start from equilibrium states.

Table 4.1 shows the settings of two scenarios. Under these two scenarios, the detailed performance of the controllers are analyzed.

Table 4.1: The settings of 2 scenarios

Number	t_d	RP	$v_r(0)$	number of on-ramp CAVs
1	1	0%	15 m/s	1
2	1	0%	15 m/s	2

The first mainline CAV is set to travel with 25 m/s all the time. Besides, a fixed feedback delay τ^S=0.2 s is also considered: $\widetilde{\mathbf{Z}^{\mathbf{t}}}(0)$=$\mathbf{Z}^{\mathbf{t}}(0-\tau^S)$ and $\widetilde{\mathbf{Z}^{\mathbf{o}}}(t_0)$=$\mathbf{Z}^{\mathbf{o}}(t_0-\tau^S)$, during the experiments.

4.5.2 Benchmark control method for comparison

To show the advantage of the designed hierarchical control approach, we compare it with the benchmark control strategy. The benchmark control strategy uses a *first-in-first-out* method, a vehicle entering into a control zone earlier leaving it earlier, to determine a merging sequence and implements the same herein designed operational layer controller to generate vehicular motions. The control zone is delimited, with a distance $\mathbf{L}$, as shown in Figure 4.1. The distance $\mathbf{L}$ is within the transmission ranges of Dedicated Short-Range Communication (DSRC). For the benchmark control strategy, t^p is 0 s. The corresponding future mainline vehicle order for the first on-ramp vehicle can be k=4 for all scenarios and k=3 or 4 when the on-ramp CAV and mainline CAV 3 enter into the control zone at the same time. When k can be 3 or 4 and on-ramp vehicles' initial speeds are 25 m/s, the future vehicle order of the second on-ramp vehicle after merging can be 5 or 6; otherwise, the future vehicle order of the second on-ramp vehicle after merging is 6.

4.5.3 Parameter settings

For our designed tactical and operational layer controller, their common parameters use the same values respectively. The parameter values representing vehicles' maximum positive and minimum negative accelerations, vehicles' length, vehicles' desired time gap, etc., are collected through V2V or V2I communication. We herein refer to parameter settings assumed in others' experiments to determine parameters' values in our experiments. The parameters are set as follows: L=62 m, T=50 s, T_p=6 s (Wang et al., 2014a), v^{limits}=30 m/s, d_{com}=-4 m/s^2, a_{com}=2 m/s^2, $d_{\max}$=-4 m/s^2 (Xiao et al., 2018), $a_{\max}$=2 m/s^2 (Xiao et al., 2018), $t_g^{\min}$=0.25 s (Chen et al., 2018a), Δt=0.1 s,

$\Delta\hat{t}$=0.5 s, x_s=0 m, x_e=300 m, l_{veh}=4 m, D_1=0.2, D_2=0.7, D_3=2, c_1=0.1, c_2=0.5, c_3=0.5, c_4=0.1, c_5=0.1, t_m=5 s, h=-3.5, s_0=2 m, and N=5. The values of weights c_1, c_2, c_3, c_4, and c_5 were manually tuned to give stable closed loop performance. Systematic tuning methods of MPC can be found in (Garriga and Soroush, 2010). 64-bit MATLAB R2018a on windows 7 system conducts the experiments with different initial settings. The third-order vehicle dynamic model is chosen to represent the behavior of vehicles. The operational layer controller regulates vehicular longitudinal accelerations and the lane-changing initiation time instants for lane changers as shown in Equation (4.12). When a lane changer steers towards the main lane and executes merging, its lateral positions change according to Equation (4.21). For each experiment, the simulation time is 50 s, long enough for the on-ramp vehicle to merge into the mainline traffic.

4.5.4 Performance indicators

Selected performance indicators are related to the actual vehicular trajectories in the simulation time and control objectives, representing the overall traffic operations. We aim to achieve efficient and safe merging of the on-ramp vehicle and to generate smooth trajectories for ride comfort. To this end, the selected performance indicators are the overall value of the objective function calculated by using the weighted sum of the actual gap errors, relative speeds, and the desired accelerations of CAVs during the merging process and the occurrence of collision. The weight parameters on gap errors, relative speeds, and the desired accelerations are c_1, c_2, and c_3 respectively. Besides, the terminal inter-vehicle gap errors with a weight parameter c_5 and relative speeds with a weight parameter c_4 are also included in the objective function.

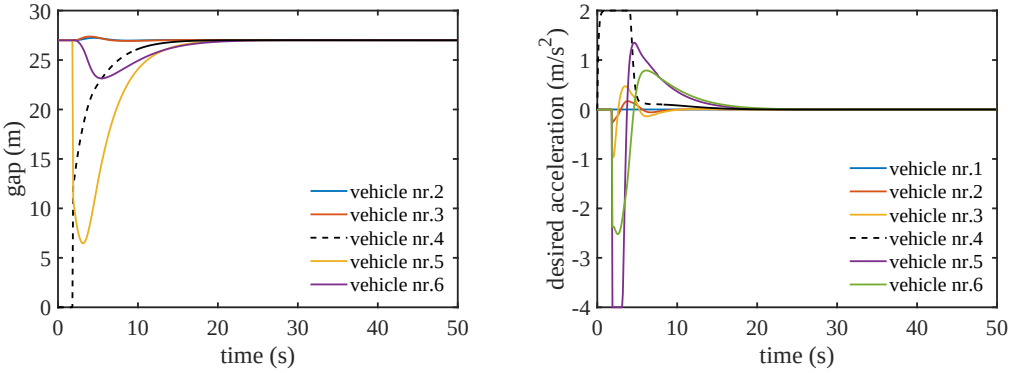

(a) Inter-vehicle gaps (b) Desired accelerations

Figure 4.3: Vehicular trajectories with the proposed hierarchical control approach under a scenario where the on-ramp CAV and mainline CAV 3 enter into the control zone at the same time

4.6 Simulation results and discussion

In this section, simulation results with two different on-ramp merging control methods under the 135 experimental scenarios are given and discussed.

Table 4.2: Experiment results of the scenarios with $v_r(0)$ is 15 m/s

t_d (s); RP (%)	Objective function value			k; t^p (s)	Improvement (%)
	k=3, t^p=0	k=4, t^p=0	HCA		
0.6;0	8414.83	2023.63	778.90	5;4	90.74 & 61.51
0.6;20		2386.19	660.01	5;4	72.34
0.6;40		3092.92	728.09	5;4	76.46
0.6;60		4171.99	967.60	5;3	76.81
0.6;80		5652.86	1200.77	5;6.5	78.76
0.8;0	9690.12	2099.76	1625.89	4;7	83.22 & 22.57
0.8;20		2344.72	1192.44	5;4	49.14
0.8;40		3098.95	957.02	5;4	69.12
0.8;60		4398.80	1004.74	5;4	57.15
0.8;80		6296.09	1247.11	5;2.5	59.76
1;0	11130.34	2337.90	1837.97	4;2	83.49 & 21.38
1;20		2402.95	2044.39	4;8	14.92
1;40		3170.85	1519.02	5;4	52.09
1;60		4687.61	1275.86	5;4	72.78
1;80		7032.86	1366.88	5;3	80.56

4.6.1 Safe performance

In all the 135 scenarios, no collision exists for the two on-ramp merging control methods. One example of the evolution of inter-vehicle gaps and the desired accelerations with the proposed hierarchical control approach (HCA) under scenario 1 (See Table 4.1). With the hierarchical control approach, the future on-ramp CAV's vehicle order after merging is k = 4, and t^p is 2 s, as shown in Table 4.2. The dashed black line

illustrates that the on-ramp vehicle is still on the on-ramp or acceleration lane, while the solid black line indicates it is on the main lane. Obviously, the merging process does not have collisions; thus, it is safe. At around 20 s, the inter-vehicle gaps and desired accelerations relax to the equilibrium values.

4.6.2 Performance of the proposed hierarchical control approach

One on-ramp vehicle: mainline vehicles starting from equilibrium states

When one on-ramp vehicle exists and mainline vehicles start from equilibrium states, for the possible 45 scenarios with different initial conditions and desired time gap settings, experimental results show that the proposed hierarchical control approach outperforms the benchmark control method in 34 scenarios, and behaves as good as the benchmark control method in 11 scenarios.

Table 4.3: Experiment results of the scenarios where the on-ramp CAV and mainline CAV 3 enter into the control zone at the same time

t_d (s);	Objective function value			k;	Improvement
$v_r(0)$ (m/s)	k=3, t^p=0	k=4, t^p=0	HCA	t^p (s)	(%)
0.6;15	8414.83	2023.63	778.90	5;4	90.74 & 61.51
0.8;15	9690.12	2099.76	1625.89	4;7	83.22 & 22.57
1;15	11130.34	2337.90	1837.97	4;2	83.49 & 21.38
0.6;20	2562.47	1106.06	741.53	4;2	71.06 & 32.96
0.8;20	3411.90	1579.01	1183.04	4;1.5	65.33 & 25.08
1;20	4396.84	2131.91	1691.02	4;1.5	61.54 & 20.68
0.6;25	1335.10	1335.10	1121.98	3;1.5	15.96
0.8;25	1985.48	1985.48	1058.95	3;2	46.67
1;25	2758.56	2758.56	1984.06	3;3	28.08

When the on-ramp vehicle's initial speed $v_r(0)$ is 15 m/s, 0.6 times of the speed of the mainline traffic 25 m/s, using HCA for on-ramp merging control brings pronounced

improvements in traffic operations as shown in Table 4.2. In Table 4.2, the first column includes different combinations of desired time gaps t_d and RP. The overall value of the objective function is calculated with the weighted sum of the actual gap errors, relative speeds, and the desired accelerations of CAVs during the merging process with a given merging sequence and t^p generated by using the *first-in-first-out* method or HCA are given in columns 2, 3, and 4. The established decisions from the HCA are presented in column 5. Column 6 indicates the improvement in traffic operations by using the proposed HCA, all higher than 14.92%. The improvement percentage is calculated by dividing the objective function value caused by using the first-in-first-out method into the deviation of the objective function value caused by using the first-in-first-out method and the HCA. Initially, the on-ramp CAV's speed deviation to the speed of the mainline traffic is large. Using the *first-in-first-out* method to establish a merging sequence does not give time for the on-ramp vehicle to increase its speed. Its potential direct follower needs to brake strongly to facilitate on-ramp CAV's merging, causing large values of desired accelerations. By contrast, HCA gives the on-ramp CAV several seconds t^p to accelerate to increase its speed; and then makes the on-ramp vehicle to adapt its speed and position to its target gap. After merging, the mainline vehicle order for the on-ramp CAV is 4 or 5.

When the on-ramp CAV's initial speed $v_r(0)$ increases to 20 m/s or 25 m/s, the HCA still outperforms the benchmark control method under scenarios where the on-ramp CAV and mainline CAV 3 enter into the control zone at the same time, RP being 0%, as shown in Table 4.3. The improvements in traffic operations by using the proposed HCA are all higher than 15.96%. When the on-ramp CAV's initial speed $v_r(0)$ is 20 m/s, the HCA chooses 4 or 5 as the on-ramp CAV's future mainline vehicle order, and gives t^p a positive value, several seconds. It is noticeable that when RP is 0%, choosing k=3 or k=4 by the benchmark control method for on-ramp merging does matter when $v_r(0)$ is not 25 m/s. The merging sequences with k=4 work better. When $v_r(0)$ is 25 m/s, choosing k=3 or k=4 by the benchmark control method achieves the same value of the objective function, and thus makes no difference to the traffic operations.

When the on-ramp CAV's initial speed $v_r(0)$ is 20 m/s, compared with the benchmark control method, using HCA brings at least 13.47% improvement in traffic operations where RP is 20% or 80%. HCA tends to give the same merging sequence as the benchmark control method when the on-ramp CAV's initial position is around the middle of the mainline CAV 3 and 4, as shown in Table 4.4. With the desired time gap increases, the possibility of the HCA to give the same merging sequence as the benchmark control method increases. When the on-ramp CAV's initial speed is 25 m/s, the same initial speed as the mainline traffic, the two control methods behave the same when initial RP is within [20%,60%].

Table 4.4: Experiment results of the scenarios with $v_r(0)$ is 20 m/s and RP is not 0%

t_d (s)	RP (%)	Objective function value		k; t^p (s)	Improvement (%)
		k=4,t^p=0	HCA		
0.6	20	873.77	700.84	4;2	19.79
0.6	40	871.97	848.00	4;2	2.75
0.6	60	1127.47	1076.66	4;3.5	4.51
0.6	80	1657.77	942.28	5;2	43.16
0.8	20	1201.85	1014.07	4;1.5	15.62
0.8	40	1128.47	1123.15	4;1.5	0.47
0.8	60			4;0	0
0.8	80	2185.79	1594.65	5;1.5	27.05
1	20	1593.79	1379.06	4;1.5	13.47
1	40	1439.35	1438.58	4;1	0.5
1	60			4;0	0
1	80	2723.37	1981.38	4;5.5	27.25

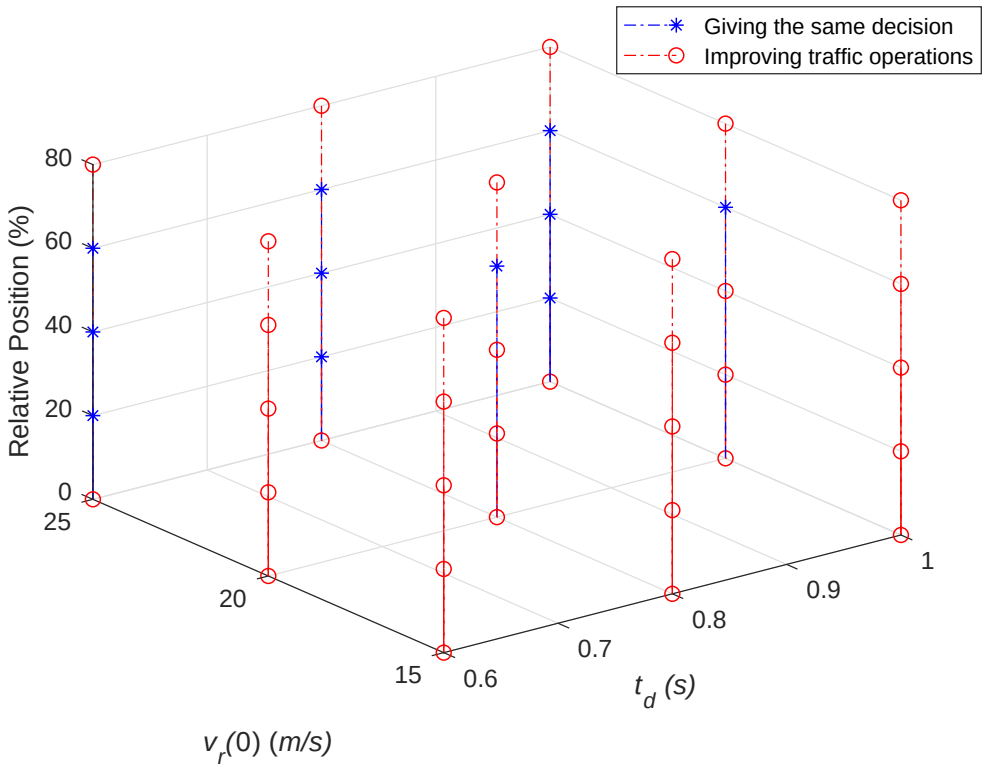

Figure 4.4: The performance of the hierarchical control approach compared with the benchmark control method

Compared with the benchmark control method, the performance of the HCA under the 45 scenarios are marked in Figure 4.4. In Figure 4.4, a circle means that using HCA brings improvement in traffic operations; a star means that HCA gives the same decision as the benchmark control method. By observing Table 4.2, Table 4.3, Table 4.4, and Figure 4.4, we conclude that the HCA outperforms the benchmark control method when the on-ramp CAV's initial speed is 15 m/s, when the desired time gap is 0.6 s or when the on-ramp CAV's relative position to mainline CAV 3 and 4 is 0%, 20%, and 80%. When the on-ramp CAV's initial speed is 20 m/s, the HCA also outperforms the benchmark control method when the on-ramp CAV's relative position to mainline CAV 3 and 4 is 40%. Under the remaining scenarios, the HCA gives the same decisions as the benchmark control method.

One on-ramp vehicle: mainline vehicles starting from non-equilibrium states

In Figure 4.3, after the on-ramp vehicle accomplishes lane changing, small inter-vehicle gaps exist. To this end, the two control methods are further tested with a small inter-vehicle gap existing in mainline traffic, checking their performance when a new on-ramp vehicle shows up after the first on-ramp vehicle changes lane. For the 45 scenarios with mainline vehicles starting from non-equilibrium states, a small inter-vehicle distance $0.5 \cdot v_2 \cdot t_d$ is given to initial vehicle 2 and other following mainline vehicles start from the equilibrium states. Before t^p, initially mainline CAV 2 decelerates to have its desired inter-vehicle distance, reducing its speed. Mainline CAV 3 decelerates to reduce relative speed to CAV 3. With these changes in vehicular states, the performance of the HCA is as shown in Figure 4.5.

By comparing with Figure 4.4, the differences exist in 5 scenarios. 3 of them are with $v_r(0)$ being 25 m/s, RP being 80%, and t_d being 0.6 s, 0.8 s, or 1 s. The remaining 2 scenarios are: (1) $v_r(0)$=20 m/s, RP=60%, and t_d=0.6 s; (2) $v_r(0)$=20 m/s, RP=40%, and t_d=1 s. For these 5 scenarios, the HCA establishes the same decision as the *first-in-first-out* method instead of outperforming in Figure 4.4. As a result, under 16 scenarios, the two control methods give the same decision; under the remaining 29 scenarios, the HCA outperforms the *first-in-first-out* method, averagely bringing 33.01% improvement in traffic operations.

When RP is 0%, for the *first-in-first-out* method using k=4 outperforms k=3 when $v_r(0)$ <25 m/s. However, when $v_r(0)$ is 25 m/s, choosing k=4 or k=3 leads to the same value of the objective function. The finding is the same as shown in Table 4.3.

Two on-ramp vehicles: mainline vehicles starting from equilibrium states

When two on-ramp vehicles exist in the on-ramp lane and the second on-ramp vehicle has the desired inter-vehicle distance to the first one, the second on-ramp vehicle's future vehicle order after merging is 6 or 5 decided by the *first-in-first-out* method.

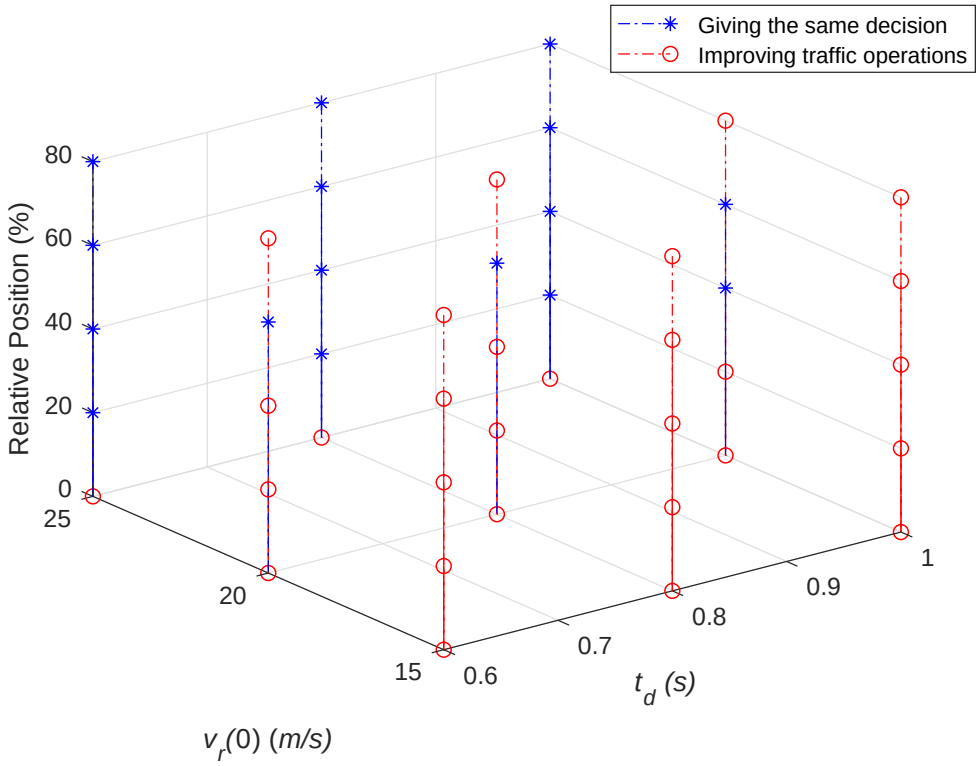

Figure 4.5: The performance of the hierarchical control approach compared with the benchmark control method when a small gap exists

Choosing 5 as the future vehicle order of the second on-ramp vehicle is only possible when RP is 0% and $v_r(0)$ is 25 m/s. For the HCA, the future vehicle order of the second on-ramp vehicle is 6 under 42 scenarios. For the remaining three scenarios where $v_r(0)$ is 25 m/s and RP is 40%, the HCA gives 5 as the second on-ramp vehicle's future vehicle order and generates 5.5 s or 6 s as its speed-adaptation time instant. Under scenario 2 (See Table 4.1), the HCA gives 2.5 s as the speed-adaptation time instant for the two on-ramp vehicles, respectively. The desired acceleration trajectories of vehicles are as shown in Figure 4.6. The black or dashed blue line illustrates that the first or second on-ramp vehicle is still on the on-ramp or acceleration lane respectively, while the solid black or blue line indicates the vehicle is on the main lane respectively. For the *first-in-first-out* method, the on-ramp vehicles are on the main lane at 8.7 s and 10.7 s respectively, bringing 5732.25 as the objective function value.

In Figure 4.6(b), the second on-ramp vehicle follows the first on-ramp vehicle before 2.5 s, bringing 37.90 to the objective function value. After 2.5 s, the two on-ramp vehicles' trajectories are regulated together with mainline vehicles. At 10.8 s and 10.6 s, the two on-ramp vehicles are on the main lane respectively. The merging process produces in total 3473,94 to be the objective function value, making 39.40% improvement compared with the *first-in-first-out* method.

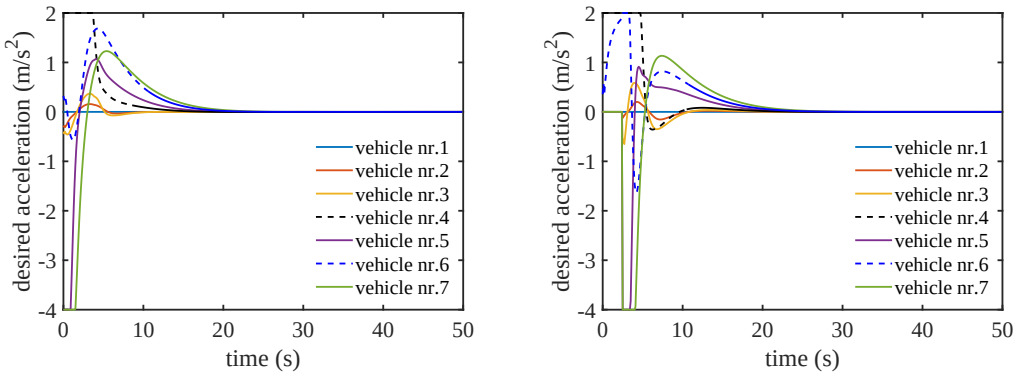

(a) *first-in-first-out* method (b) HCA

Figure 4.6: Vehicular trajectories with the hierarchical control approach under a scenario where the on-ramp CAV and mainline CAV 3 enter into the control zone at the same time

The comparison results of the two control methods are as shown in Figure 4.7. An upward-pointing triangle shows that the HCA deteriorates traffic operations compared with the *first-in-first-out* method. By comparison, for 7 scenarios, the two control methods generate the same decisions. For 4 scenarios, the HCA deteriorates traffic operations, averagely binging 1.2% deterioration. However, for the remaining 34 scenarios, the HCA makes an averagely 26.65% improvement. To this end, the HCA still has superiority.

Under scenarios where two on-ramp vehicles exist and are close to each other, when RP is 0% and $v_r(0)$ is 25 m/s, choices of k=3 or k=4 for the first on-ramp or of using 5 or 6 as the future vehicle order of the second on-ramp vehicle by the *first-in-first-out* method work the same as scenarios where only one on-ramp vehicle exist. When RP is 0% and $v_r(0)$ is less than 25 m/s, using k=4 and 6 as the future vehicle order of the second on-ramp vehicle by the *first-in-first-out* method brings improvement in traffic operations compared with other choices.

4.6.3 Results of and Recommendations on using the *first-in-first-out* method

Because the *first-in-first-out* method is a simple way to determine a merging sequence, compared with the proposed hierarchical control approach, we give recommendations on when to use the *first-in-first-out* method reasonably and suitably to traffic operators and researchers. For all the scenarios where the first on-ramp CAV and the mainline CAV 3 enter into the control zone at the same time, using the *first-in-first-out* method to establish merging sequences lose quite some traffic benefits, as shown in Table 4.3, Figure 4.4, Figure 4.5, and Figure 4.7, with k=4 having an overall better performance than with k=3 for the *first-in-first-out* method. To this end, priority can be given to

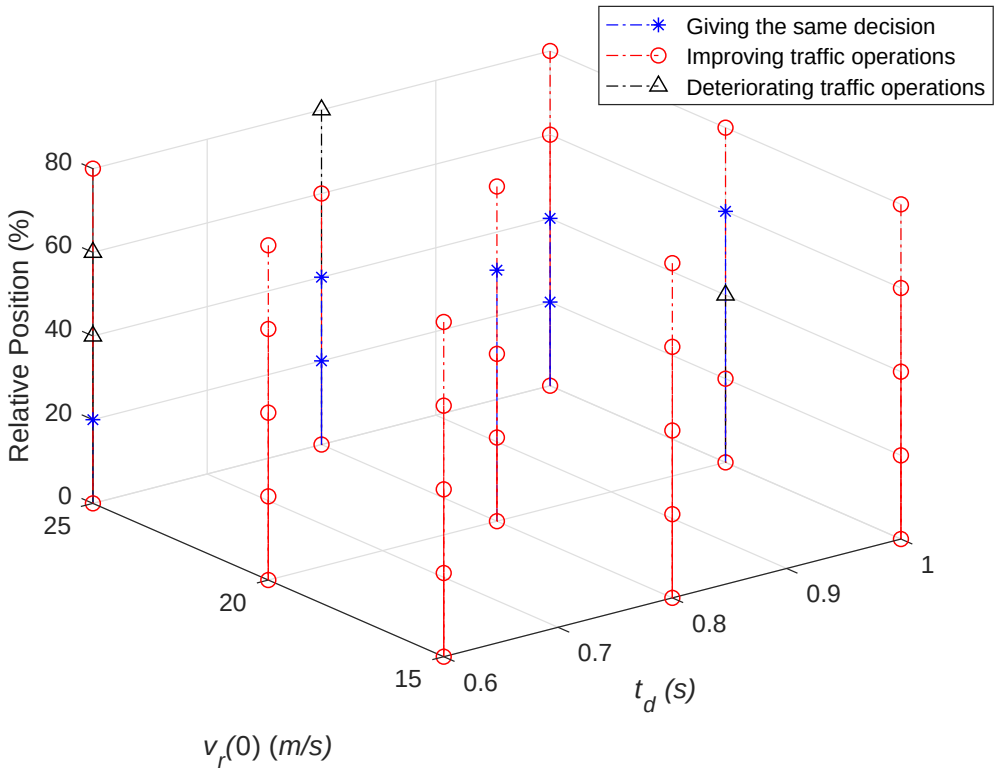

Figure 4.7: The performance of the proposed hierarchical control approach compared with the benchmark control method under scenarios starting with two on-ramp vehicles

mainline traffic when a mainline vehicle and an on-ramp vehicle enter into the control zone at the same time. When the first on-ramp vehicle's initial speed $v_r(0)$ is 15 m/s, 0.6 times of the speed of the mainline traffic 25 m/s, the *first-in-first-out* method, does not reach a good overall traffic performance as the proposed hierarchical control approach, as shown in Table 4.2. To this end, using the *first-in-first-out* to establish merging sequences is not suitable when the initial speed of the first on-ramp vehicle is significantly lower than the mainline traffic. When the first on-ramp CAV enters into the control zone between two mainline CAVs, with the on-ramp vehicle's initial speed increasing to 20 m/s, the *first-in-first-out* method is possibly suitable as shown in Table 4.4 and Figure 4.4. The possibility is higher when CAV 2 has a small inter-vehicle gap compared to its desired value as shown in Figure 4.5. When the on-ramp vehicle's initial speed reaches 25 m/s, the possibility of using the *first-in-first-out* method to have the same decision as the proposed hierarchical control approach greatly increases, as shown in Figure 4.4.

Compared with the optimal vehicle merging sequences and the speed-adaptation time instants of on-ramp vehicles under 135 scenarios, determined by the proposed hierarchical control approach, we recommend researchers or traffic operators to use the *first-in-first-out* method when the initial speed of the first on-ramp vehicle $v_r(0)$ is close to the mainline traffic and its initial relative position to two mainline vehicles is within [40%,60%]. When $v_r(0)$ is slower than the speed of the mainline traffic, it

is better for the on-ramp vehicle to accelerate for several seconds to reach or slightly exceed the speed of the mainline traffic before using the *first-in-first-out* method to establish a merging sequence. The distance of the control zone **L** is thus shrinking with the rear of the on-ramp vehicle. If the on-ramp CAV has the same speed as the mainline traffic and enters into the control zone at the same time instant as a mainline CAV, the *first-in-first-out* method is not recommended to be implemented immediately, as shown in Table 4.3; the on-ramp CAV is recommended to accelerate for 1 or 2 *s* and to choose an anterior slot or gap for merging, compared to initial option decided by *first-in-first-out* method.

4.6.4 Discussion

The proposed hierarchical control approach generates a combination of an optimal merging sequence and speed-adaptation time instants of the on-ramp merging vehicles. Instead of making an on-ramp vehicle to adapt its speed and position for merging immediately after it enters into an on-ramp lane employed by existing methods, our tactical layer controller allows an on-ramp vehicle to move with desired speeds for a certain time period before it starts to adapt its speed and position to prepare merging into the target gap. The time period allows the on-ramp vehicle to increase its speed, reducing speed deviation to the mainline traffic, and to adjust its relative position to two mainline vehicles where the target gap locates. As a result of the speed and position adaptation, its direct follower does not need to brake strongly to facilitate the merging maneuver, when the initial speed of the on-ramp vehicle is significantly lower than the mainline traffic, or when the on-ramp CAV and a mainline CAV enter into the control zone at the same time.

The proposed hierarchical control approach overall works better than the *first-in-first-out* method in improving traffic operations. The experimental results show the superiority of the proposed hierarchical control approach. To this end, without repeating the detailed merging process exhaustively with the operational layer controller, an optimal merging sequence can also be established. Besides, considering a speed-adaptation time instant for an on-ramp vehicle can bring extra improvement in traffic operations even though the idea is not explicitly addressed in other researches. Preparing on-ramp vehicles to reach a merging or certain speed before establishing a merging sequence implicitly supports the idea of considering speed-adaptation time instant (Schmidt and Posch, 1983; Posch and Schmidt, 1984). For 4 scenarios, the proposed hierarchical control approach brings 1.2% deterioration. This deterioration may be caused by mismatches between the tactical and operational layer controllers or the feedback delay. Reducing the mismatches or considering feedback delay in the design may attenuate the deterioration.

The third-order vehicle dynamics model rests on a linearization approach to create a linear representation of a nonlinear longitudinal vehicle dynamics model (Wang et al., 2016b). The linearized model captures driveline dynamics, finite bandwidth of vehicle

actuators, and time lag for the torque available at the tires to achieve a desired acceleration. The third-order vehicle dynamics model is preferred than the second-order model because it is closer to real vehicle behavior and brings reasonable control commands for real-world implementation (Wang et al., 2016b). Besides, parameter uncertainties in the vehicle dynamics model can be considered using the third-order vehicle dynamics model (Chen et al., 2018c). The tactical layer controller usually uses a large value, 0.5 s or 1 s, larger than the actuator lag, as the time step to save computation time; thus, the third-order vehicle dynamics model is not necessary and the second-order vehicle dynamics model is employed. If for some automated vehicles, actuator lags are quite large, a third-order vehicle dynamics model can be used in the tactical layer controller to reduce the mismatch in vehicle dynamics models. Besides, a car-following mode and a cooperative merging mode are utilized by the tactical layer controller to generated actual accelerations based on analytical models rather than numerical optimization in the operational layer. These differences make the computation time of the tactical layer controller tractable. In all our experiments, these differences or mismatches do not contradict the feasibility and applicability of the tactical layer controller to generate optimal merging sequences. This finding may support other researchers to explore simpler optimal control methods to establish merging sequences under different market penetrations of CAVs.

When one on-ramp vehicle exists and five mainline vehicles exist, with a looking-ahead horizon T=50 s, the computation time of the tactical layer controller is 0.32 s. When the number of on-ramp vehicles increases to two, the computation of the tactical layer controller becomes 4.8 s when all the possible merging sequences and speed-adaptation time instants are evaluated. The incremental computation time is caused by the added numbers of possible combinations and the selected solution method: enumeration algorithm. If the merging sequences or speed-adaptation time instants can be restricted to limited choices according to experimental results, the computation time can be reduced. Besides, efficient solutions for mixed-integer programming problems may also reduce computation time, which is one of our future research directions. It takes the operational layer controller around 0.91 s to solve the problem of 6 vehicles with a time horizon 6 s. The computation time of the operational layer controller turns to be around 1.12 s when 7 vehicles are involved. In practical usage, the computation time of the operational layer controller should be considered when it is large. The computation time of the operational layer controller can be reduced with distributed model predictive control (Camponogara et al., 2002).

In our work, imperfect state observation/estimation is already included with a small state delay in the tactical layer. For our 135 experiments, a feedback delay is included, which means the tactical layer controller uses previous vehicular information to establish merging sequences and the merging sequences are established at 0 s, without using the designed feedback nature. The experimental results show that the established merging sequences are feasible. Besides, with feedback nature, the tactical layer controller

has a self-correction mechanism already, though it may update at larger intervals, e.g. 5 to 10 s. To this end, small disturbances in vehicular information do not likely change the feasibility of the established merging sequences. However, we cannot prove that feasibility is guaranteed with the finite number of experiments, especially when the state observation deviates largely from the ground truth. To this end, we add another mechanism in our control architecture. The additional function allows the operational layer controller to reject decisions from the tactical layer controller if no feasible solution is found for an on-ramp vehicle among $\Delta\hat{t}$. If no feasible solution can be found by the operational controller under the current tactical command and the on-ramp vehicle is far away from the end of the acceleration lane, the operational layer controller then requests a new command from the tactical layer controller. Triggered by the rejection event, the tactical layer controller establishes new decisions before $\Delta\hat{t}$. To address safety-critical situations where no feasible solution exists and the on-ramp vehicle is close to the end of the acceleration lane, the operational layer controller is given the autonomy to choose the next gap after the previous target gap for the on-ramp vehicle directly to accomplish merging.

In the tactical layer, the Helly car-following model is employed to predict the future vehicular longitudinal accelerations of a CAV instead of using the operational layer controller. At this stage, all vehicles are assumed to be CAVs. However, our design can be extended to adapt to mixed traffic where human-driven vehicles coexist with CAVs. To include human-driven vehicles, reasonable car-following and lane-changing models can be assumed to represent the behaviors of human-driven vehicles for both the tactical and operational controllers to predict the future development of the surrounding traffic scene. Safety should be ensured at the operational layer controller. To ensure safety, the current and predicted inter-vehicle distances should be large enough for a lane changer to change lane as shown in Equation (4.14). Besides, because the human-driven vehicles do not tend to cooperate to facilitate a lane changing process and their behaviors can not be perfectly modeled or predicted, a trade-off between merging efficiency and the risk to collide can be considered at the operational layer controller in the future.

Noise in actuators or sensors may deteriorate the performance of the controllers to regulate vehicular motions. Noise in detected measurements can be filtered out with data fusion methods in the hierarchical architecture of the merging control system if a filter is added to the estimator. When the uncertainties in actuators cause actuator lag to vary in a small range of values, the deterioration is small. However, when the uncertainties bring a large range of values of the actuator lag, a robust control method is needed to ensure the string stability of the operational layer controller (Chen et al., 2018c).

Because the *first-in-first-out* method is common and easy to be implemented, we give recommendations for using the *first-in-first-out* method to get the same or similar decisions as or to the proposed hierarchical control approach. To improve traffic operations, traffic operators and researchers can use those recommendations when using the

first-in-first-out method to establish merging sequences. One point should not be neglected that optimal merging sequences are established based on a certain performance indicator. For different performance indicators, different merging sequences may be optimal.

4.7 Conclusions and future research

This chapter puts forward a hierarchical control approach for efficient and safe on-ramp merging of Connected Automated Vehicles. A tactical layer controller uses a car-following and a cooperative merging mode to represent the regimes to generate vehicular trajectories during the merging process and gives optimal tactical decisions that bring efficient traffic operations. During the optimization, on-ramp vehicles are allowed to drive with their desired speeds for certain time periods respectively before they start to adapt their speeds and positions to prepare merging into the target gaps, respectively. An operational layer controller is designed based on model predictive control. It employs a third-order vehicle dynamics model, regulates desired accelerations of CAVs, and gives commands on the lane-changing executions of the on-ramp vehicles based on current and predicted inter-vehicle time gaps. The performance of the proposed hierarchical control approach and a benchmark control approach, using the *first-in-first-out* method to determine merging sequences, is tested under 135 scenarios with different initial conditions and desired time gap settings. Experimental results suggest that the proposed hierarchical control approach may outperform the benchmark control method and the superiority may be kept when multiple on-ramp vehicles exist.

We conclude that different settings of initial conditions and the desired time gap do affect an optimal combination of a merging sequence and time instants when on-ramp CAVs start to adapt their speeds and positions to prepare merging into the target gaps respectively. The proposed hierarchical control approach seems to bring pronounced improvements in traffic operations when the initial speed of the on-ramp vehicle is significantly lower than the mainline traffic, when the desired time gap is small, such as 0.6 s, or when an on-ramp CAV and a mainline CAV enter into the control zone at the same time. Allowing on-ramp vehicles to travel with their desired speeds for certain time periods respectively can bring improvements in traffic operations.

After comparing the simulation results of the proposed hierarchical control approach and the benchmark on-ramp merging method, we give recommendations to use the *first-in-first-out* method to establish merging sequences. The main idea of the recommendations is to adapt the initial speed and position of the on-ramp CAV to meet conditions where the *first-in-first-out* method probably gives the same decision as the tactical controller of the proposed hierarchical control approach.

The future research will dive into merging with multiple main lanes. The cooperative merging strategy should be extended to allow CAVs on the outermost main lane to per-

form courtesy lane change. The future research will also focus on on-ramp merging under mixed traffic by extending the proposed hierarchical control approach. Macroscopic characteristics of traffic flow will be analyzed to evaluate the benefits of our design on traffic operations. In the next chapter, we tackle merging with multiple main lanes. On-ramp CAVs are allowed to change lane to facilitate motorway on-ramp merging.

APPENDIX

A polynomial equation for a vehicle's lateral motion during the lane changing maneuver

$$y_r(t) = \begin{cases} y_r(t_0) & t < t^l, \xi_r(t) = 0 \\ f(t) & t^l \leq t \leq t^l + t_m, \xi_r(t^l) = 1 \\ y_r(t_0) + h & t > t^l + t_m \end{cases} \tag{4.21}$$

$$f(t) = \frac{-6h}{t_m^5} \cdot (t - t_0)^5 + \frac{15h}{t_m^4} \cdot (t - t_0)^4 + \frac{-10h}{t_m^3} \cdot (t - t_0)^3 + y_r(t_0) \tag{4.22}$$

where, h denotes maximum lateral position variation whose absolute value equals to lane width. For changing lane to the left side of the road, h is a negative value.

Chapter 5

Hierarchical optimal maneuver planning and trajectory control at on-ramps with multiple mainstream lanes

---

Chapters 3 and 4 focus on coordination of CAVs in one on-ramp lane and one main lane. This chapter relaxes one main lane to multiple main lanes. It addresses the final sub-objective. We propose a hierarchical cooperative merging control approach that ensures collision-free and traffic-efficient merging through the interaction of a maneuver planner and an operational trajectory controller. State-of-the-art approaches in cooperative merging either build on heuristics solutions or prohibit mainline CAVs to change lane on multilane highways. The planner predicts future vehicular trajectories, including acceleration trajectories and time instants when lane changes start, in a long horizon up to 50 seconds with a linear prediction model. It establishes the optimal dynamic vehicle sequence in each lane by minimizing predicted traffic disturbances that can propagate upstream and lead to traffic breakdown. Mainline vehicles may be made to change lane. The operational controller follows the established instructions from the planner and regulates vehicular trajectories with model predictive control in a shorter horizon of 6 seconds. The performance of the designed hierarchical cooperative merging control approach is compared to a cooperative merging method utilizing widely used *first-in-first-out* rule to establish merging sequences and the same operational controller to generate vehicular trajectories. Systematic comparison shows that the proposed approach consistently results in less disturbances during merging.

This chapter is an edited version of the article:

Chen, N., Van Arem, B., and Wang, M., ”Hierarchical optimal maneuver planning and trajectory control at on-ramps with multiple mainstream lanes”, under review.

5.1 Introduction

The spatial and temporal dimensions of interactions between mainline and on-ramp traffic on highway trigger congestion, traffic oscillation, and incidents if inter-vehicle spaces are less than desired values (Ntousakis et al., 2016). Connected automated vehicles are effective countermeasures to improve traffic operations near on-ramps (Ntousakis et al., 2016; Van Arem et al., 2006; Wang et al., 2013; Pueboobpaphan et al., 2010; Zhou et al., 2017). CAVs are equipped with on-board sensors to detect ambient driving environment. Besides, CAVs have communication units and share information among themselves or with other entities through vehicle-to-everything communication to enhance situation awareness, thus having high potential to bring benefits in traffic operations (Van Arem et al., 2006; Xiao and Gao, 2010; Shladover et al., 2012; Rios-Torres and Malikopoulos, 2017b; Chen et al., 2018c,0; Zhao et al., 2018). The movement of automated vehicles are generally controlled by a maneuver planning and trajectory control and a trajectory following controllers (Schmidt and Posch, 1983; Milanés et al., 2011; Guanetti et al., 2018). The maneuver planning and trajectory control controller schedules dynamic vehicle sequences in each lane and plans reference trajectory online or offline in advance (See Figure 1.1). The trajectory following controller commands vehicular actuators to track the planned trajectory as close as possible. In this study, our scope focuses on the maneuver planning and trajectory control.

The maneuver planning and trajectory control controller, in general, predicts interaction-aware maneuvers of the surrounding vehicles, schedules a merging sequence, and guides a lane changer to a given slot safely by regulating trajectories of ambient controlled vehicles (Bahram et al., 2016; Evestedt et al., 2016; Scarinci et al., 2015). The merging sequence reflects the dynamic sequences of vehicles in each lane during merging, thus indicating a vehicle's future directly preceding and following vehicles respectively. Both merging sequence scheduling and trajectory control impact traffic efficiency or traffic operations.

5.1.1 Literature review

Feasible trajectory control

Initially motion planning is given more attention. Automated vehicles have a great potential to improve traffic throughput by maintaining small inter-vehicle distances. Regulating automated vehicles to have desired speeds and small inter-vehicle distances before reaching a merging point or the end of the acceleration lane becomes the main research focus in Milanés et al. (2011); Wang et al. (2013); Chen et al. (2018b); Rios-Torres and Malikopoulos (2017b); Posch and Schmidt (1984). A merging sequence, at this stage, can be coupled together with the trajectory or motion planning. In Schmidt and Posch (1983), each vehicle is assumed to reach a prescribed merging velocity with

a constant acceleration. A sequence control layer calculates predicted times-to-go of all vehicles in a control zone to a merging point and establishes a merging sequence by ascending the predicted times-to-go. Besides, the sequence control layer detects possible conflicts by comparing successive values in the ordered set of times-to-go and then assigns appropriate motion control law to a motion control layer. The motion control layer accordingly generates trajectories for vehicles to reach the predefined merging velocity and have large enough time intervals at the merging point. Moreover, when a merging sequence is predefined or given by mapping vehicles in one lane to another lane, vehicles' are controlled to reach desired inter-vehicle distances at a merging point. Remarkably, V2X communication becomes essential to transmit vehicular information (Wang et al., 2013). Different control algorithms, e.g. model predictive control, are proved to plan feasible trajectories for automated vehicles to merge safely with desired speeds or inter-vehicle distance through simulation or field tests (Milanés et al., 2011; Wang et al., 2013; Cao et al., 2015; Chen et al., 2018b). Control strategies for facilitating merging process with automated vehicles before 2013 are summarized in Scarinci and Heydecker (2014).

Efficient trajectory control with given sequence or with simple sequencing methods

Traffic efficiency and operations are then considered in trajectory control strategies for automated vehicles. In Ntousakis et al. (2016), a merging sequence is assumed to be given. Merging trajectories are planned for a vehicle by minimizing a cost function, subject to estimated final states of the vehicle at a merging point. The cost function is a weighted sum of vehicular acceleration, jerk and its first derivative. The planned trajectories ensure comfort and bring traffic efficiency. In Rios-Torres and Malikopoulos (2017a), a control zone is presented before a merging zone. CAVs inside the control zone are controlled by a centralized controller. The merging zone is the region with potential lateral collisions of the vehicles. A *first-in-first-out* rule is used to decide merging sequences. If two vehicles enter the control zone simultaneously, the centralized controller randomly selects one to have a smaller vehicle order. Vehicles are assumed to have a constant speed in the merging zone. Only one vehicle can be crossing the merging zone at a time. The controller plans an acceleration trajectory for each vehicle by minimizing a weighted sum of the accelerations during the merging process and the time headway when the vehicles are leaving the merging zone, thus reducing fuel consumption and travel time. In Xie et al. (2017), a merging sequence is scheduled by projecting on-ramp vehicles to the right-most mainline lane using a merging point as the reference. A centralized controller plans vehicular trajectories by minimizing a weighted sum of minus speeds and standard deviation of accelerations during the merging process. In Zhou et al. (2019), a state-constrained optimal control based trajectory control strategy is proposed. The speeds of mainline facilitating CAVs were bounded from below to mitigate the negative impact on the safety of the their following vehicles. However, the aforementioned studies mainly focus on trajectory control

and do not explore an optimal or sub-optimal merging sequence.

Efficient trajectory control with vehicle sequence optimization

Without changing trajectory control strategies, extra improvement on traffic efficiency can be achieved by using an optimal or sub-optimal merging sequence. Generally, different merging sequences can be evaluated when both detailed trajectory control strategies and vehicle dynamics models are known. In Athans (1969), a merging sequence is given by an assumed command and control center. The merging of two strings of vehicles into a single guideway is reduced to controlling vehicles in a single string. The merging problem is formulated as an optimal control problem. All possible merging sequences are used to get the corresponding values of the objective function of the optimal control problem. The optimal merging sequence corresponding to the minimum value is chosen. In Awal et al. (2013), the upstream vehicle closest to a defined decision point acts as a leader and establishes merging sequences for its upstream vehicles within vehicle-to-vehicle communication range. Prospective merging sequences are selected based on the estimated arriving times of mainline and on-ramp vehicles to a merging point. With each of the merging sequences, merging delay is calculated. The one corresponding to the minimum merging delay is selected as optimal. Besides, when checking different merging sequences, interaction-aware maneuver prediction can rely on surrogate linear models. In Chapter 4, a tactical layer controller uses constrained linear models to predict vehicular trajectories during merging. All possible merging sequences are successively evaluated in order to find the optimal one. An operational layer controller accepts the given optimal merging sequence and plans vehicular trajectories based on model predictive control. Moreover, sub-optimal merging sequences can be given by using certain assumptions on final vehicular states or rules. In Ding et al. (2019), the arrival times of mainline and on-ramp vehicles are assigned to form a merging sequence. The merging sequence is then adjusted according to four rules to have small time intervals between consecutive vehicles. The acceleration profile for each vehicle is generated by minimizing the square of accelerations within the assigned arrival time. If a newly detected vehicle is instructed to follow an existing vehicle in the same lane and has a short inter-vehicle distance with the target, the newly detected vehicle utilizes a linear control law to update its acceleration. In Duret et al. (2019), a tactical layer controller gives a merging sequence based on two assumptions: 1) CAVs in two platoons travels with a constant free-flow speed between their initial positions and a merging position. 2) the final platoon settles down to equilibrium at the merging location with all vehicles following Newell equilibrium conditions. A merging sequence is established by projecting initial positions of vehicles with the free-flow speed along a shock wave starting from the merging position. Besides, the tactical layer controller gives time instants when yielding vehicles start to create gaps by increasing time shifts, respectively. An operational layer is designed based on MPC. It receives tactical decisions and then plans acceleration trajectories for CAVs. In Min et al. (2020), the first controlled vehicles

in a main or an on-ramp lane accelerates to its desired speed and following vehicles utilize intelligent driver model to update accelerations in a divided game area. When one controlled vehicle is leaving the game area, a centralized controller utilizes game theory to give a merging sequence by evaluating weighted sum of three aspects: 1) the number of vehicles in each lane; 2) a vehicle's distance from a predefined merging point; and 3) the mean space distance of a vehicle from its preceding and following one. The weight vector is determined by searching the Pareto solution of minimizing fuel consumption caused by velocity and acceleration, respectively. In a divided adjusting area, vehicles follow their preceding vehicles given in the merging sequence and utilize constrained IDM to update their accelerations, respectively.

Trajectory control in mixed traffic

Improving merging efficiency in mixed traffic also draws significant attention. In Scarinci et al. (2015), CAVs in the main lane adjacent to the acceleration lane act as leaders of different platoons and collect small partial headways to form single longer ones to facilitate merging, thus reducing merging disruption. In Zhou et al. (2017), the acceleration rates of automated vehicles are determined by using a cooperative intelligent driver model. This model considers actions of surrounding vehicles. Mainline automated vehicles create larger gaps for on-ramp human-driven vehicles within their detection ranges in advance. As a result, automated vehicles eliminate freeway oscillations. In Sun et al. (2020), a ramp merging mechanism is formulated as a bi-level optimization program to give merging sequences and plan vehicular trajectories together. With the mechanism, the throughput can be further increased by 10%-15%. The mechanism can be used for mixed traffic. In some studies, lane changing behaviors of CAVs are described by lane changing models or rules for human-driven vehicles with or without certain changes (Nilsson et al., 2016; Xiao et al., 2018; Bahram et al., 2016). These lane changing models or rules lack considering possible cooperation among CAVs.

Trajectory control at on-ramp merging areas with multiple main lanes

Allowing mainline CAVs to change lane to facilitate on-ramp merging increases complexity. In Hu and Sun (2019), a rule-based lane changing decision is utilized for upstream mainline CAVs in the outer main lane in a lane changing region to balance future downstream lane flow distribution. The rule decides the lane changing proportion, thus determining the number of mainline vehicles that need to change lane. Mainline vehicles are then randomly chosen as lane changers. The lane changers' future vehicle sequences are decided by mapping their positions to their target lane. In the lane changing region, CAVs' trajectories are generated together by maximizing the total speed. In a cooperative merging region, merging sequences are assumed to be given. A CAV's trajectory is planned by maximizing its speed during merging. In Xu et al. (2020), a

bi-level cooperative driving strategy is utilized to reduce delay. An upper-level planning checks some promising passing orders generated by Monte Carlo Tree Search. The search is based on some heuristic rules and a passing-order-to-trajectory interpretation algorithm. The passing-order-to-trajectory interpretation algorithm is presented in a lower-level planning. The algorithm gives the total travel time and CAVs' acceleration trajectories. In Hang et al. (2021), each vehicle minimizes its driving safety, ride comfort, and travel efficiency cost by playing a game. Besides, an on-ramp CAV and its two adjacent passive participants in two different main lanes: a follower in its adjacent main lane and the follower of the mainline vehicle in the left main lane, play in a cooperative game to check whether extra total cost can be reduced without sacrificing each vehicle's benefit. The vehicle in the right main lane may change lane to the left to further reduce the total cost. Driving characteristics of the CAVs can be considered. Different driving characteristics bring different optimal choices for CAVs. In Ding et al. (2021), estimated delay time in an induction zone of mainline is minimized by instructing some upstream controlled CAVs in the rightmost main lane to change lane to the left. On-ramp CAVs join outer mainline traffic in the merging zone by using a *first-in-first-out* principle. The earliest and latest time instants for on-ramp CAVs to join mainline traffic at a fixed position are calculated based on vehicular initial position, speed, and allowed acceleration range, respectively. Their joining time instants are optimized together to make on-ramp vehicles join mainline traffic quickly and reduce affected CAVs' delay.

5.1.2 Knowledge gap

In summary, trajectory control methods, merging or vehicle sequences selections, and mainline facilitating lane changing maneuvers affect traffic efficiency or traffic operations during cooperative merging of CAVs. By comparison, the first two aspects are extensively studied. When CAVs travel in multiple main lanes near on-ramps, allowing mainline vehicles to change lane for facilitating merging increases both flexibility to create large spaces for merging vehicles and complexity of the controlled system. Existing control methods only allow upstream mainline vehicles to change lane to the left before entering a given merging zone, check several possible vehicle sequence combinations based on safe lane changing constraints and with an assumption that each CAV has a constant acceleration in the process, or allow at most three CAVs to play a game without sacrificing each CAV's benefit. These methods restrict lane change locations, ignore chances for CAVs to cooperatively create safe lane changing conditions, or fail to optimize overall traffic efficiency. A centralized control method is needed to systematically address lane changing maneuvers of mainline CAVs to optimize overall traffic performance during on-ramp merging.

5.1.3 Our contribution

This chapter proposes a hierarchical cooperative merging control approach to address automated merging procedures of on-ramp vehicles when mainline CAVs are allowed to change lane to facilitate on-ramp merging process. Main contributions are summarized as follows: (i) the maneuver planner centrally predicts future merging procedures in a long time horizon T, e.g. $T \geq 50$ s, by using a uniform prediction model to represent *car-following*, *cruising*, and *cooperative lane changing* maneuvers during merging and optimizes dynamic vehicle sequences in each lane by minimizing disturbances reflected by negative acceleration to upstream traffic (Daganzo et al., 1999). The prediction model is constructed based on linear microscopic traffic models. Mainline CAVs' lane changing positions are not restricted and potential vehicle sequences are not restricted by initial vehicular states. (ii) The operational trajectory controller centrally regulate vehicle accelerations by using MPC in a short time horizon T_p, e.g. T_p=6 s, and decides the time instants for lane changers to turn left. The predictive and feedback nature of MPC scheme can check feasibility of established vehicle sequences and handle predicted possible failures in time. (iii) Both the planner and operational controller considers vehicle-vehicle interaction and constrains on acceleration and speed to have safe and feasible dynamics.

5.1.4 Chapter organization

The remainder of the chapter is organized as follows. Section 5.2 presents the hierarchical cooperative merging control approach. Sections 5.3 and 5.4 elaborate on the mathematical formulations of the planner and operational controller, respectively. Section 5.5 presents simulation set-up and experimental results. Finally, Section 5.6 concludes the contribution.

5.2 Hierarchical cooperative merging control approach

A typical on-ramp merging scenario (See Figure 5.1) has two main lanes, one on-ramp lane and one acceleration lane. The lanes are numbered from right to left, with the on-ramp lane and the acceleration lane both numbered 1. On-ramp CAVs have to merge into mainline traffic, thus having path conflicts with mainline CAVs in lane 2.

The hierarchical cooperative merging control approach (See Figure 5.2) resolves possible conflicts by regulating both mainline and on-ramp CAVs' trajectories to have large enough inter-vehicle distances during merging near on-ramps. Both the planner and operational controller locate in a roadside unit (See Figure 5.1 and Figure 5.2), so that the trajectories of all CAVs can be controlled together. The roadside unit collects initial vehicle sequence, position and speed through Vehicle-to-Infrastructure communications. The planner utilizes model-based prediction and decides dynamic

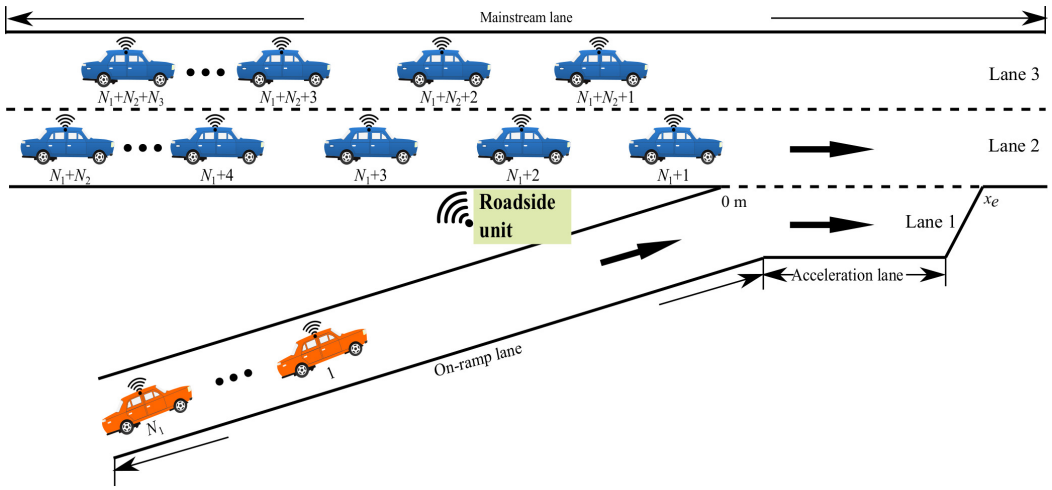

Figure 5.1: Schematic illustration of a typical on-ramp merging scenario with multiple main lanes

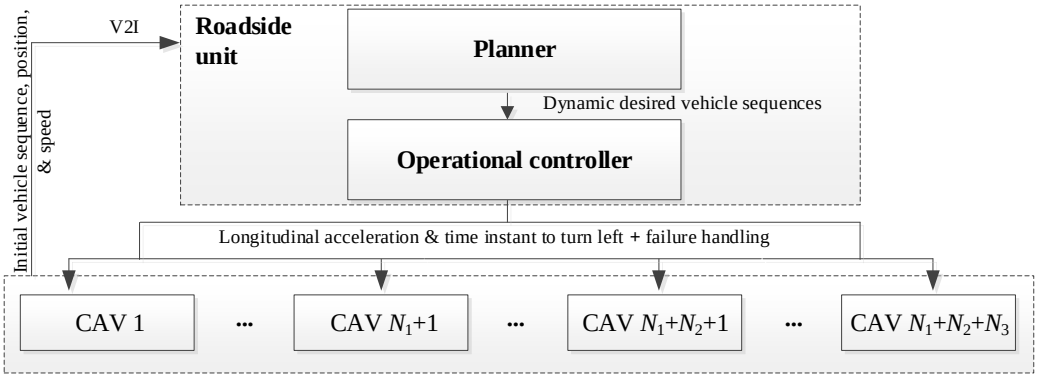

Figure 5.2: Cooperative control hierarchy for maneuver planning and trajectory control of CAVs near on-ramps

vehicle sequences in each lane by considering the mandatory lane changing demand of on-ramp vehicles and by minimizing overall disturbances to upstream mainline traffic during prediction time horizon T. The dynamic vehicle sequences are then sent to the operational controller which commands longitudinal acceleration for CAVs and time instants to turn left for lane changers respectively. On-ramp CAVs merge into mainline traffic before reaching the end of the acceleration lane. The planner performs the same function as the tactical layer controller in Chapter 4. Whereas, the planner does not explicitly establish speed-adaptation time instants.

The T in the planner is up to 50 seconds (s). The planner updates its decision at low frequencies, e.g. every 5-10 s. The operational controller updates commands at high frequencies, e.g. every $dt \leq 0.1$ s. To explore optimal vehicle trajectories near on-ramps, centralized control methods are utilized by the planner and operational controller. However, the hierarchical cooperative merging control approach is not restricted to centralized control methods and it can be extended to adapt to mixed traffic. If

the operational controller finds that an on-ramp CAV does not have large enough inter-vehicle distances with its target preceding and following CAVs for lane changing when it is approaching the end of the acceleration lane based on prediction, the operational controller overrules the given vehicle sequence for the on-ramp vehicle to find feasible and safe trajectories.

5.3 Maneuver planner: model-based optimization

The merging of on-ramp CAVs in lane 1 into mainline traffic is mandatory. The planner thus has to give feasible dynamic vehicle sequences that ensure the on-ramp CAVs to merge into mainline traffic before reaching the end of the acceleration lane. The planner answers under which conditions mainline CAVs change lane to facilitate merging attenuates disturbances to upstream traffic, which mainline vehicles change lane, and what the final vehicle orders of the mainline lane changers are. Time argument t is omitted to improve readability when no ambiguity exists.

All CAVs are numbered from 1 to N_1+N_2+N_3 (See Figure 5.1). N_i represents the initial number of CAVs in lane i. $O_{i,j}$ and $P_{i,j}$ are 0-1 variables. $O_{i,j}$ denotes the vehicle sequence between CAV i and j based on all CAVs' lateral and longitudinal positions. $O_{i,j}$=1 indicates that CAV i is CAV j's directly preceding vehicle in the same lane. Otherwise, $O_{i,j}$=0. $P_{i,j}$ denotes the desired vehicle sequence between CAV i and j according to the planner. $P_{i,j}$=1 indicates that CAV i is CAV j's target directly preceding vehicle. All CAVs in lane 1 have to change lane safely before reaching the end of the acceleration lane. To this end, at T, $\sum_{i=1}^{N_1}\sum_{1}^{N_1+N_2+N_3} O_{i,j}$+$\sum_{i=1}^{N_1+N_2+N_3}\sum_{j=1}^{N_1} O_{i,j}$=$N_1$.

5.3.1 Linear bounded models for merging prediction

The longitudinal behavior of a CAV is expressed by a second-order vehicle dynamics model. The open-loop system dynamics for each vehicle are described in Equation (5.1), where x_i, v_i, and a_i denote the location, speed, and acceleration of CAV i, respectively.

$$\dot{x}_i = v_i, \dot{v}_i = a_i, \qquad i = 1,2,\cdots,N_1+N_2+N_3 \tag{5.1}$$

To predict vehicular trajectories during future merging process, the planner borrows models from traffic flow community to represent CAVs' behavior during on-ramp merging process. Considering cases when vehicle may conflict with or directly influence each other, vehicles' motions are categorized into three maneuvers: *car-following*, *cruising*, and *cooperative lane changing*.

The *car-following* maneuver works when a vehicle follows its future directly preceding vehicle which is in the same lane, i.e., $O_{j,i}$=$P_{j,i}$. The *car-following* operation is

modeled using a car-following model used in Van Arem et al. (2006) for automated vehicles with bounded accelerations, as shown in the car-following part in the prediction model shown in Equation (5.2). The *cruising* maneuver applies to the first vehicle in each lane according to the dynamic vehicle sequences and its formulation is as shown in the cruising part in Equation (5.2), where v^{limits} can also be replaced with a desired speed set by a driver or traffic control system. The *cooperative lane changing* maneuver computes the accelerations in the cooperative lane changing process as a special case of car-following maneuver. When a vehicle's target lane is the left of its original lane according to the dynamic vehicle sequences, it starts to prepare itself to create sufficient inter-vehicle distances to execute lane change. To achieve large enough inter-vehicle distances, it and its future directly follower in the target lane are in cooperation maneuver until it accomplishes the lane change. The cooperation maneuver is formulated in the cooperative lane changing part in Equation (5.2).

$$\begin{aligned} a_i &= \underbrace{P_i^B \cdot \left[(D_1 \cdot \Delta V_i + D_2 \cdot \Delta S_i + D_3 \cdot a_j)\right] \cdot P_i^A}_{\text{car following}} \\ &+ \underbrace{P_i^C \cdot \left[(D_5 \cdot \Delta V_i + D_6 \cdot \Delta S_i + D_7 \cdot a_j)\right] \cdot (1 - P_i^A)}_{\text{cooperative lane changing}} \\ &+ \underbrace{(1 - P_i^C) \cdot D_4 \cdot \Delta V_i}_{\text{cruising}} \end{aligned} \tag{5.2}$$

where, D_1, D_2, D_3, D_4, D_5, D_6, and D_7 are model parameters; P_i^C=$\sum_{j=1}^{N_1+N_2+N_3} P_{j,i}$ and P_i^B=$\sum_{j=1}^{N_1+N_2+N_3}(P_{j,i} \cdot O_{j,i})$; ΔV_i=$(1 - \sum_{j=1}^{N_1+N_2+N_3} P_{j,i}) \cdot v_i^d + \sum_{j=1}^{N_1+N_2+N_3}(v_j \cdot P_{j,i}) - v_i$ and ΔS_i=s_i-s_i^d; s_i=$(1 - \sum_{j=1}^{N_1+N_2+N_3} P_{j,i}) \cdot (s_i^d + x_i + l_{veh}) + \sum_{j=1}^{N_1+N_2+N_3}(x_j \cdot P_{j,i}) - x_i - l_{veh}$; l_{veh} denotes vehicle length, $s_i^d = v_i \cdot t^d + s_0$ is the desired gap of CAV i, and v_i^d is the desired speed if no predecessor exists; P_i^A= $\prod_{j=1}^{N_1+N_2+N_3}(O_{j,i} \equiv P_{j,i})$ differentiates whether a CAV's directly preceding vehicle in the same lane is the desired one. P_i^C, P_i^B, and P_i^A are equal 0 or 1. If vehicle i has a desired preceding vehicle, P_i^C is 1. P_i^B is 1 when vehicle i has a desired preceding vehicle in its target lane and has a preceding vehicle in its original lane. If P_i^A is 1, vehicle i is following its desired preceding vehicle in its target lane. t^d and s_0 represent the desired time gap and the minimum inter-vehicle gap at standstill, respectively.

The acceleration calculated by the *car-following* and *cooperative lane changing* maneuvers are bounded to $[a_{\min}, a_i^s]$ to be realistic and safe, where $a_{\min}$ is the minimal negative acceleration, and a_i^s is the lower bound of maximum acceleration $a_{\max}$ and safe vehicle-vehicle interaction acceleration a_i^{int} shown in Equation (5.3).

$$a_i^{int} = \sum_{j=1}^{N_1+N_2+N_3} ((D_1 \cdot \Delta V_i + D_2 \cdot \Delta S_i + D_3 \cdot a_j) \cdot (1 - (\Delta S_i \leq 0 \wedge a_j < 0)) \cdot O_{j,i}) \tag{5.3}$$

where, $t^d_{\min}$ is the minimum safe time gap. When a vehicle is decelerating, its directly following vehicle in its original lane does not accelerate if their inter-vehicle distance is less than the follower's desired value.

5.3.2 Safe inter-vehicle distance for changing lane

When inter-vehicle distances are large enough between a lane-changer and both its future directly preceding and following vehicle, it changes lane. For on-ramp lane changers traveling in the acceleration lane, they accept a smaller but safe time gap to change lane while approaching the end of the acceleration lane, which is reflected by an acceptable time gap t^{atg} shown in Equation (5.4) (Chen et al., 2020a). x_e (See Figure 5.1) stands for the end of the acceleration lane. For a mainline lane changer, it accepts $t^d_{\min}$ to accomplish its merging maneuver. When lane-changing conditions are met, lane-changers start to steer to the left, with a fixed time duration t_m (Samiee et al., 2016; Chen et al., 2020a); after $0.5 \cdot t_m$, the lane-changer is in its target lane.

$$t^{atg} = x_i \cdot (t^d_{\min} - t^d)/x_e + t^d; \tag{5.4}$$

5.3.3 Optimization formulation: dynamic vehicle sequences

The planner is a model-based optimization model that optimizes dynamic vehicle sequences by minimizing disturbances to upstream traffic and by explicitly ensuring successful lane changing of on-ramp vehicles. Its state vector is represented by $\mathbf{Z^P}$=$(x_1, y_1, v_1, a_1, \cdots, x_{N_1+N_2+N_3}, y_{N_1+N_2+N_3}, v_{N_1+N_2+N_3}, a_{N_1+N_2+N_3})^T$ and the control vector $\mathbf{U^P} = (P_{1,1}, \cdots, P_{N_1+N_2+N_3, N_1+N_2+N_3})^T$ shows time-varying vehicle sequence for every two vehicles in each lane, where y_i denotes lateral position of CAV i.

Vector Q_2 and Q_3 representing negative accelerations of the last vehicles in main lane 2 and 3 respectively in T are chosen to reflect disturbances to upstream traffic and the Euclidean norm (or 2-norm) of them is included in the performance measure shown in Equation (5.5) (Daganzo et al., 1999). Given that On-ramp CAVs are mandatory to change lane, a vector M=$[m_1, \cdots, m_{N_1}]^T$ and a binary vector B=$[b_1, \cdots, b_{N_1}]^T$ are introduced, where m_i is a large number and b_i=0 means that on-ramp vehicle i has accomplished merging within T. To this end, b_i=1-$\sum_{j=1}^{N_1+N_2+N_3} O_{i,j}$-$\sum_{j=1}^{N_1+N_2+N_3} O_{j,i}$ at T.

$$\min_{U^P}(\|Q_2\|_2 + \|Q_3\|_2 + M^T \cdot B) \tag{5.5}$$

subject to:

- the system dynamics model shown in Equation (5.1), maneuver prediction model shown in Equation (5.2).
- the initial condition: $\mathbf{Z^P}(0) = \widetilde{\mathbf{Z}}^{\mathbf{P}}(0)$ and $\sum_{i=1}^{N_1+N_2+N_3}\sum_{j=1}^{N_1+N_2+N_3} P_{i,j}(0) = N_1 + N_2 + N_3 - 3$.
- the final condition: $N_1 + N_2 + N_3 - 2 \leq \sum_{i=1}^{N_1+N_2+N_3}\sum_{j=1}^{N_1+N_2+N_3} P_{i,j}(T) \leq N_1 + N_2 + N_3 - 1$.
- speed constraints: $0 \leq v_i \leq v^{\text{limits}}$.
- acceleration constraints: $a_{\min} \leq a_i \leq a_i^s$.

where, $\widetilde{\mathbf{Z}}^{\mathbf{P}}(0)$ is initial state at 0 s.

Equation (5.5) is a generic formulation. Extra assumptions can be made to reduce randomness and freedom of lane changing choices of mainline CAVs. To restrict lane changing times of CAV i during T, the sum of the absolute values of lateral position changes can be constrained. Besides, lane changing directions can be restricted to reduce complexity. In section 5.5, only limited number of CAVs are considered with different initial settings, and thus Equation (5.5) can be solved effectively using enumeration. However, more efficient solution methods are left to be explored for situations where enumeration is difficult or time consuming.

5.4 Operational trajectory controller: MPC approach

The operational controller optimizes vehicle trajectories by taking into account the dynamic vehicle sequences established by the planner. It is formulated as model predictive control to regulate longitudinal acceleration trajectory to reach desired vehicular states and to safely lead lane changers to their target lanes, respectively. In Chapter 4, the proposed operational layer controller regulates CAVs in one lane together. Unlike it, the operational controller in this Chapter controls all CAVs together.

The desired vehicular state for the first vehicle in each lane is to reach the desired speed. The following vehicles wish to have the same speed as their directly predecessor in target lane while keeping safe or the desired inter-vehicle distances, respectively. To this end, $\mathbf{Z^o} = (\Delta V_1, s_1, \Delta y_1, \cdots, \Delta V_{N_1+N_2+N_3}, s_{N_1+N_2+N_3}, \Delta y_{N_1+N_2+N_3})^T$ is defined as the state vector. Δy_i=y_i^t-y_i is deviation between the target and actual lateral position

of vehicle i. If Δy_i is not 0, vehicle i changes lane when ξ_i=1 and the lane changing direction depends on Δy_i. ξ_i stands for the safe lane-changing acceptability for vehicle i and is evaluated by the operational controller based on the planned acceleration trajectories and predicted vehicular positions. The control vector is defined as $\mathbf{U^o} = (a_1, \xi_1, \cdots, a_{N_1+N_2+N_3}, \xi_{N_1+N_2+N_3})^T$.

An optimal $\mathbf{U^o}$ in a finite time horizon [t_0,t_0+T_p) is given by minimizing a constructed objective function as shown in Equation (5.6). The constructed objective function penalizes deviations of vehicular states to equilibrium states where the first vehicles in each lane travel to reach desired speeds and following vehicles travel at desired inter-vehicle distances, with the same speed with directly preceding vehicles, and with zero accelerations, as shown in Equation (5.7). The minimization of the three types of deviations leads vehicles to longitudinally reach their equilibrium states gradually. Lateral decisions are established based on the planned longitudinal acceleration trajectory. ξ_i is 1 when the predicted inter-vehicle distances are larger than the accepted inter-vehicle distances of vehicle i for changing lane during T_p. The inter-vehicle distances between vehicle i with both its directly predecessor and follower in the target lane are considered. The accepted inter-vehicle distance for lane changing is the same as given in 5.3.2. When Δy_i is not 0 and ξ_i is 1, vehicle i starts to turn to its target lane. A lane changer follows a polynomial equation with a fixed time duration t_m to accomplish merging (Samiee et al., 2016; Chen et al., 2020a).

$$\min_{\mathbf{U^o}} \zeta(\mathbf{Z^o}, \mathbf{U^o}) = \min_{\mathbf{U^o}} \left(\int_{t_0}^{t_0+T_p} \psi(\mathbf{Z^o}, \mathbf{U^o}) dt \right) \tag{5.6}$$

$$\begin{aligned} \psi &= c_1 \cdot \sum_i (s_i - s_i^d)^2 + c_2 \cdot \sum_i \Delta v_i^2 + c_3 \cdot \sum_i a_i^2 \\ &= c_1 \cdot (X_1 - S^d)^2 + c_2 \cdot X_2^2 + c_3 \cdot \mathbf{A}^2 \end{aligned} \tag{5.7}$$

subject to:

- the system longitudinal dynamics model shown in Equation (5.1).
- an initial state: $\mathbf{Z^o}(t_0) = \widetilde{\mathbf{Z}}^{\mathbf{o}}(t_0)$.
- speed constraints: $0 \leq v_i \leq v^{\text{limits}}$.
- gap constraints: $s_i \geq s_0 \cdot \sum_{j=1}^{N_1+N_2+N_3} P_{j,i}$.
- acceleration constraints: $a_{\min} \leq a_i \leq a_i^{sp}$. a_i^{sp} is the maximum value of $a_{\max}$ and the first value of the optimal solution to the following optimization problem:

$$\begin{aligned} \min_{\mathbf{a_i^*}} \quad & \int_{t_0}^{t_0+T_p} \sum_{j=1}^{N_1+N_2+N_3} ((c_1 \cdot \Delta V_i^2 + c_2 \cdot \Delta S_i^2 + c_3 \cdot a_i^2) \\ & \cdot (1 - (\Delta S_i \leq 0 \wedge a_j < 0)) \cdot O_{j,i}) dt \end{aligned}$$

where, $\widetilde{\mathbf{Z}}^{\mathbf{o}}(t_0)$ is the value of the state vector at updated time instant t_0. c_1, c_2, and c_3 are weight parameters. The initial value of t_0 is 0 s. Given Δt as the control time step of the operational controller, the control command is updated periodically with $1/\Delta t$ and t_0 are multiples of Δt. With $\mathbf{X_1} = (s_1, \cdots, s_{N_1+N_2+N_3})^T$, $\mathbf{S^d} = (s_1^d, \cdots, s_{N_1+N_2+N_3}^d)^T$, $\mathbf{X_2} = (\Delta v_1, \cdots, \Delta v_{N_1+N_2+N_3})^T$, and $\mathbf{A} = (a_1, \cdots, a_{N_1+N_2+N_3})^T$, vehicle longitudinal dynamics can be described by Equation (5.8).

$$\begin{pmatrix} \mathbf{P^1} \cdot \dot{\mathbf{X}}_\mathbf{1} \\ \dot{\mathbf{X}}_\mathbf{2} \end{pmatrix} = \begin{pmatrix} \mathbf{P^1} \cdot \mathbf{X_2} \\ (\mathbf{P^2})^T \cdot \mathbf{A} - \mathbf{A} \end{pmatrix} \tag{5.8}$$

where,

$$\mathbf{P^1} = \begin{bmatrix} P_1^C & \mathbf{0} & \mathbf{0} \\ \mathbf{0} & \ddots & \mathbf{0} \\ \mathbf{0} & \mathbf{0} & P_{N_1+N_2+N_3}^C \end{bmatrix},$$

$$\mathbf{P^2} = \begin{bmatrix} P_{1,1} & \cdots & P_{1,N_1+N_2+N_3} \\ \vdots & \ddots & \vdots \\ P_{N_1+N_2+N_3,1} & \cdots & P_{N_1+N_2+N_3,N_1+N_2+N_3} \end{bmatrix}$$

5.4.1 Solution to the optimal control problem

Equation (5.6) is solved by using Pontryagin's Minimum Principle (Wang et al., 2015; Duret et al., 2019; Chen et al., 2018b). The corresponding Hamiltonian function of the optimization problem is created as shown in Equation (5.9).

$$\begin{aligned} \mathscr{H} &= c_1 \cdot (\mathbf{X_1} - \mathbf{S^d})^2 + c_2 \cdot \mathbf{X_2}^2 + c_3 \cdot \mathbf{A}^2 \\ &+ \boldsymbol{\lambda_1}^T \cdot \mathbf{P^1} \cdot \mathbf{X_2} + \boldsymbol{\lambda_2}^T \cdot ((\mathbf{P^2})^T \cdot \mathbf{A} - \mathbf{A}) \end{aligned} \tag{5.9}$$

where, $\boldsymbol{\lambda_1}$ and $\boldsymbol{\lambda_2}$ are co-state cost of the first-order differential equations of $\mathbf{P^1} \cdot \mathbf{X_1}$ and $\mathbf{X_2}$, respectively. The necessary conditions for the optimal solutions are listed in Equation (5.10), with initial state $\mathbf{Z^o}(t_0)$ given, final time t_0+T_p specified, and $\boldsymbol{\lambda_1}(t_0)$=0, $\boldsymbol{\lambda_2}(t_0)$=0, $\boldsymbol{\lambda_1}(t_0+T_p)$=0, and $\boldsymbol{\lambda_2}(t_0+T_p)$=0. We are then faced with a two-point boundary-value problem which is solved by using an iterative algorithm presented in detail in Duret et al. (2019).

$$\begin{aligned} a_i^* &= \arg\min_{a_i} \mathscr{H} \\ -d\boldsymbol{\lambda_1}/dt &= \partial\mathscr{H}/\partial(\mathbf{P^1} \cdot \mathbf{X_1}) \\ -d\boldsymbol{\lambda_2}/dt &= \partial\mathscr{H}/\partial\mathbf{X_2} \end{aligned} \tag{5.10}$$

5.5 Experiment and numerical results

A micro-simulation environment is built by coding in MATLAB R2018a. The proposed hierarchical cooperative merging control approach is then tested and validated under different merging scenarios in the simulation environment.

5.5.1 Simulation set-up

Figure 5.1 and Figure 5.3 present the basic configuration of the simulated highway on-ramp segment. Initially (See Figure 5.1) four CAVs are in lane 3 (N_3=4), five CAVs are in lane 2 (N_2=5), and one CAV is considered in the on-ramp lane (N_1=1).

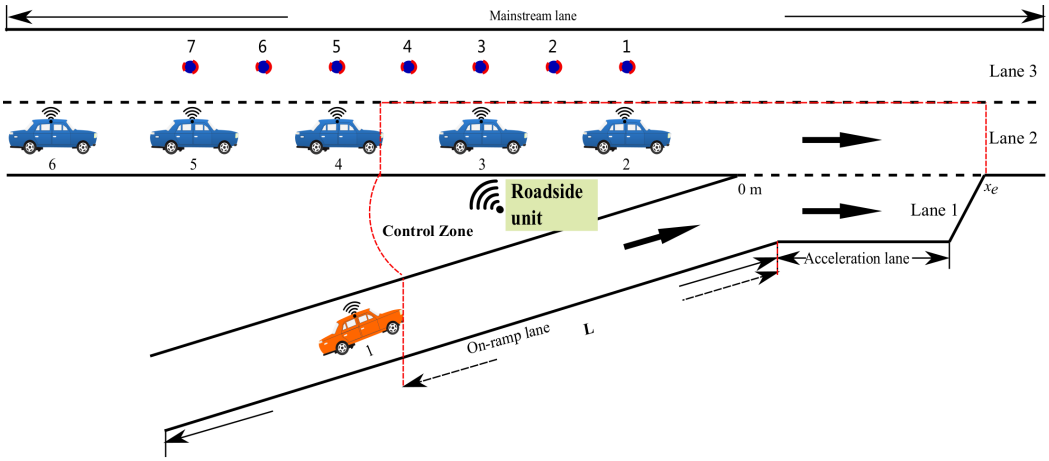

Figure 5.3: Choices of initial position for the leader of inner platoon

To understand how a mainline CAV changes lane to facilate on-ramp merging, following assumptions are made: 1) only one CAV in lane 2 may be instructed to change lane to lane 3 for facilitating the merging process; 2) CAVs in lane 3 are not allowed to change lane to the right in the mering section; 3) the on-ramp CAV has a following CAV after merging, i.e. $\sum_{j=1}^{N_1+N_2+N_3} P_{1,j}$=1. These assumptions reduce feasible dynamic vehicle sequences to Equation (5.5), and thus it can be solved effectively using enumeration.

To validate whether extra improvement in traffic operations can be brought, the proposed hierarchical cooperative merging control approach is compared with a control method which uses a *first-in-first-out* rule to establish merging sequences and the operational controller to regulate acceleration. The control zone used by the *first-in-first-out* rule is plotted with red dotted lines in Figure 5.3. A vehicle enters into the control zone first is instructed to leave first. When two vehicles enter into the control zone together, priority is given to the mainline vehicle. Vehicles in lane 2 are not instructed to change lane to lane 3. To avoid confusion, the selected control method for comparison is called the *first-in-first-out* method. Besides, a lower-level steering and longitudinal

control controller is assumed to follow the planned trajectories precisely without any delay.

The initial setting for CAVs includes vehicular position, speed, and desired time gap at 0 s. 528 different initial settings are chosen. The on-ramp CAV initially starts from the upstream boundary of the control zone -L (See Figure 5.3). Two distinguishable situations are considered based on the initial longitudinal position of the on-ramp CAV 1, mainline CAV 4 and 5: (a) the on-ramp CAV has the same value as mainline CAV 4 (See Figure 5.3), and (b) the on-ramp CAV is in the middle of the two mainline CAVs (See Figure 5.1). The initial speed of the on-ramp CAV entering into the control zone is given 15 m/s, 20 m/s, or 25 m/s.

The desired time gap for all CAVs is set to be 0.6 s, 0.8 s, 1 s, or 1.2 s. CAVs' initial speeds in lane 2 are 25 m/s and inter-vehicle distances are desired values. CAV 2 keeps 25 m/s. Given inter-vehicle distances, CAV 1's position, and (a) or (b), the initial vehicular positions of CAVs in lane 2 are set by calculation.

Two types of situations are constructed in lane 3: (i) free flow where CAVs travel with speed limits respectively and are sparsely distributed; and (ii) crowded traffic where CAVs are traveling with speeds lower than the speed limits and are affected by their directly preceding vehicles in the same lane. For the free flow situation, the CAVs in lane 3 travel with v^{limits}, 30 m/s, and are far away downstream. By comparison, for the crowded traffic situation, CAVs in lane 3 travel with 25 m/s and are close to CAVs in lane 2. The longitudinal position of the first CAV in lane 3, CAV 7, is given 7 potential positions which are shown with numbered dots in Figure 5.3. Starting from a dot with an odd number, it longitudinally has the same position as a mainline CAV in lane 2; otherwise, it is in the middle of two consecutive mainline CAVs. The initial inter-vehicle distance for CAV 8 is given three different options: equilibrium state, a large gap, or a small gap, with time gap being 1, 2 or 0.5 times of its desired value, respectively.

Table 5.1 shows the setting of one scenario. Under the scenario, the detailed performance of the controllers are analyzed in subsection 5.5.3.

Table 5.1: The setting of 1 scenario

Scenario type	$v_2(0)$	$v_7(0)$	t_d	RP	$v_1(0)$	$x_1(0)$	$x_7(0)$
Large gap	25 m/s	25 m/s	1	0%	25 m/s	type (b)	dot 2

The parameters selected for the defined variables are based on published literature or off-line calibration. T=50 s, $\Delta\hat{t}$=0.5 s, T_p=6 s, Δt=0.1 s, L=62 m, v^{limits}=30 m/s, s_0=2 m, l_{veh}=4 m, t_m=2 s, D_1=0.2, D_2=0.7, D_3=0.6, D_4=0.8, D_5=0.2, D_6=0.5, D_7=0, $a_{\max}$=2 m/s^2, $a_{\min}$=-4 m/s^2, x_e=300 m, $t^d_{\min}$=0.25 s, c_1=0.1, c_2=0.5, and c_3=0.5. The simulation time is 50 s.

5.5.2 Overall simulation results

Figure 5.4 presents the overall performance comparison between the proposed hierarchical cooperative merging control approach and the *first-in-first-out* method, by considering the generated disturbances to upstream traffic caused by utilizing the two control methods throughout simulation, respectively. The reduction rate is calculated by dividing the difference between them by the disturbances caused by using the *first-in-first-out* method and then multiplying the answer by 100. The negative values, from -11% to -91%, show the reduction in disturbances with the the hierarchical cooperative merging control approach.

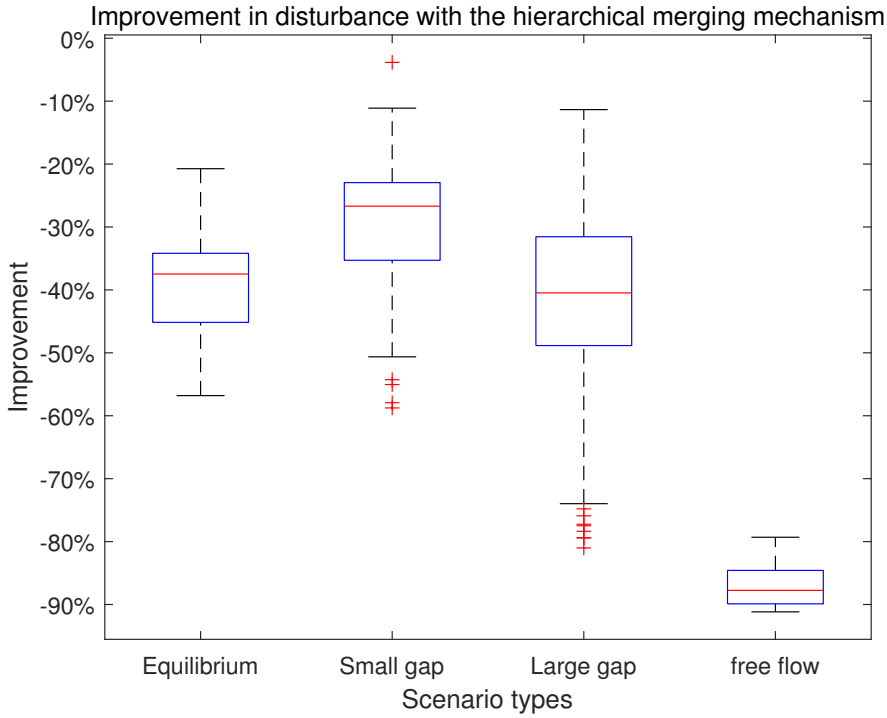

Figure 5.4: Performance comparison between the proposed hierarchical cooperative merging control approach and the *first-in-first-out* method

The *first-in-first-out* method assigns the on-ramp CAV to follow CAV 4 under all simulation scenarios. By comparison, the hierarchical cooperative merging control approach schedules different dynamic vehicle sequences based on all CAVs' vehicular states. Under equilibrium scenarios, it tends to make CAV 1 accelerate to a higher speed if CAV 1's initial speed is low or gives CAV 1 a small vehicle order in lane 2 , without making a mainline CAV change lane. For the remaining simulation scenarios, when no mainline CAV is instructed to change lane, vehicular states in lane 3 do not influence the scheduled merging sequences and thus the merging sequences are given the same as the equilibrium scenarios, respectively. Under small gap scenarios, for 70 out of the 168 scenarios, a mainline CAV in lane 2 is instructed to change lane to lane 3. Because the existence of small gaps introduces extra disturbances to lane 3 compared

with the equilibrium scenarios, the average reduction in disturbances does not excel the equilibrium scenarios obviously (See Figure 5.4). However, instructing a mainline CAV in lane 2 to change lane when a small gap exists in lane 3 during merging may bring extra benefits, which is shown by the outliers in Figure 5.4). Obviously, large reduction rate in disturbances shows up when a large space exists in lane 3. The average reduction rates in disturbances for the large gap are bigger than equilibrium scenarios, even though large gaps, like the small gaps, also introduce extra disturbances to lane 3. Under the large gap scenarios, a mainline CAV in lane 2 is instructed to change lane during merging for 109 out of the 168 scenarios. Compared with the small gap scenarios, large gap scenarios have higher potential to further reduce disturbances through lane changing behavior of mainline CAVs (See Figure 5.4). For the free flow scenarios, the on-ramp CAV occupies the gap created by a lane changer in lane 2, thus bringing even bigger reduction rates in disturbances.

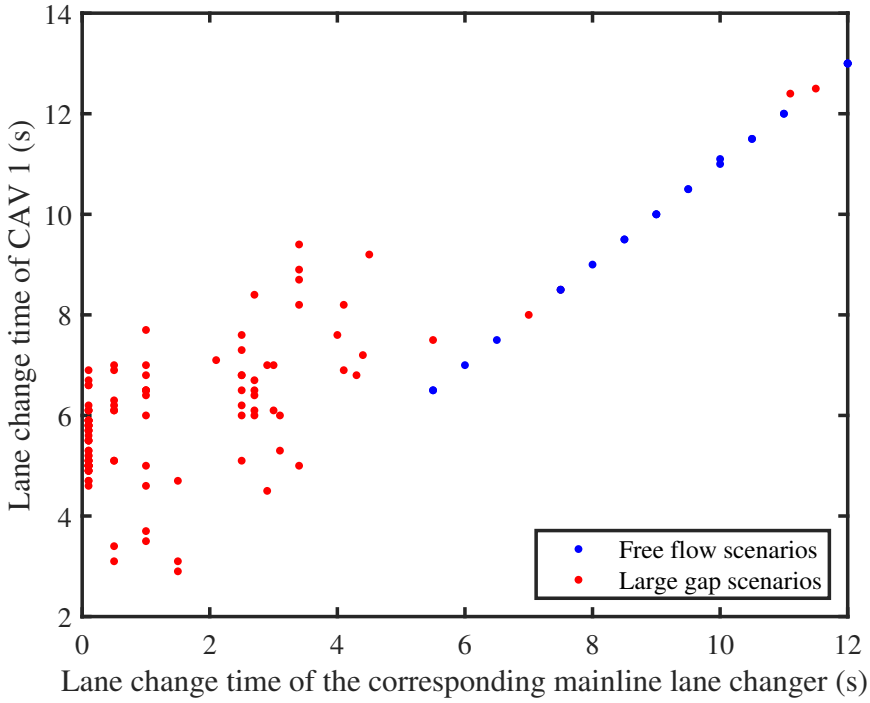

Figure 5.5: Correlation between lane change time of CAV 1 and the corresponding mainline lane changer under the 109 large gap scenarios and free flow scenarios

Figure 5.5 visualizes the correlation between time instants to change lane of the on-ramp CAV and the mainline lane changers under the 109 large gap scenarios and free flow scenarios. Under these scenarios, CAV 1's lane change time is at least 1 s later than the mainline lane changer. Noticeably, mainline lane changers are given 2 s to accomplish lane changing. 1 s after their lane change time instants, they have already left lane 2, respectively. To this end, the on-ramp CAV 1 starts to change lane after mainline lane changers have left lane 2, respectively. This indicates that disturbances to upstream traffic in lane 2 can reduce with a large gap following or being utilized by CAV 1. Under free flow scenarios, the deviation of the two lane changers' lane

change time is 1 s and CAV 1 utilizes the slots created by mainline lane changers for merging. For free flow scenarios, lane changers do not bring extra disturbances to lane 3; and thus, the control target relaxes to reduce disturbances to upstream traffic in lane 2. A small vehicle order is given to CAV 1 to further reduce disturbances. The mainline lane changers start to change lane when CAV 1's target lane changes to lane 2. The differences in lane change times for mainline lane changers are caused by the differences in on-ramp CAV 1's initial speed and position. For the 109 large gap scenarios, the behavior of a mainline lane changer may reduce disturbances in lane 3. As a result, the lane change times for lane changers are results of trade-offs to have minimal disturbances to upstream traffic.

5.5.3 A large gap scenario

The performance of the hierarchical cooperative merging control approach is presented in detail for a large gap scenario (See Table 5.1). The large gap scenario has the following initial settings: 1) all CAVs start from 25 m/s; 2) the on-ramp CAV's position type is (b); 3) longitudinal position of 7 starts from dot 2 in Figure 5.3; 4) the desired time gap is 1 s.

Planner results

Before 0.5 s, the planner instructs no CAV to change its target lane. At 0.5 s, the CAV 3 is instructed to follow CAV 7. At 3 s, the on-ramp CAV's target preceding vehicle is given CAV 4. The vehicle orders of other CAVs in each lane change accordingly when a CAV's desired vehicle sequence changes.

Trajectories

Figure 5.6 and Figure 5.7 show the acceleration and position trajectories in lane 1, lane 2, and lane 3, respectively, with the *first-in-first-out* method. Figure 5.6(b) shows CAV 1's acceleration in lane 1 with black dashed line when CAVs in lane 2 and lane 1 affect each other to generate acceleration.

Acceleration trajectories are reasonable based on the control objective of the operational controller with the *first-in-first-out* method. The *first-in-first-out* method assigns the on-ramp CAV to follow CAV 4 at 0 s. As a result, the initial gap errors for CAV 1 and 5 are negative. They decelerate and CAV 4 accelerates to reduce the gap errors. The deceleration of CAV 5 makes CAV 6's relative speed positive and gap error negative, and thus CAV 6 decelerate. Similarly, because the acceleration of CAV 4 makes its relative speed negative and gap error negative, CAV 3 accelerates. CAVs in lane 2 relax to equilibrium states respectively at around 20 s. At 5.2 s, CAV 1 is on the acceleration lane and has large enough inter-vehicle distances to CAV 4 and 5 respectively,

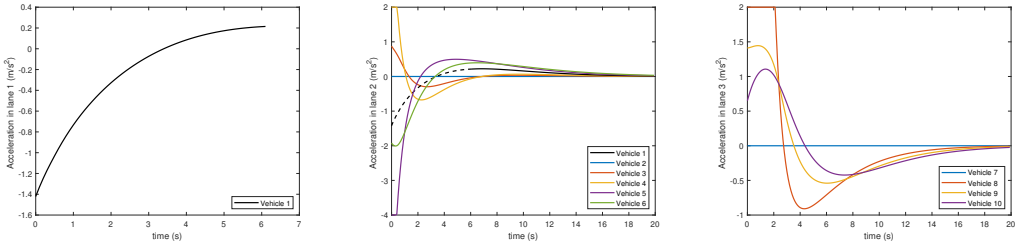

(a) lane 1 (b) Lane 2 (c) Lane 3

Figure 5.6: Acceleration trajectories with the *first-in-first-out* method

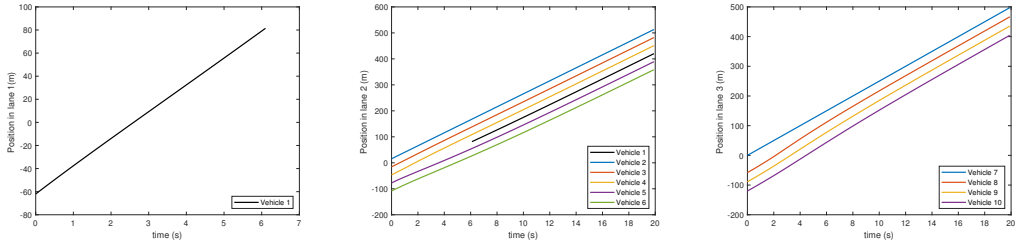

(a) lane 1 (b) Lane 2 (c) Lane 3

Figure 5.7: Position trajectories with the *first-in-first-out* method

and thus CAV 1 starts to turn left (See Figure 5.7(b)). In lane 3, initially CAV 8 has positive gap error and thus it accelerates. This makes CAV 9's relative speed and gap error negative, and thus CAV 9 accelerates. Likewise, CAV 10 accelerates to reduce negative relative speed and gap error brought by CAV 9's acceleration.

Figure 5.8 and Figure 5.9 illustrate the acceleration and position trajectories with the proposed hierarchical cooperative merging control approach in lane 1, lane 2, and lane 3, respectively. To clear show the interaction of CAVs from two different lanes during lane changing processes, Figure 5.8(b) uses black dashed line to show corresponding CAV 1's acceleration trajectory in lane 1; Figure 5.8(c) uses red dashed line to show corresponding CAV 3's acceleration trajectory in lane 2.

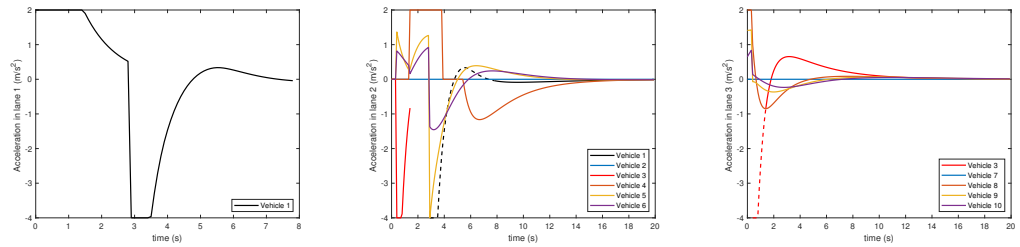

(a) lane 1 (b) Lane 2 (c) Lane 3

Figure 5.8: Acceleration trajectories with the proposed hierarchical cooperative merging control approach

Figure 5.8(b) shows three different obvious stages divided by 0.5 s, 1.5 s, and 3 s. At

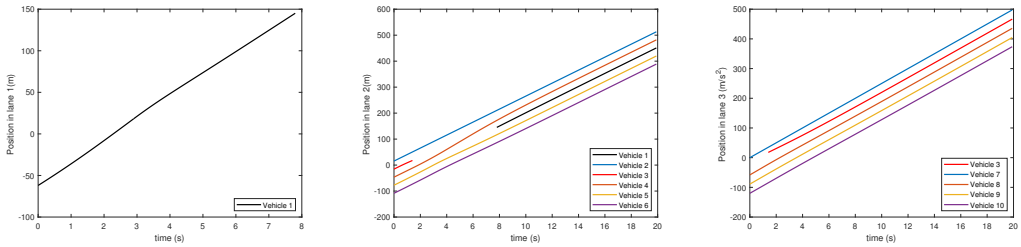

(a) lane 1 (b) Lane 2 (c) Lane 3

Figure 5.9: Position trajectories with the proposed hierarchical cooperative merging control approach

0.5 s, CAV 3 is given CAV 7 as its desired directly preceding CAV. CAV 4 has a positive gap error and it is instructed to accelerate if the acceleration constraints are ignored. CAV 5 and CAV 6 accelerate accordingly to reduce gap errors and relative speeds caused by their directly preceding vehicles' acceleration, respectively. However, CAV 3 decelerates with -4 m/s^2, CAV 4 is constrained to not accelerate, thus remaining 0 m/s^2. At 0.5 s, CAV 3 has large enough inter-vehicle distances to its surrounding vehicles and starts to turn left (See Figure 5.9(b) and Figure 5.9(c)). At 1.5 s, CAV 3 is in lane 3, it no longer affects CAV 4 and CAV 4 starts to accelerate to reduce its gap error. Before 3 s, the CAV 1 accelerates to reach the speed limits. At 3 s, the on-ramp CAV is given CAV 4 as its desired directly preceding vehicle. CAV 4 still has a positive gap error and it accelerates. CAV 1 has negative gap error (See Figure 5.9(b)) and negative relative speed, and thus it decelerates. CAV 5 has negative relative speed, and thus it decelerates. CAVs in lane 2 relax to their equilibrium states respectively at around 17 s, quicker than the situation with the *first-in-first-out* method.

In lane 3, before 0.5 s, CAV 8 accelerates to reduce its positive gap error. CAV 9 and 10 accelerates as well to lessen their gap error and relative speed caused by their preceding vehicle's acceleration, respectively. At 0.5 s, CAV 3 has negative gap error and decelerates. CAV 8 still has a positive gap error and accelerates (See Figure 5.9(c) and Figure 5.6(c)). CAVs in lane 3 relax to their equilibrium states respectively at around 15 s, quicker than the situation with the *first-in-first-out* method.

Performance indicators

The total disturbances for the upstream traffic during simulation and average speed before leaving the end of the acceleration lane are selected by comparison. Their values are recorded to the nearest two decimal points. With the *first-in-first-out* method, the overall disturbances is 10.40 m/s^2 and the average speed is 25.03 m/s. The proposed hierarchical cooperative merging control approach brings 6.45 m/s^2 and 25.12 m/s. By comparison, the hierarchical cooperative merging control approach reduces the disturbances by 37.94% and improves average speed by 0.36%.

5.5.4 Discussion

By considering only one on-ramp CAV and assuming one mainline CAV may change lane to the left during merging, the possible combination of vehicle orders are countable and can be solved easily by enumeration. When more on-ramp CAVs are considered together and mainline CAVs are given more freedom to change lane, an effective solution for Equation (5.5) is needed to enhance computation efficiency.

Simulation results show that the proposed hierarchical cooperative merging control approach outperforms the *first-in-first-out* method to reduce disturbances to upstream traffic (See Figure 5.4). This implies that extra improvement in traffic operations can be achieved by exploring an optimal or a sub-optimal merging sequence.

By observation, the hierarchical cooperative merging control approach tends to make the on-ramp CAV (CAV 1) have a small vehicle order in lane 2 under equilibrium situations or when no mainline CAV is instructed to change lane, and allows CAV 1 to accelerate for several seconds to get closer to downstream mainline CAVs in lane 2. The on-ramp CAV can reach the speed limits 30 m/s before it is given its desired future directly preceding vehicle or a merging sequence. Compared with the situations when a small gap exists in lane 3, when a large space exists in lane 3, the hierarchical cooperative merging control approach is more likely to instruct a mainline CAV close to the large gap in lane 2 to change lane. Besides, the on-ramp CAV is given a new merging sequence no earlier than the mainline lane changer. The possibility that the on-ramp CAV utilizes the space generated by the mainline lane changer is high.

Under the 109 large gap scenarios and free flow scenarios where a mainline CAV is instructed to change lane by the hierarchical cooperative merging control approach, the on-ramp CAV 1 waits to change lane until the mainline lane changers have left lane 2 (See Figure 5.5). However, under some scenarios, the CAV 1 do not directly use the gap created by the mainline lane changers to change lane. Compared with the choices of not allowing a mainline CAV to change lane, disturbances to upstream traffic have obviously reduced (See Figure 5.4). This implies that the existence of large gaps in lane 2 during on-ramp merging is helpful to reduce traffic disturbances. Assuming not taking other measures, if a mainline CAV's lane changing behavior does not add much disturbances to lane 3, making it to change lane may improve overall traffic operations during on-ramp merging.

Optimal merging sequences are affected by both the planner's control objectives and the restrictions on mainline CAVs. The disturbances to upstream traffic are selected as a performance indicator to choose an optimal merging sequence by the planner. Besides, average speed, total travel time, control objectives of the operational controller, or time duration for on-ramp CAVs to accomplish merging can also be chosen as a performance indicator. The optimal merging sequences can be different accordingly (Chen et al., 2020a; Athans, 1969; Awal et al., 2013; Duret et al., 2019; Chen et al., 2020b; Ding et al., 2021). Distinguishing which performance indicators are critical in traffic management is an important research direction. When a mainline CAV is

allowed to change lane, traffic operations can be further improved (See Figure 5.4). Relaxing restriction on lane changing maneuvers of mainline CAVs during merging is a promising research direction for efficient on-ramp merging in the future.

In subsection 5.5.3, the hierarchical cooperative merging control approach reduces the disturbances by 37.94%. Surprisingly, the average speed is only improved by 0.36%. To this end, attenuating traffic disturbances during merging may not bring significant improvement in average speed.

CAVs in lane 2 may change lane to improve merging efficiency when a CAV's inter-vehicle distance is smaller than its desired value in lane 3 (See Figure 5.4). Existing lane changing models cannot cover this point. To this end, exploring new lane changing models for CAVs which consider possible cooperation among CAVs is another promising research direction for merging.

5.6 Conclusion and outlook

The proposed hierarchical cooperative merging control approach has a maneuver planner and an operational trajectory controller which are formulated as model-based optimization, respectively. Importantly, the planner uses a linear prediction model to represent interactions among CAVs during merging. The planner, thus, can evaluate different dynamic vehicle sequences with a performance indicator (See Equation (5.5)), and then establish optimal dynamic vehicle sequences in multiple lanes in a long time horizon. The operational controller regulates longitudinal acceleration trajectories and time instants for lane changers to change lane by utilizing model predictive control, subject to admissible gap, speed, and acceleration constraints.

Figure 5.4 shows that the proposed hierarchical cooperative merging control approach may outperform the *first-in-first-out* method under 528 different initial settings including desired time gap, speed, and position of CAVs, bringing 11% to 91% reduction ratios in traffic disturbances.

Remarkably, the hierarchical control approach does not have restrictions on formulations of controllers, vehicle types, road layouts, or assumptions on lane changing choices. To this end, it can be easily extended. To adapt to mixed traffic conditions, the hierarchical control approach can be further extended by including the interaction between automated vehicles and human-driven vehicles in the planner and operational controller, respectively. This will be addressed in our future research. In the next chapter, the main findings of this thesis are summarized and future research directions are given.

Chapter 6

Conclusions

The thesis is motivated by the research needs in cooperative merging control for CAVs near on-ramps outlined in Chapter 1. The main objective is to design cooperative driving strategies for CAVs near on-ramps considering controller performance, safe lane changing, maneuver planning, and trajectory control. Four sub-objectives are stated under the research objective. They are answered by chapters 2-5. This chapter summarizes the main findings in Section 6.1. Section 6.2 draws conclusions based on the findings. The implications of the thesis work for practice are discussed in Section 6.3. Section 6.4 recommends future research directions.

6.1 Findings

This thesis deals with the development of coordination strategies near on-ramps. They mainly focus on different aspects regarding controller performance, safe lane changing conditions, merging sequence, and acceleration trajectory control. Their performance, impacts on traffic operations, and flexibility to adapt to mixed traffic are examined via numerical simulations. The main findings are highlighted here. We structure the main findings around a number of contributions.

Robust control approach

Chapter 2 addresses the first sub-objective *to develop a robust platooning control method* by design a robust MPC controller. The key feature of the approach is that at each control time step, a Min-Max MPC problem is solved, which entails predicting the behavior of involved vehicles based on the current vehicular states and generating optimal acceleration trajectories by minimizing the maximum value of a cost function brought by model uncertainties. At the following new control time step, the optimal trajectories are computed with updated measurements. The cost function reflects control objectives, such as maximizing efficiency, keeping safety, and minimizing control effort. In mixed traffic, the behavior of human-driven vehicles is roughly predicted with a car-following model. In comparison to a nominal MPC method that using a nominal model, the experimental results have shown that the proposed approach has superiority and is robust to have string stability regardless of model uncertainties and feedback delay in both 100% CAV environment and mixed traffic.

The difference between the Min-Max MPC controller and a nominal MPC controller, which uses a nominal model for prediction without considering uncertainty, is the Min-Max formulation. To this end, the robustness of a MPC approach to model uncertainties can be ensured by adding Min-Max. This finding may support researchers in ignoring the robustness of a MPC approach to mainly focus on other control objectives in the design stage.

Safe merging condition

In Chapter 3, longitudinal acceleration trajectories for CAVs are generated by using our MPC controller. We present a safe merging evaluation approach based on predicted vehicular states. An on-ramp CAV meets its safe lane changing condition when its predicted inter-vehicle time gaps with surrounding vehicles are larger than the accepted time gaps for merging. The acceptable time gap decreases while it is approaching the end of the acceleration lane. When its safe merging condition is met, it is instructed to follow a lateral trajectory equation to achieve automatic merging. To this

end, the second sub-objective, *to develop a cooperative merging strategy which allows on-ramp CAVs to merge before they reach their desired inter-vehicle distances to preceding vehicles and their desired speeds, and assists CAVs to accomplish merging automatically*, is achieved. Noticeably, the traffic efficiency is not sacrificed for merging safety in the merging process. Simulation experiments showed no collision existed with the corresponding merging strategy and on-ramp CAVs can merge safely with shorter inter-vehicle distances than their desired values.

Hierarchical control architecture

A hierarchical control architecture is proposed in Chapters 4 and 5. It is generic and has no restrictions on control approaches for its two layers. The generality and application of it are shown in Chapters 4 and 5. In Chapters 4 and 5, the upper-level controller establishes optimal merging sequences for two streams of traffic or vehicle sequence in each lane. The lower-level controller generates longitudinal acceleration trajectories and time instants for lane changers to change lane. The two controllers work together to coordinate trajectories of CAVs to improve traffic operations near on-ramps.

Without repeating future detailed merging process exhaustively, the optimal merging or vehicle sequence can be established. Surrogate linear models of real vehicle trajectories regulated by the lower-level controller have been used to predict future vehicles' cruising, car-following, and cooperative lane changing maneuvers during the maneuver planning stage. Simulation results showed that the established optimal merging or vehicle sequences outperformed those generated by applying the $first-in-first-out$ rule to improve traffic operations.

Using different control objectives, the established optimal merging sequences by the upper-level controller can be different. Chapter 4 focuses on exploring a new approach to have optimal merging sequences. Thus, optimal merging sequences are established to minimizing the same objective function as the lower-level controller. By observing the optimal merging sequences, we found that on-ramp CAVs with lower initial speeds were given time to reduce the speed difference with the mainline traffic. Besides, relative positions affected the given vehicle sequence for an on-ramp CAV after it finished cruising. If it was around the middle of two mainline CAVs longitudinally, it was potentially instructed to follow the mainline downstream CAV. The sub-objective *to develop a cooperative merging strategy which uses a new approach to seek the optimal merging sequence and regulates CAVs' lateral and longitudinal trajectories to accomplish merging* is achieved.

By comparison, Chapter 5 establishes optimal dynamic vehicle sequences by minimizing disturbances to upstream traffic. Mainline CAVs may change lane to facilitate the merging of on-ramp CAVs. Simulation results have shown that a mainline CAV may be instructed to change lane to facilitate the merging of on-ramp CAVs when its left lane has large gaps. If no mainline CAV changes lane, on-ramp CAVs are found

to have a small vehicle sequence in their final target lanes. Note it is allowed to cruise for several seconds to be close to downstream mainline vehicles before its target lane changes. The sub-objective *to develop a cooperative merging strategy which allows mainline CAVs to change lane to facilitate the merging process of on-ramp CAVs* is fulfilled.

Computational performance of centralized control approaches

In Chapter 4, centralized control approaches are used in formulating both the upper-level and lower-level controllers. The upper-level controller has a looking-ahead horizon 50 seconds (s) and the lower-level controller's control time horizon is 6 s. When one on-ramp CAV and five mainline CAVs exist, the computation time of the upper-level controller is 0.32 s and the computation time of the lower-level controller is 0.91 s. When the number of on-ramp CAVs increases to two, the computation times for the two controllers become 4.8 s and 1.12 s. The incremental computation for the upper-level controller may be caused by the increasing numbers of possible combinations and by utilizing the enumeration algorithm as a solution approach. The computation times of the centralized control approaches are not small enough to be negligible.

Initiation time for cooperation

According to the optimal merging or vehicle sequence in the simulation experiments of Chapters 4 and 5, on-ramp CAVs were allowed to cruise for several seconds to increase speed, adjust position, or get close to downstream traffic. Even though the optimal merging sequence relates to the constructed control objectives of the upper-level controller, the observed phenomenon is sufficient to show that allowing on-ramp CAVs to cruise can bring benefits to improve traffic operations.

6.2 Conclusions

This thesis has proposed several control strategies for CAVs to improve traffic operations near on-ramps on motorways. We present the main conclusions here based on the formulations of those control strategies and findings.

In Chapter 2, the Min-Max MPC controller seemed to have robust performance to keep string stability in 100% CAV environment and mixed traffic. This may suggest the Min-Max MPC controller is robust and flexible to different traffic scenarios, although only two simulation experiments were conducted. Noticeably, the difference between Min-Max MPC and MPC is the Min-Max formulation. This may show that MPC approaches can ignore robustness at design stages.

In Chapter 3, on-ramp CAVs merged by accepting smaller time gaps than their desired values and accomplished merging automatically without collision. Possible collisions were prevented by checking the predicted time gaps were all larger than the accepted one. This suggests with model-based prediction, on-ramp CAVs can merge with smaller time gaps, and thus merging efficiency can be improved. Besides, safe lateral maneuvers were accomplished by following trajectory equations which generate human-like lateral trajectories for people.

In Chapter 4, our hierarchical model-based control approach seems to establish optimal merging sequence and generate plausible behaviors for CAVs during on-ramp merging. In fact, simulation results have shown the established merging sequence improves traffic operations better than that by using the first-in-first-out rule. We found that surrogate linear models instead of the detailed MPC approach may be used to predict future merging process. Besides, coordination between mainline and on-ramp CAVs to prepare for merging started when on-ramp CAVs had close speeds to mainline traffic. We could guess that allowing on-ramp CAVs with lower speeds to cruise for several seconds to increase their speeds brought benefits in improving traffic operations.

In Chapter 5, with our proposed maneuver planning strategy, lane changing behaviors of mainline CAVs brought extra improvement in traffic operations. When a large gap existed in the left main lane, a mainline CAV in the right main lane potentially changed lane. Safe and plausible trajectories of CAVs during merging were observed. This suggests that our trajectory control approach is feasible. Chapters 4 and 5 together suggest that using different objective functions may generate different decisions on lateral maneuvers.

6.3 Implications for practice

The findings and conclusions of this thesis provide several practical implications regarding the design and assessment of cooperative merging strategies for CAVs. The proposed robust control strategy can be referred to or applied by researchers, CAV developers, fleet owners, and vehicle manufacturers to develop robust controllers for CAVs. Traffic operators and policymakers are supported to design different test fields and assess manufactured CAVs under different road and weather conditions. They are advised to admit those manufactured CAVs only if they maintain string stability in all the tests.

Researchers are provided with a prediction-based approach to check whether accepting a gap for lane changing is safe. It can be utilized by researchers: (i) to evaluate whether collisions are avoidable when a lane changer uses a gap for lane changing; (ii) to design new efficient cooperative merging strategies for CAVs; (iii) to design new safe lane changing strategies for CAVs in mixed traffic.

Merging sequences or vehicle sequences matter in improving traffic operations. The best location for the upper-level controllers of our hierarchical control approaches is a roadside infrastructure near the start of the acceleration lane. The road operator is advised to deploy a roadside infrastructure that can contain the upper-level centralized controller in the future. We have given recommendations on using the first-in-first-out rule to establish merging sequences based on the simulation results. Those recommendations can be used by traffic operators and researchers. Besides, researchers and traffic operators can use our upper-level controllers to schedule merging or vehicle sequences.

The designed hierarchical control architecture support researchers to design new cooperative merging strategies. Besides, the centralized trajectory control approach for CAVs in three different lanes is presented in Chapter 5. This approach can be referred to or used by researchers in designing new cooperative merging strategies that allow mainline CAVs to change lane.

6.4 Recommendations for future research

This thesis presents a robust Min-Max MPC controller for homogeneous and heterogeneous platooning control by considering parametric uncertainties of the vehicle dynamics model. Noticeably, unmeasured disturbance or noises may exist in driving environments and affect the performance of designed controllers. To this end, a future step is to design a robust MPC controller considering both model uncertainties and unmeasured noises. Besides, future research is recommended to investigate analytic approaches using Lyapunov theory to guarantee string stability of vehicle platoons and robust lane change control in mixed traffic to improve traffic operations.

The proposed flexible cooperative merging strategy checks lane changing safety by using predicted vehicular states. It is tested without considering possible model mismatches. A future research direction is to construct a robust control approach based on it if necessary. Besides, it is designed considering a 100% CAV environment. When human-driven vehicles exist and the market penetration of the CAVs is low, safe lane changing conditions are still challenging. A future step is to design a merging strategy which ensures safe lane changing in mixed traffic. A trade-off between safety and traffic efficiency should be considered in the design.

Optimal merging sequences for two streams of traffic are considered by this thesis in 100% CAV market penetration. Centralized control methods are utilized by the tactical layer controller and the operational layer controller to plan lateral maneuvers and control trajectory. A future research direction can be to develop decentralized control methods to achieve the same functions because the computation time of the centralized control approaches are found computationally complex. In mixed traffic, determining optimal merging sequences or planning safe trajectories for on-ramp CAVs during merging becomes challenging because human-driven vehicles cannot be controlled and

possible cooperation among CAVs is thus limited. Consequently, a future direction is to investigate optimal merging sequences and design trajectory control methods in mixed traffic.

This thesis have constructed a uniform prediction model for vehicular behavior anticipation during merging in the planner. The operational controller is formulated to easily implement established dynamic vehicle sequences in a centralized way. Both the planner and the operational controller can address complex merging scenarios allowing mainline CAVs to change lane. To have insights on the correlation between on-ramp lane changers and mainline lane changers, only one mainline CAV is assumed to change lane and it is only allowed to turn left during each control cycle of the planner. A future research direction is to relax constraints on the number of mainline lane changers and lane changing directions to systematically explore how mainline CAVs behave to have a safe and efficient merging process. Apart from that, a future research direction is to explore decentralized control approaches to establish lane changing decisions for mainline CAVs and/or on-ramp CAVs to improve traffic operations near on-ramps under different CAV market penetrations.

Bibliography

Arnold, E. et al. (1998). Ramp metering: a review of the literature.

Athans, M. (1969). A unified approach to the vehicle-merging problem. *Transportation Research*, 3(1):123–133.

Awal, T., Kulik, L., and Ramamohanrao, K. (2013). Optimal traffic merging strategy for communication-and sensor-enabled vehicles. In *16th International IEEE Conference on Intelligent Transportation Systems (ITSC 2013)*, pages 1468–1474. IEEE.

Bahram, M., Hubmann, C., Lawitzky, A., Aeberhard, M., and Wollherr, D. (2016). A combined model-and learning-based framework for interaction-aware maneuver prediction. *IEEE Transactions on Intelligent Transportation Systems*, 17(6):1538–1550.

Barth, M. and Boriboonsomsin, K. (2009). Traffic congestion and greenhouse gases. *Access Magazine*, 1(35):2–9.

Boggs, P. T. and Tolle, J. W. (1995). Sequential quadratic programming. *Acta Numerica*, 4:1–51.

Brackstone, M. and McDonald, M. (1999). Car-following: a historical review. *Transportation Research Part F: Traffic Psychology and Behaviour*, 2(4):181–196.

Camponogara, E., Jia, D., Krogh, B. H., and et al. (2002). Distributed model predictive control. *IEEE Control Systems Magazine*, 22(1):44–52.

Cao, W., Mukai, M., Kawabe, T., Nishira, H., and Fujiki, N. (2014). Gap selection and path generation during merging maneuver of automobile using real-time optimization. *SICE Journal of Control, Measurement, and System Integration*, 7(4):227–236.

Cao, W., Mukai, M., Kawabe, T., Nishira, H., and Fujiki, N. (2015). Cooperative vehicle path generation during merging using model predictive control with real-time optimization. *Control Engineering Practice*, 34(1):98–105.

Chen, L. and Englund, C. (2016). Cooperative intersection management: a survey. *IEEE Transactions on Intelligent Transportation Systems*, 17(2):570–586.

Chen, N., van Arem, B., Alkim, T., and Wang, M. (2020a). A hierarchical model-based optimization control approach for cooperative merging by connected automated vehicles. *IEEE Transactions on Intelligent Transportation Systems*.

Chen, N., van Arem, B., and Wang, M. (2020b). optimization of traffic efficiency at on-ramps with connected automated vehicles. In *2020 Forum on Integrated and Sustainable Transportation Systems (FISTS)*, pages 230–235. IEEE.

Chen, N., Wang, M., Alkim, T., and Van Arem, B. (2018a). A flexible strategy for efficient merging maneuvers of connected automated vehicles. In *18th COTA International Conference of Transportation Professionals*, pages 46–55. COTA.

Chen, N., Wang, M., Alkim, T., and Van Arem, B. (2018b). A flexible strategy for efficient merging maneuvers of connected automated vehicles. In *18th COTA International Conference of Transportation Professionals*, pages 46–55. COTA.

Chen, N., Wang, M., Alkim, T., and van Arem, B. (2018c). A robust longitudinal control strategy of platoons under model uncertainties and time delays. *Journal of Advanced Transportation*, 2018.

Daamen, W., Loot, M., and Hoogendoorn, S. P. (2010). Empirical analysis of merging behavior at freeway on-ramp. *Transportation Research Record*, 2188(1):108–118.

Daganzo, C. F., Cassidy, M. J., and Bertini, R. L. (1999). Possible explanations of phase transitions in highway traffic. *Transportation Research Part A: Policy and Practice*, 33(5):365–379.

Dey, K. C., Yan, L., Wang, X., Wang, Y., Shen, H., Chowdhury, M., Yu, L., Qiu, C., and Soundararaj, V. (2016). A review of communication, driver characteristics, and controls aspects of Cooperative Adaptive Cruise Control (CACC). *IEEE Transactions on Intelligent Transportation Systems*, 17(2):491–509.

Ding, H., Di, Y., Zheng, X., Bai, H., and Zhang, W. (2021). Automated cooperative control of multilane freeway merging areas in connected and autonomous vehicle environments. *Transportmetrica B: transport dynamics*, 9(1):437–455.

Ding, J., Li, L., Peng, H., and Zhang, Y. (2019). A rule-based cooperative merging strategy for connected and automated vehicles. *IEEE Transactions on Intelligent Transportation Systems*, 21(8):3436–3446.

Duan, Z., Zhang, J., Zhang, C., and Mosca, E. (2006). Robust H2 and H- filtering for uncertain linear systems. *Automatica*, 42(11):1919–1926.

Duret, A., Wang, M., and Ladino, A. (2019). A hierarchical approach for splitting truck platoons near network discontinuities. *Transportation Research Part B: Methodological*.

Evestedt, N., Ward, E., Folkesson, J., and Axehill, D. (2016). Interaction aware trajectory planning for merge scenarios in congested traffic situations. In *2016 IEEE 19th International Conference on Intelligent Transportation Systems (ITSC)*, pages 465–472. IEEE.

Feng, S., Zhang, Y., Li, S. E., Cao, Z., Liu, H. X., and Li, L. (2019). String stability for vehicular platoon control: Definitions and analysis methods. *Annual Reviews in Control*, 47:81–97.

Feng, Y., Head, K. L., Khoshmagham, S., and Zamanipour, M. (2015). A real-time adaptive signal control in a connected vehicle environment. *Transportation Research Part C: Emerging Technologies*, 55:460–473.

Gao, F., Li, S. E., Zheng, Y., and Kum, D. (2016). Robust control of heterogeneous vehicular platoon with uncertain dynamics and communication delay. *IET Intelligent Transport Systems*, 10(7):503–513.

Garriga, J. L. and Soroush, M. (2010). Model predictive control tuning methods: A review. *Industrial & Engineering Chemistry Research*, 49(8):3505–3515.

Ghasemi, A., Kazemi, R., and Azadi, S. (2015). Exact stability of a platoon of vehicles by considering time delay and lag. *Journal of Mechanical Science and Technology*, 29(2):799–805.

Guanetti, J., Kim, Y., and Borrelli, F. (2018). Control of connected and automated vehicles: State of the art and future challenges. *Annual reviews in control*, 45:18–40.

Guo, J., Luo, Y., and Li, K. (2017). Adaptive fuzzy sliding mode control for coordinated longitudinal and lateral motions of multiple autonomous vehicles in a platoon. *Science China Technological Sciences*, 60(4):576–586.

Hang, P., Lv, C., Huang, C., Xing, Y., and Hu, Z. (2021). Cooperative decision making of connected automated vehicles at multi-lane merging zone: A coalitional game approach. *IEEE Transactions on Intelligent Transportation Systems*.

Hedrick, J. K., Tomizuka, M., and Varaiya, P. (1994). Control issues in automated highway systems. *IEEE Control Systems Magazine*, 14(6):21–32.

Hirunyanitiwattana, W. and Mattingly, S. P. (2006). Identifying secondary crash characteristics for california highway system. Technical report.

Hu, X. and Sun, J. (2019). Trajectory optimization of connected and autonomous vehicles at a multilane freeway merging area. *Transportation Research Part C: Emerging Technologies*, 101:111–125.

Jacobson, L., Stribiak, J., Nelson, L., Sallman, D., et al. (2006). Ramp management and control handbook. Technical report, United States. Federal Highway Administration.

Jia, D. and Ngoduy, D. (2016). Platoon based cooperative driving model with consideration of realistic inter-vehicle communication. *Transportation Research Part C: Emerging Technologies*, 68:245–264.

Jin, I. G. and Orosz, G. (2014). Dynamics of connected vehicle systems with delayed acceleration feedback. *Transportation Research Part C: Emerging Technologies*, 46:46–64.

Jin, L., Cicici, M., Amin, S., and et al. (2018). Modeling the impact of vehicle platooning on highway congestion: A fluid queuing approach. *Proceedings of the 21st International Conference on Hybrid Systems: Computation and Control (part of CPS Week)*, pages 237–246.

Jin, P. J., Fang, J., Jiang, X., DeGaspari, M., and Walton, C. M. (2017). Gap metering for active traffic control at freeway merging sections. *Journal of Intelligent Transportation Systems*, 21(1):1–11.

Knoop, V. L., Wang, M., Wilmink, I., Hoedemaeker, D. M., Maaskant, M., and Van der Meer, E.-J. (2019). Platoon of sae level-2 automated vehicles on public roads: Setup, traffic interactions, and stability. *Transportation Research Record*, 2673(9):311–322.

Kothare, M. V., Balakrishnan, V., and Morari, M. (1996). Robust constrained model predictive control using linear matrix inequalities. *Automatica*, 32(10):1361–1379.

Letter, C. and Elefteriadou, L. (2017). Efficient control of fully automated connected vehicles at freeway merge segments. *Transportation Research Part C: Emerging Technologies*, 80:190–205.

Li, Y., Li, K., Zheng, T., Hu, X., Feng, H., and Li, Y. (2016). Evaluating the performance of vehicular platoon control under different network topologies of initial states. *Physica A: Statistical Mechanics and its Applications*, 450:359–368.

Li, Y., Yang, B., Zheng, T., Li, Y., Cui, M., and Peeta, S. (2015). Extended-state-observer-based double-loop integral sliding-mode control of electronic throttle valve. *IEEE Transactions on Intelligent Transportation Systems*, 16(5):2501–2510.

Li, Y., Zhang, L., Zheng, H., He, X., Peeta, S., Zheng, T., and Li, Y. (2018). Nonlane-discipline-based car-following model for electric vehicles in transportation-cyber-physical systems. *IEEE Transactions on Intelligent Transportation Systems*, 19(1):38–47.

Li, Z., Elefteriadou, L., and Ranka, S. (2014). Signal control optimization for automated vehicles at isolated signalized intersections. *Transportation Research Part C: Emerging Technologies*, 49:1–18.

Liang, C. and Peng, H. (1999). Optimal adaptive cruise control with guaranteed string stability. *Vehicle System Dynamics*, 32(4-5):313–330.

Lin, P.-W., Kang, K.-P., and Chang, G.-L. (2004). Exploring the effectiveness of variable speed limit controls on highway work-zone operations. In *Intelligent transportation systems*, volume 8, pages 155–168. Taylor & Francis.

Ma, J., Leslie, E., Ghiasi, A., Huang, Z., and Guo, Y. (2020). Empirical analysis of a freeway bundled connected-and-automated vehicle application using experimental data. *Journal of Transportation Engineering, Part A: Systems*, 146(6):04020034.

Marinescu, D., Čurn, J., Bouroche, M., and Cahill, V. (2012). On-ramp traffic merging using cooperative intelligent vehicles: A slot-based approach. In *Intelligent Transportation Systems (ITSC), 2012 15th International IEEE Conference on*, pages 900–906. IEEE.

McCartt, A. T., Northrup, V. S., and Retting, R. A. (2004). Types and characteristics of ramp-related motor vehicle crashes on urban interstate roadways in northern virginia. *Journal of Safety Research*, 35(1):107–114.

Mehar, A., Chandra, S., and Velmurugan, S. (2013). Speed and acceleration characteristics of different types of vehicles on multi-lane highways. *European Transport*, 55(1):1–12.

Michaud, F., Lepage, P., Frenette, P., Letourneau, D., and Gaubert, N. (2006). Coordinated maneuvering of automated vehicles in platoons. *IEEE Transactions on Intelligent Transportation Systems*, 7(4):437–447.

Milanés, V., Godoy, J., Villagrá, J., and Pérez, J. (2011). Automated on-ramp merging system for congested traffic situations. *IEEE Transactions on Intelligent Transportation Systems*, 12(2):500–508.

Milanés, V., Shladover, S. E., Spring, J., Nowakowski, C., Kawazoe, H., and Nakamura, M. (2014). Cooperative adaptive cruise control in real traffic situations. *IEEE Transactions on Intelligent Transportation Systems*, 15(1):296–305.

Min, H., Fang, Y., Wang, R., Li, X., Xu, Z., and Zhao, X. (2020). A novel on-ramp merging strategy for connected and automated vehicles based on game theory. *Journal of Advanced Transportation*, 2020.

Morales, A. and Nijmeijer, H. (2016). Merging strategy for vehicles by applying cooperative tracking control. *IEEE Transactions on Intelligent Transportation Systems*, 17(12):3423–3433.

Naus, G. J., Vugts, R. P., Ploeg, J., van de Molengraft, M. J., and Steinbuch, M. (2010). String-stable CACC design and experimental validation: A frequency-domain approach. *IEEE Transactions on Vehicular Technology*, 59(9):4268–4279.

Nilsson, J., Silvlin, J., Brannstrom, M., Coelingh, E., and Fredriksson, J. (2016). If, when, and how to perform lane change maneuvers on highways. *IEEE Intelligent Transportation Systems Magazine*, 8(4):68–78.

Ntousakis, I. A., Nikolos, I. K., and Papageorgiou, M. (2016). Optimal vehicle trajectory planning in the context of cooperative merging on highways. *Transportation Research Part C: Emerging Technologies*, 71:464–488.

Öncü, S., Ploeg, J., van de Wouw, N., and Nijmeijer, H. (2014). Cooperative adaptive cruise control: Network-aware analysis of string stability. *IEEE Transactions on Intelligent Transportation Systems*, 15(4):1527–1537.

Posch, B. and Schmidt, G. (1984). A comprehensive control concept for merging of automated vehicles under a broad class of traffic conditions. In *Control in Transportation Systems*, pages 187–194. Elsevier.

Pueboobpaphan, R., Liu, F., and van Arem, B. (2010). The impacts of a communication based merging assistant on traffic flows of manual and equipped vehicles at an on-ramp using traffic flow simulation. In *13th International IEEE Conference on Intelligent Transportation Systems*, pages 1468–1473. IEEE.

Rajamani, R. and Shladover, S. (2001). An experimental comparative study of autonomous and co-operative vehicle-follower control systems. *Transportation Research Part C: Emerging Technologies*, 9(1):15–31.

Raza, H. and Ioannou, P. (1996). Vehicle following control design for automated highway systems. *IEEE Control Systems Magazine*, 16(6):43–60.

Rios-Torres, J. and Malikopoulos, A. A. (2017a). Automated and cooperative vehicle merging at highway on-ramps. *IEEE Transactions on Intelligent Transportation Systems*, 18(4):780–789.

Rios-Torres, J. and Malikopoulos, A. A. (2017b). A survey on the coordination of connected and automated vehicles at intersections and merging at highway on-ramps. *IEEE Transactions on Intelligent Transportation Systems*, 18(5):1066–1077.

Ryu, J. and Gerdes, J. C. (2004). Integrating inertial sensors with Global Positioning System (GPS) for vehicle dynamics control. *Transactions-American Society of Mechanical Engineers Journal of Dynamic Systems Measurement and Control*, 126(2):243–254.

SAE International (2021). Taxonomy and definitions for terms related to driving automation systems for on-road motor vehicles.

Samiee, S., Azadi, S., Kazemi, R., and Eichberger, A. (2016). Towards a decision-making algorithm for automatic lane change manoeuvre considering traffic dynamics. *PROMET-Traffic&Transportation*, 28(2):91–103.

Scarinci, R. and Heydecker, B. (2014). Control concepts for facilitating motorway on-ramp merging using intelligent vehicles. *Transport reviews*, 34(6):775–797.

Scarinci, R., Heydecker, B., and Hegyi, A. (2015). Analysis of traffic performance of a merging assistant strategy using cooperative vehicles. *IEEE Transactions on Intelligent Transportation Systems*, 16(4):2094–2103.

Schakel, W., Knoop, V., and van Arem, B. (2012). Integrated lane change model with relaxation and synchronization. *Transportation Research Record: Journal of the Transportation Research Board*, 1(2316):47–57.

Schmidt, G. K. and Posch, B. (1983). A two-layer control scheme for merging of automated vehicles. In *Decision and Control, 1983. The 22nd IEEE Conference on*, pages 495–500. IEEE.

Sheikholeslam, S. and Desoer, C. A. (1993). Longitudinal control of a platoon of vehicles with no communication of lead vehicle information: A system level study. *IEEE Transactions on Vehicular Technology*, 42(4):546–554.

Shladover, S., Su, D., and Lu, X.-Y. (2012). Impacts of cooperative adaptive cruise control on freeway traffic flow. *Transportation Research Record: Journal of the Transportation Research Board*, 1(2324):63–70.

Skabardonis, A., Varaiya, P., and Petty, K. F. (2003). Measuring recurrent and nonrecurrent traffic congestion. *Transportation Research Record*, 1856(1):118–124.

Sun, Z., Huang, T., and Zhang, P. (2020). Cooperative decision-making for mixed traffic: A ramp merging example. *Transportation research part C: emerging technologies*, 120:102764.

Tak, S., Kim, S., and Yeo, H. (2016). A study on the traffic predictive cruise control strategy with downstream traffic information. *IEEE Transactions on Intelligent Transportation Systems*, 17(7):1932–1943.

Treiber, M., Hennecke, A., and Helbing, D. (2000). Congested traffic states in empirical observations and microscopic simulations. *Physical Review E*, 62(2):1805.

Van Arem, B., Van Driel, C. J., and Visser, R. (2006). The impact of cooperative adaptive cruise control on traffic-flow characteristics. *IEEE Transactions on Intelligent Transportation Systems*, 7(4):429–436.

van den Broek, T. H., Ploeg, J., and Netten, B. D. (2011). Advisory and autonomous cooperative driving systems. In *2011 IEEE International Conference on Consumer Electronics (ICCE)*, pages 279–280. IEEE.

VanderWerf, J., Shladover, S., Kourjanskaia, N., Miller, M., and Krishnan, H. (2001). Modeling effects of driver control assistance systems on traffic. *Transportation Research Record: Journal of the Transportation Research Board*, 1(1748):167–174.

Wang, M., Daamen, W., Hoogendoorn, S. P., and van Arem, B. (2014a). Rolling horizon control framework for driver assistance systems. Part I: Mathematical formulation and non-cooperative systems. *Transportation Research Part C: Emerging Technologies*, 40:271–289.

Wang, M., Daamen, W., Hoogendoorn, S. P., and van Arem, B. (2014b). Rolling horizon control framework for driver assistance systems. Part II: Cooperative sensing and cooperative control. *Transportation Research Part C: Emerging Technologies*, 40:290–311.

Wang, M., Daamen, W., Hoogendoorn, S. P., and van Arem, B. (2016a). Cooperative car-following control: Distributed algorithm and impact on moving jam features. *IEEE Transactions on Intelligent Transportation Systems*, 17(5):1459–1471.

Wang, M., Hoogendoorn, S. P., Daamen, W., van Arem, B., and Happee, R. (2015). Game theoretic approach for predictive lane-changing and car-following control. *Transportation Research Part C: Emerging Technologies*, 58(1):73–92.

Wang, M., Hoogendoorn, S. P., Daamen, W., van Arem, B., Shyrokau, B., and Happee, R. (2016b). Delay-compensating strategy to enhance string stability of adaptive cruise controlled vehicles. *Transportmetrica B: Transport Dynamics*, pages 1–19.

Wang, Y., Wenjuan, E., Tang, W., Tian, D., Lu, G., and Yu, G. (2013). Automated on-ramp merging control algorithm based on Internet-connected vehicles. *IET Intelligent Transport Systems*, 7(4):371–379.

Wen, Y., Zhang, S., Zhang, J., Bao, S., Wu, X., Yang, D., and Wu, Y. (2020). Mapping dynamic road emissions for a megacity by using open-access traffic congestion index data. *Applied Energy*, 260:114357.

Xiao, L. and Gao, F. (2010). Effect of information delay on string stability of platoon of automated vehicles under typical information frameworks. *Journal of Central South University of Technology*, 17(6):1271–1278.

Xiao, L. and Gao, F. (2011). Practical string stability of platoon of adaptive cruise control vehicles. *IEEE Transactions on Intelligent Transportation Systems*, 12(4):1184–1194.

Xiao, L., Wang, M., Schakel, W., and van Arem, B. (2018). Unravelling effects of cooperative adaptive cruise control deactivation on traffic flow characteristics at merging bottlenecks. *Transportation Research Part C: Emerging Technologies*, 96:380–397.

Xie, Y., Zhang, H., Gartner, N. H., and Arsava, T. (2017). Collaborative merging strategy for freeway ramp operations in a connected and autonomous vehicles environment. *Journal of Intelligent Transportation Systems*, 21(2):136–147.

Xu, H., Zhang, Y., Cassandras, C. G., Li, L., and Feng, S. (2020). A bi-level cooperative driving strategy allowing lane changes. *Transportation research part C: emerging technologies*, 120:102773.

Xu, L., Lu, J., Ran, B., and et al. (2019). Cooperative merging strategy for connected vehicles at highway on-ramps. *Journal of Transportation Engineering, Part A: Systems*, 145(6):04019022.

Xu, Q. and Sengupta, R. (2003). Simulation, analysis, and comparison of ACC and CACC in highway merging control. In *Intelligent Vehicles Symposium, 2003. Proceedings. IEEE*, pages 237–242. IEEE.

Yang, K., Guler, S. I., and Menendez, M. (2016). Isolated intersection control for various levels of vehicle technology: Conventional, connected, and automated vehicles. *Transportation Research Part C: Emerging Technologies*, 72:109–129.

Zhao, W., Liu, R., and Ngoduy, D. (2018). A bilevel programming model for autonomous intersection control and trajectory planning. *Transportmetrica A: Transport Science*, 1(1):1–26.

Zhou, M., Qu, X., and Jin, S. (2017). On the impact of cooperative autonomous vehicles in improving freeway merging: a modified intelligent driver model-based approach. *IEEE Transactions on Intelligent Transportation Systems*, 18(6):1422–1428.

Zhou, Y., Chung, E., Bhaskar, A., and Cholette, M. E. (2019). A state-constrained optimal control based trajectory planning strategy for cooperative freeway mainline facilitating and on-ramp merging maneuvers under congested traffic. *Transportation Research Part C: Emerging Technologies*, 109:321–342.

Summary

The aim of the thesis is to design coordination strategies for connected automated vehicles near on-ramps considering controller performance, safe lane changing conditions, maneuver planning, and trajectory control. CAVs have enhanced situation awareness with their onboard detection units and vehicle-to-everything communications. They have the potential to improve traffic operations by manoeuvring together under a common goal and by accepting a small time gap. Existing model predictive control controllers rarely check their controllers' robustness considering the mismatch between vehicle dynamics and prediction models. The existing cooperative merging strategies constrain that on-ramp CAVs merge into mainline traffic after reaching the final desired inter-vehicle distance and/or (merging) speed. That constraint may make them not be applied to scenarios where the length of the on-ramp lane is short and on-ramp CAVs cannot reach desired states before merging. Few methods investigate optimal merging sequences for two conflicting streams of traffic. Besides, mainline CAVs are rarely allowed to change lane during cooperation. This thesis consecutively tackles the aforementioned four points by presenting four coordination strategies that address the mentioned limitations. It consists of four stand-alone research papers corresponding to chapters 2-5.

Chapter 2 proposes a robust platooning control approach. It can be used for homogeneous and heterogeneous platooning control. In a homogeneous platoon, all vehicles are CAVs. CAVs and human-driven vehicles coexist in a heterogeneous platoon. The proposed control approach explicitly considers parametric uncertainties of the vehicle dynamics model. Human-driven vehicles' behavior cannot be controlled but can be affected by preceding CAVs. The intelligent driver model plus is used to represent the behavior of human-driven vehicles. The parameters of IDM+ are not perfect and thus uncertainties exist. A min-max MPC formulation is presented. At each control time step, optimal acceleration trajectories are generated by minimizing the maximum value of a cost function brought by model uncertainties. The cost function is constructed by using the predicted behavior of involved vehicles based on the current vehicular states and the generated accelerations. Simulation results suggest the proposed control approach may be robust to keep string stability.

In Chapter 3, a virtual platoon formed by mainline and on-ramp CAVs is controlled, with an assumed merging sequence. Longitudinal acceleration trajectories of CAVs are generated by using MPC. We present a new prediction-based merging condition. An

on-ramp CAV steers towards mainline traffic in the acceleration lane when its predicted inter-vehicle time gaps with surrounding vehicles are larger than its accepted time gap for merging. Like human drivers, it accepts a smaller time gap than its desired time gap for merging while it is approaching the end of the acceleration lane. The lateral maneuver of the on-ramp vehicle is accomplished by following a human-like trajectory equation without the intervention of a driver. Simulation results show that on-ramp CAVs accomplish merging automatically and safely with our proposed control strategy.

Chapter 4 addresses the optimal merging sequences for two conflicting streams of traffic. A hierarchical control approach is proposed. A tactical layer controller seeks the optimal merging sequences for two conflicting streams of traffic by solving a model-based optimization problem. Future vehicles' behavior during merging is estimated by using surrogate linear models of real vehicle trajectories regulated by an operational layer controller. During the planning process, on-ramp CAVs are allowed to cruise for several seconds to adjust their positions and speeds before being coordinated to merge into target slots, respectively. The operational layer controller is designed based on MPC. It regulates optimal acceleration trajectories for CAVs and time instants for on-ramp CAVs to change lane. Both the controllers explicitly consider safe interaction among vehicles and constraints on speed, acceleration, and safety. Without changing the operational layer controller, the decisions from the tactical layer controller outperform those from the first-in-first-out merging rule in improving traffic operations.

Chapter 5 extends the hierarchical control approach in Chapter 4 to allow mainline CAVs to change lane to facilitate merging of on-ramp CAVs. A uniform linear model is constructed to represent cruising, car-following, and cooperative lane changing maneuvers of vehicles. A planner optimizes dynamic vehicle sequences in each lane by minimizing predicted disturbances reflected by negative acceleration to upstream traffic in a long time horizon. An operational controller is designed based on MPC. It regulates acceleration trajectories and time instants for lane changers to change lane. Simulation results have shown, lane changing behaviors of mainline CAVs can improve traffic operations. Our control approach outperforms the first-in-first-out merging rule to schedule vehicle sequences in each lane under 528 different initial settings including desired time gap, speed, and position of CAVs, bringing 11% to 91% reduction ratios in traffic disturbances.

The main findings and conclusions are drawn in Chapter 6. We suggest that developed CAVs should be assessed under different scenarios and be admitted to the market when they are robust to have string stability. Low-speed on-ramp CAVs should be allowed to accelerate to reach the speed of the mainline traffic before they are coordinated with mainline CAVs for merging. Future research directions include investigating analytic approaches using Lyapunov theory to guarantee string stability of vehicle platoons, robust lane change control in mixed traffic, designing safe lane changing conditions in mixed traffic, and formulating cooperative merging strategies in mixed traffic.

Samenvatting

Het doel van dit proefschrift is om coördinatiestrategieën te ontwerpen voor 'connected automated vehicles' nabij opritten, rekening houdend met de prestaties van de voertuigbesturing, veiligheid van rijstrookwisselingen, manoeuvreplanning en het volgen van een trajectorie. CAVs hebben een verbeterd situatie bewustzijn met hun ingebouwde sensoren en draadloze communicatie met andere voertuigen en wegkantsystemen. Ze hebben het potentieel om de verkeersafwikkeling te verbeteren door samen te werken bij manoeuvres met een gemeenschappelijk doel en door snel te kunnen reageren. Bestaande regelaars voor 'Model Predictive Control' zijn zelden robuust, door de discrepantie tussen voertuigdynamica en voorspellingsmodellen. Bestaande coöperatieve invoegstrategieën laten CAVs pas vanaf de toerit invoegen in het hoofdverkeer na het bereiken van de uiteindelijke gewenste afstand tussen voertuigen en/of (invoeg)snelheid. Die beperking kan ertoe leiden dat ze niet geschikt zijn voor situaties waarin de lengte van de toerit kort is en CAVs op de toerit de gewenste volgafstand en invoegsnelheid niet kunnen bereiken voordat kan worden ingevoegd. Er zijn maar weinig methoden die de optimale invoegvolgorde onderzoeken voor twee conflicterende verkeersstromen. Bovendien mogen CAVs op de hoofdrijbaan tijdens de samenwerking zelden van strook wisselen. Dit proefschrift behandelt achtereenvolgens de bovengenoemde vier punten door vier coördinatiestrategieën te presenteren die de genoemde beperkingen aanpakken. Het bestaat uit vier op zichzelf staande wetenschappelijke artikelen.

Hoofdstuk 2 formuleert een robuuste benadering voor het regelen van homogene en heterogene pelotons. In een homogeen peloton zijn alle voertuigen CAVs. In een heterogeen peloton rijden CAVs en Human Driven Vehicles. De voorgestelde regelbenadering houdt expliciet rekening met parametrische onzekerheden van het voertuigdynamicamodel. Het gedrag van HDVs wordt niet direct geregeld maar wel beïnvloed door voorafgaande CAVs. Het intelligent driver model wordt gebruikt om het gedrag van HDVs weer te geven. Door een min-max MPC-formulering worden bij elke regeltijdstap optimale versnellingstrajecten gegenereerd door het minimaliseren van de maximale waarde van een kostenfunctie die wordt veroorzaakt door modelonzekerheden. De kostenfunctie wordt geconstrueerd door gebruik te maken van het voorspelde gedrag van betrokken voertuigen op basis van de huidige voertuigtoestanden en de gegenereerde versnellingen. Simulatieresultaten laten zien dat deze robuuste aanpak leidt tot een beter stabiliteit van het verkeer.

In Hoofdstuk 3 wordt een virtueel peloton bestuurd dat bestaat uit CAVs op de hoofdrijbaan en CAVs op de toerit met een gegeven invoegvolgorde. De longitudinale versnellingen van de CAVs worden gegenereerd met behulp van een MPC model. Een CAV voegt van de toerit in op de hoofdrijbaan wanneer de voorspelde volgtijden met andere voertuigen groter zijn dan een minimaal geaccepteerde volgtijd voor invoegen. Net als bij HDVs wordt de minimaal geaccepteerde volgtijd kleiner naarmate het einde van de toerit wordt genaderd. De laterale manoeuvre van het voertuig op het oprit wordt gemodelleerd door een automatische verplaatsing langs een baan die vergelijkbaar is met een menselijke rijstrookwisseling. Simulatieresultaten laten zien dat CAVs met de voorgestelde controle strategie automatisch en veilig invoegen,

Hoofdstuk 4 bestudeert de optimale invoegvolgorde voor twee conflicterende verkeersstromen door een hiërarchische regelaanpak. Een tactische regelaar zoekt de optimale invoegvolgorde door een modelgebaseerd optimalisatieprobleem op te lossen. Het gedrag van de voertuigen tijdens het samenvoegen wordt geschat met behulp van vereenvoudigde lineaire modellen van de voertuigtrajectoriën die worden gemodelleerd door een operationele regelaar. Tijdens het planningsproces hebben CAVs op de oprit enkele seconden om hun posities en snelheden aan te passen voordat ze worden gecoördineerd om respectievelijk in te voegen in een geselecteerd hiaat tussen twee voertuigen op de hoofdrijbaan. De operationele regelaar is ontworpen op basis van MPC. Het regelt optimale acceleratietrajectoriën voor CAVs en tijdsmomenten voor CAVs om van de toerit om naar de hoofdrijbaan te wisselen. Zowel de tactische als de operationele regelaar houden expliciet rekening met een veilige interactie tussen voertuigen en begrenzingen ten aanzien van snelheid, acceleratie en veiligheid. De resultaten laten zien dat de tactische regelaar tot een betere verkeersprestatie leidt vergeleken met een first-in-first-out invoegtactiek, wanneer gebruik gemaakt wordt van dezelfde operationele regelaar.

Hoofdstuk 5 breidt de hiërarchische regelaanpak van hoofdstuk 4 uit door CAVs op de hoofdrijbaan toe te staan om van rijstrook te wisselen om het invoegen van CAVs vanaf de toerit te vergemakkelijken. Er wordt een eenvoudig lineair model opgesteld om weef, volg en coöperatieve rijstrookwisselmanoeuvres te representeren. Een planner optimaliseert de dynamische voertuigvolgorde in elke rijstrook door voorspelde verstoringen te minimaliseren, in de vorm van negatieve versnellingen van stroomopwaarts verkeer over een langere tijdshorizon. Een operationele regelaar op basis van MPC regelt acceleraties en tijdstippen voor CAVs om van rijstrook te wisselen. Simulatieresultaten tonen aan dat rijstrookwisselingen door CAVs op de hoofdrijbaan de verkeersprestatie kunnen verbeteren. De gecombineerde planner en regelaar plant de voertuigsequenties in elke rijstrook beter dan een first-in-first-out onder 528 verschillende initiële instellingen voor gewenste volgtijd, snelheid en positie van CAVs. Dit leidt tot 11% tot 91% vermindering in verstoringen.

Hoofdstuk 6 vat de belangrijkste bevindingen en conclusies samen. CAVs moeten onder verschillende scenario's worden beoordeeld om hun robuustheid en stabiliteit in het verkeer te kunnen vaststellen. Toeritten moeten ruimte bieden voor acceleraties van

CAVs om vanaf lage snelheid de snelheid van verkeer op de hoofdrijbaan te bereiken voordat ze worden gecoördineerd met CAVs op het hoofdrijbaan om in te voegen. Toekomstige onderzoeksrichtingen omvatten het onderzoeken van analytische benaderingen met behulp van de Lyapunov-theorie om de stabiliteit van voertuigpelotons te garanderen en het ontwerpen van robuuste, veilige en coöperatieve rijstrookwisselingen in gemengd verkeer.

About the author

Na Chen was born in Anhui, China, in 1991. She received the Bachelor of Engineering degree in Traffic and Transportation and the Master of Engineering degree in Traffic and Transportation Planning and Management from Beijing Jiaotong University, Beijing, China, in 2013 and 2016, respectively. In 2016, she started her PhD under the supervision of Prof. dr. ir. Bart van Arem and Dr. Meng Wang, in the Department of Transport & Planning at Delft University of Technology. The PhD research was funded by China scholarship council, Rijkswaterstaat of the Ministry of Infrastructure and Water Management in the Netherlands, and Delft University of Technology. Her research interests include intelligent transport systems and traffic management.

Publications

Journal articles

- **Chen, N.**, van Arem, B., & Wang, M., "Hierarchical Optimal Maneuver Planning and Trajectory Control at On-ramps with Multiple Mainstream Lanes," under review.
- **Chen, N.**, van Arem, B., Alkim, T., & Wang, M., "A Hierarchical Model-Based Optimization Control Approach for Cooperative Merging by Connected Automated Vehicles," IEEE Transactions on Intelligent Transportation Systems, vol. 22, no. 12, pp. 7712-7725, Dec. 2021, doi: 10.1109/TITS.2020.3007647.
- **Chen, N.**, Wang, M., Alkim, T., & van Arem, B., "A Robust Longitudinal Control Strategy of Platoons under Model Uncertainties and Time Delays," Journal of Advanced Transportation, vol. 2018, Article ID 9852721, 13 pages, 2018. https://doi.org/10.1155/2018/9852721
- Jia, L., **Chen, N.**, Li, H., & Dong, H., "Intersection Queue Length Estimation with Single Magnetic Sensor," Journal of Jilin University (Engineering and Technology Edition), vol. 46, no. 3, pp. 756-763, 2016.

Peer-reviewed conference contributions

- **Chen, N.**, Van Arem, B., & Wang, M., "Optimization of Traffic Efficiency at On-ramps with Connected Automated Vehicles," 2020 Forum on Integrated and Sustainable Transportation Systems (FISTS). IEEE, pp. 230-235, 2020.
- **Chen, N.**, Wang, M., Alkim, T., & Van Arem, B., "A Flexible Strategy for Efficient Merging Maneuvers of Connected Automated Vehicles," CICTP 2018: Intelligence, Connectivity, and Mobility-Preceedings of the 18th COTA International Conference of Transportation Professionals, pp. 46-55, 2018.
- Li, H., **Chen, N.**, Qin, L., Jia, L., & Rong, J., "Queue Length Estimation at Signalized Intersections Based on Magnetic Sensors by Different Layout Strategies," World Conference on Transport Research – WCTR 2016, vol. 25, pp. 1626-1644, 2017.
- **Chen, N.**, Wang, L., Jia, L., Dong, H., & Li, H., "Parking Survey Made Efficient in Intelligent Parking Systems," Green Intelligent Transportation System and Safety (GITSS 2015), vol. 137, pp. 487-495, 2016.
- **Chen, N.**, Jia, L., Dong, H., Qin, Y., Pang, S., & Chen, J., "Design and Development of High-Speed Railway Infrastructure Detection Database," Proceedings of the 2013 International Conference on Electrical and Information Technologies for Rail Transportation (EITRT2013)-Volume I, pp. 433-439, 2014.

- **Chen, N.**, Chen, J., Zhong, F., Dong, H., & Gao, Y., "Secure Transmission Model Technology Scheme of Massive Train Information," Applied Science, Materials Science and Information Technologies in Industry, vol. 513, pp. 699-702, 2014.

- Dong, H., Wu, M., Shan, Q., **Chen, N.**, et al., "Urban Residents Travel Analysis Based on Mobile Communication Data," 16th International IEEE Conference on Intelligent Transportation Systems (ITSC 2013), pp. 1487-1492, 2013.

Patents

- Beijing Jiaotong University. A Method to Improve the Utilization of Parking Spaces Using Wireless Sensor Networks (In Chinese): China, CN201310301031.6 [P].2013-10-9.
  Inventors: Li, H., Jia, L., Dong, H., **Chen, N.**, Li, K., Liu, C., & Hu, Y.

- Beijing Jiaotong University. A Frequency Domain Spectral Energy Vehicle Classification Method Based on Magnetic Sensor (In Chinese): China, CN201310244509.6 [P].2015-10-21.
  Inventors: Li, H., Jia, L., Dong, H., Tian, Y., Liu, C, Hu, Y., Yang, Y., & **Chen, N.**

Software Copyright

- Name: Transmission Simulation System Software of Urban Rail Train On-board Sensor Network (In Chinese) V1.0. Registration number: 2014SRBJ0239. Development organization: Beijing Jiaotong University.
  Inventors: Dong, H., Xia, X, Jia, L., Qin, Y., Tian, Y., Tang, J., & **Chen, N.**

- Name: Dynamic Monitoring and Warning System of Urban Rail Train Safe State (In Chinese) V1.0. Registration number: 2014SRBJ0238. Development organization: Beijing Jiaotong University.
  Inventors: Tang, J., Dong, H., Jia, L., Qin, Y., Tian, Y., & **Chen, N.**

- Name: High Speed Railway Infrastructure Service Status Supervision System (In Chinese) V1.0. Registration number: 2014SRBJ0237. Development organization: Beijing Jiaotong University.
  Inventors: Dong, H., Tang, J., Jia, L., Qin, Y., Li, H., Xia, X., & **Chen, N.**

TRAIL Thesis Series

The following list contains the most recent dissertations in the TRAIL Thesis Series. For a complete overview of more than 275 titles see the TRAIL website: www.rsTRAIL.nl.

The TRAIL Thesis Series is a series of the Netherlands TRAIL Research School on transport, infrastructure and logistics.

Chen, N., *Coordination Strategies of Connected and Automated Vehicles near On-ramp Bottlenecks on Motorways*, T2021/29, December 2021, TRAIL Thesis Series, the Netherlands

Onstein, A.T.C., *Factors influencing Physical Distribution Structure Design*, T2021/28, December 2021, TRAIL Thesis Series, the Netherlands

Olde Kalter, M.-J. T., *Dynamics in Mode Choice Behaviour*, T2021/27, November 2021, TRAIL Thesis Series, the Netherlands

Los, J., *Solving Large-Scale Dynamic Collaborative Vehicle Routing Problems: an Auction-Based Multi-Agent Approach*, T2021/26, November 2021, TRAIL Thesis Series, the Netherlands

Khakdaman, M., *On the Demand for Flexible and Responsive Freight Transportation Services*, T2021/25, September 2021, TRAIL Thesis Series, the Netherlands

Wierbos, M.J., *Macroscopic Characteristics of Bicycle Traffic Flow: a bird's-eye view of cycling*, T2021/24, September 2021, TRAIL Thesis Series, the Netherlands

Qu, W., *Synchronization Control of Perturbed Passenger and Freight Operations*, T2021/23, July 2021, TRAIL Thesis Series, the Netherlands

Nguyen, T.T., *Highway Traffic Congestion Patterns: Feature Extraction and Pattern Retrieval*, T2021/22, July 2021, TRAIL Thesis Series, the Netherlands

Pudāne, B., *Time Use and Travel Behaviour with Automated Vehicles*, T2021/21, July 2021, TRAIL Thesis Series, the Netherlands

Gent, P. van, *Your Car Knows Best*, T2021/20, July 2021, TRAIL Thesis Series, the Netherlands

Wang, Y., *Modeling Human Spatial Behavior through Big Mobility Data*, T2021/19, June 2021, TRAIL Thesis Series, the Netherlands

Coevering, P. van de, *The Interplay between Land Use, Travel Behaviour and Attitudes: a quest for causality*, T2021/18, June 2021, TRAIL Thesis Series, the Netherlands

Landman, R., *Operational Control Solutions for Traffic Management on a Network Level*, T2021/17, June 2021, TRAIL Thesis Series, the Netherlands

Zomer, L.-B., *Unravelling Urban Wayfinding: Studies on the development of spatial knowledge, activity patterns, and route dynamics of cyclists*, T2021/16, May 2021, TRAIL Thesis Series, the Netherlands

Núñez Velasco, J.P., *Should I Stop or Should I Cross? Interactions between vulnerable road users and automated vehicles*, T2021/15, May 2021, TRAIL Thesis Series, the Netherlands

Duivenvoorden, K., *Speed Up to Safe Interactions: The effects of intersection design and road users' behaviour on the interaction between cyclists and car drivers*, T2021/14, April 2021, TRAIL Thesis Series, the Netherlands

Nagalur Subraveti, H.H.S., *Lane-Specific Traffic Flow Control*, T2021/13, March 2021, TRAIL Thesis Series, the Netherlands

Beirigo, B.A., *Dynamic Fleet Management for Autonomous Vehicles: Learning- and optimization-based strategies*, T2021/12, March 2021, TRAIL Thesis Series, the Netherlands

Zhang, B., *Taking Back the Wheel: Transition of control from automated cars and trucks to manual driving*, T2021/11, February 2021, TRAIL Thesis Series, the Netherlands

Boelhouwer, A., *Exploring, Developing and Evaluating In-Car HMI to Support Appropriate use of Automated Cars*, T2021/10, January 2021, TRAIL Thesis Series, the Netherlands

Li, X., *Development of an Integrity Analytical Model to Predict the Wet Collapse Pressure of Flexible Risers*, T2021/9, February 2021, TRAIL Thesis Series, the Netherlands

Li, Z., *Surface Crack Growth in Metallic Pipes Reinforced with Composite Repair System*, T2021/8, January 2021, TRAIL Thesis Series, the Netherlands

Gavriilidou, A., *Cyclists in Motion: From data collection to behavioural models*, T2021/7, February 2021, TRAIL Thesis Series, the Netherlands

Methorst, R., *Exploring the Pedestrians Realm: An overview of insights needed for developing a generative system approach to walkability*, T2021/6, February 2021, TRAIL Thesis Series, the Netherlands

Walker, F., *To Trust or Not to Trust? Assessment and calibration of driver trust in automated vehicles*, T2021/5, February 2021, TRAIL Thesis Series, the Netherlands